Fuzzy Logic Based Localization for Mobile Robots

Mohammad Molhim

A Thesis

in

The Department

of

Mechanical and Industrial Engineering

Presented in Partial Fulfillment of the Requirements

for the Degree of Doctor of Philosophy at

Concordia University

Montréal, Québec, Canada

December 2002

ABSTRACT

Fuzzy Logic Based Localization for Mobile Robots

Mohammad Molhim, Ph.D. Student

Concordia Unviersity, 2002

This thesis deals with the localization and map updating problems of mobile robots. We introduce three new fuzzy logic based localization and map updating algorithms for mobile robots that are equipped with a ring of sonar sensors. The first algorithm deals with the global localization problem, the second deals with detailed localization and location updating, and the third deals with map updating.

Sonar sensors are inexpensive but inaccurate. To deal with sonar uncertainty, we introduce models for angular and radial uncertainty of sonar readings based on possibility theory, mainly possibility distributions (fuzzy sets).

The concept of the fuzzy local composite map is introduced. This map utilizes the uncertainty models associated with sonar readings to give a description of the robot's surroundings. This map consists of a set of components, each of which represent the shortest distance between the robot and a detected object, and the orientation of the detected object with respect to the robot.

In the proposed global localization algorithm, the constructed fuzzy local composite map is matched with the given global map to identify the robot's location. In cases where multiple locations are obtained, the robot moves to accumulate range information to be used to reduce the number of candidate locations. This process continues until a unique location is obtained.

In the proposed detailed localization and map updating algorithms, two sets

of fuzzy composite map components are identified. The first set includes the components that have matching counterparts in the global map and are used to update the robot's location. The second set includes the components that do not have matching components in the global map and are used to update the robot's global map by adding new line segments.

The proposed algorithms are designed for implementation on any mobile robot equipped with a ring of sonar sensors. Moreover, these algorithms are dynamic algorithms where the robot's location and map can be estimated and updated in real-time. The proposed algorithms are implemented on a Nomad 200 mobile robot in an indoor environment. The results demonstrate the effectiveness of the proposed algorithms.

I dedicate this thesis to my parents and lovely wife ...

ACKNOWLEDGEMENTS

The author would like to express appreciation and gratitude to his supervisor, Dr. K. Demirli, who was extremely helpful during the course of this research work. Dr. Demirli's efforts were instrumental in the realization of this work. His vision played an important role in the achievement of this work. His continued guidance and support fueled my work with passion and motivation.

Special thanks goes to Dr. Akif Bulgak, the former director of the Canadian International Development Agency (CIDA)/Jordan University of Science and Technology (JUST)/Concordia University project, and to Mrs. Marie Berryman, the former coordinator of this project, both of whom were extremely encouraging and helpful throughout all stages of this work.

The financial support of CIDA, JUST and the National Research Council of Canada (NSERC) is gratefully acknowledged.

I am indebted to my colleagues who graduated from Concordia University during the course of this research, Dr. Mohanad AL-Atta and Dr. Malak Naji, for their support and encouragement during my research and study. I am further indebted for my colleagues Omar Banimelhem, Khalid Banimelhem, Murad El-Shibly, Hussien AL Wedyan, Alaa Al Hawari, and Khalid AL-Wedyan for their constant help and encouragement.

I also want to thank my father, mother, brothers and sisters for their deep love, encouragement, support and the help they have given me throughout my life. Thank you Hassan, Omaymeh, Areej, Arwa, Isra, Afnan and Osama.

My warm thanks to my wife's family for the encouragement and help they have provided me with during my life.

My biggest thanks goes to my lovely wife, Aseel Shajrawi, for her care, encouragement and patience. Without her support, this work would not have been possible.

TABLE OF CONTENTS

LIST OF FIGURES x
LIST OF TABLES xiii
LIST OF SYMBOLS xv

1 Introduction **1**

1.1 Problem Definition 3
1.2 Literature Review 6
1.3 Motivations 14
1.4 Objectives, Methodology and Contributions 16
1.5 Thesis Organization 21

2 Sonar Sensors **23**

2.1 Introduction 23
2.2 Time of Flight Measurement (TOF) 24
2.3 Sonar Sensor Design 26
2.4 Performance of Sonar Sensors 26

3 Fuzzy Logic Based Uncertainty Modeling **34**

3.1 Introduction 34
3.2 Modeling Uncertainty 40
3.3 Fuzzy Sets and Logic 42
3.4 Classical and Fuzzy Sets 43
3.5 Classical Set Operators 48
3.6 Basic Operations on Fuzzy Sets 50
3.7 Possibility Theory Approaches 57
3.8 Two Approaches for Possibility theory 58
3.9 Fuzzy Measures 59

3.10 Evidence Theory 60
3.11 Possibility and Necessity Measures 64
3.12 Possibilistic Approach for Modeling Uncertainty in Physical Measurements 66
3.13 Fuzzy Sets and Possibility Distributions 73

4 Modeling Uncertainty in Sonar Readings and Identifying the Objects in the Environment 75
4.1 Introduction 75
4.2 The Nomad 200 76
4.3 Experimental Setup 77
4.4 Modeling Angular and Radial Uncertainty of Sonar Readings Reflected From a Wall 84
4.5 Reduction of Angular and Radial Uncertainty in The Wall Case . . . 89
4.6 Modeling Angular and Radial Uncertainty for Sonar Readings Reflected From a Corner 97
4.7 Identifying The Objects in The Robot's Environment 101

5 Fuzzy Logic Based Localization 106
5.1 Introduction 106
5.2 Global Localization Problem 107
5.3 Concurrent Localization and Map Updating 123

6 Experimental Results and Discussions 136
6.1 Applications of The Global Localization Problem 136
6.2 Applications of The Concurrent Localization and Map Updating Problem 149

7 Conclusions and Future Work 156
7.1 Conclusions 156

7.2 Future Work 161

REFERENCES 163

A Appendix A **173**

LIST OF FIGURES

2.1 The Polaroid ultrasonic ranging system 25
2.2 Radial beam pattern of the sonar transducer. 27
2.3 The effect of the beam width on the sonar readings. 29
2.4 The incidence angle increases above a certain critical angle and reflected waves are no longer detected by the sonar sensor 31
2.5 False reflections. 32

3.1 The support, core, *alpha*-cut and height of a fuzzy set 46
3.2 Trapezoidal fuzzy set 47
3.3 Basic operations on fuzzy sets 51
3.4 A simple possibilistic histogram with its candidate points (top). Three examples of piecewise linear continuous approximation (bottom) . . . 74

4.1 The Nomad 200. 78
4.2 The Sensus 200 sonar ranging system. 79
4.3 Experiments for studying the behavior of the sonar sensor when it is in front of a wall (top) and a corner (bottom). 81
4.4 Error calculation for a sonar reading coming from a wall at a certain distance d and incidence angle γ. 82
4.5 Error calculation for a sonar reading coming from a corner at a certain distance d and incidence angle γ. 82
4.6 Polar coordinates for actual and sonar measured distances at different angles from a wall. 83
4.7 Polar coordinates for actual and sonar measured distances at different angles from a corner. 83

4.8 A measurement record (top), focal set (middle), and components of possibilistic histogram (bottom). 88
4.9 Possibility distribution for the radial uncertainty of sonar readings when the sensor is at distances between 50 cm and 100 cm. 88
4.10 Two sonar sensors detecting the same wall. 90
4.11 Three possible cases for the readings obtained from two sensors. . . . 92
4.12 Reduced angular uncertainty for readings coming from a wall, $d_1 < d_2$ (top), $d_2 < d_1$ (middle), and $d_1 = d_2$ (bottom). 93
4.13 Three sensors detecting the same wall. 94
4.14 Reduced radial uncertainty model when the incidence angle is 2.5^o for different values of d from a wall. 98
4.15 Reduced radial uncertainty model when the incidence angle is -11.5^o for different values of d from a wall. 98
4.16 Radial uncertainty model when the sonar sensor is at different values of d from a corner. 100
4.17 The reduced radial uncertainty model when the incidence angle is 2.5^o for different values of d from a corner. 100
4.18 The reduced radial uncertainty model when the incidence angle is -11.5^o for different values of d from a corner. 101
4.19 Conjunctive fusion of two pieces of information to obtain the shortest distance to a wall. 104
4.20 Conjunctive fusion of two pieces of information to obtain the shortest distance to a corner. 104

5.1 Elements of the global map. 110
5.2 Local map. 111
5.3 Example of a possible fuzzy local composite map of Figure 5.2. . . . 113
5.4 Fuzzy location region. 116
5.5 Scalar measures of matching between two fuzzy patterns. 118

5.6 Localization algorithm. 120
5.7 Obtaining a hypothesized location based on the traveled distance. . 123
5.8 Local map 127
5.9 (a) Fuzzy composite map is fit to the global map; (b) Shortest distances between the robot and different objects are obtained; (c) Combination of the shortest distances; (d) The fuzzy region that represents the estimated position of the robot. 130
5.10 Created line segment. 134
5.11 Line segments extraction algorithm. 135

6.1 The global map. 137
6.2 Angular uncertainty of the fuzzy local composite map. 138
6.3 Candidate locations of the robot. 139
6.4 The x, y and θ components of Loc_{12}. 140
6.5 Fuzzy candidate locations in the second scan. 141
6.6 The x, y and θ components of Loc_{23} 142
6.7 Hypothesized fuzzy location, $Loc_{12,h}$. 142
6.8 Fuzzy matching between Loc_{12} and Loc_{23}: (a) x-components match, (b) y-components match. 143
6.9 Tree search to obtain the current location. 143
6.10 The two sets of candidate locations shown in the same map. 144
6.11 Different unique fuzzy locations in the global map. 146
6.12 Fuzzy location region. 147
6.13 Experimental verification of the proposed localization algorithm. . . 152
6.14 Localization error versus localization iterations. 153
6.15 Experimental verification of the proposed localization algorithm. . . 154
6.16 Localization error versus localization iterations. 155

LIST OF TABLES

3.1 The truth table of the logical operator AND 49

3.2 The truth table of the logical operator OR 49

3.3 The truth table of the logical operator NOT 49

4.1 Radial imprecision intervals when the sensor is at different values of d from a wall. 84

4.2 The reduced radial imprecision intervals when the incidence angle is 2.5^o for different values of d from a wall. 97

4.3 The reduced radial imprecision intervals when the incidence angle is -11.5^o for different values of d from a wall. 97

4.4 Radial imprecision intervals when the sensor is at different values of d from a corner. 99

4.5 The reduced radial imprecision intervals when the incidence angle is 2.5^o for different values of d from a corner. 99

4.6 The reduced radial imprecision intervals when the incidence angle is -11.5^o for different values of d from a corner. 99

6.1 Components of identified fuzzy unique locations in the global map. . 147

6.2 Number of iterations and candidate locations obtained until a unique location is identified. 148

6.3 Actual components of the unique locations in the global map. 148

A.1 Sonar readings from a wall approximately 50 cm away from the sensor for $0 \leq \gamma \leq 25$. 174

A.2 Sonar readings from a wall approximately 50 cm away from the sensor for $0 > \gamma \geq -25$. 175

A.3 Sonar readings from a corner approximately 100 cm away from the sensor for $0 \leq \gamma \leq 25$. 176
A.4 Sonar readings from a corner approximately 100 cm away from the sensor for $0 > \gamma \geq -25$. 177

LIST OF SYMBOLS

A	Arbitrary fuzzy sets
$\bar{A}$	Complement of set A
$\mathcal{A}_i$	Set of objects that have negative surface normals in $\Pi_{\Theta \mid sd_i}$
B	Arbitrary fuzzy sets
$\vec{B}$	General measuring record
D	Distance between (X_i, Y_i) and (X_E, Y_E)
$C(\cdot)$	Number of occurrences
$\mathcal{C}$	Corner in the global map
E	Set of endpoints with duplicates omitted from $\vec{E}$
$\hat{E}$	Ordered endpoints vector
$\vec{E}$	Vector of endpoints
$\vec{E}^l$	Left endpoints vector
$\vec{E}^r$	Right endpoints vector
E^l	Set of endpoints with duplicates omitted from $\vec{E}^l$
E^r	Set of endpoints with duplicates omitted from $\vec{E}^r$
$\mathcal{E}$	Wall in the global map
$\mathcal{F}$	Focal elements
$\mathcal{F}^{\mathcal{E}}$	Empirical focal set
G	Object in the global map
$\mathcal{G}$	Global map
H	Hypothesized location
I	Set of sonar sensors that are detecting objects
K	Set of all the points to which a continuous curve actually will be fit
K'	Set of all the points to which a continuous curve may be fit
L	Line links (X_r, Y_r) and (X_i, Y_i)
$\mathcal{L}$	Set of fuzzy candidate locations

$\mathcal{M}$	Fuzzy local composite map
N	New location
O_j	Object belongs to $\mathcal{A}_i$
P	Intensity of the sound wave
$\mathcal{P}$	Power set
$PI(\cdot)$	Plausibility measure
P_0	Maximum initial intensity of the sound wave
Q	Number of elements of E
Q^r	Number of elements of E^r
Q^l	Number of elements of E^l
S	Crisp value of the shortest distance
$\mathcal{S}$	Random set
T_k	Candidate points of a possibilistic histogram
U	Universe of discourse of a fuzzy set
V	Distance between (X_i, Y_i) and the object O_j
X_E	X coordinate of the intersection point between L and O_j
X_e	X coordinate of the endpoint of a created line segment
X_i	X coordinate of $\mathcal{A}_i$
X_r	Robot's global x coordinate
X_s	X coordinate of the starting point of a created line segment
Y_E	Y coordinate of the intersection point between L and O_j
Y_e	Y coordinate of the endpoint of a created line segment
Y_i	Y coordinate of $\mathcal{A}_i$
Y_r	Robot's global y coordinate
Y_s	Y coordinate of the starting point of a created line segment
and, AND	Linguistic conjunction
$Bel(\cdot)$	Belief measure
Loc	Fuzzy candidate location

NC	Angle of corner
$Nec(\cdot)$	Necessity measure
NL	Negative surface normal of a wall
NOT	Linguistic negation
OB	Actual distance between the sonar sensor and the object
or, OR	Linguistic disjunction
$Poss(\cdot)$	Possibility measure
TOF	Time-of-flight
a	Radius of the sonar sensor
c	Midpoint of the $core(\cdot)$
d	Distance between the sonar sensor and a detected object
e	Error in sonar reading
f	Transmission frequency of the sonar sensor
$g(\cdot)$	Fuzzy measure
h_k	Midpoint of T_k
l	Distance traveled by the robot
$m(\cdot)$	Basic probability assignment
$m^E(\cdot)$	Set frequency distribution
$n(\cdot)$	Negation functions
r	Sonar reading
s	t-conorms
s_{bold}	Bold–union
s_{max}, max	Maximum
s_{sum}	Algebraic sum
s_w	Drastic sum
s_1, s_2	Endpoints of $supp(A)$
t	t-norms
t_{bold}	Bold–intersection

t_k^l	Left endpoint of T_k
t_k^r	Right endpoint of T_k
t_{min}, min	Minimum
t_{prod}	Algebraic product
t_w	Drastic product
v	Speed of sound
$\bar{x}_f$	Defuzzified robot's x coordinate
$\bar{y}_f$	Defuzzified robot's y coordinate
$core(A)$	Core of set A
$supp(A)$	Support of set A
Λ_Θ	Degree of match between the Θ components of two fuzzy locations
Λ_X	Degree of match between the X components of two fuzzy locations
Λ_Y	Degree of match between the Y components of two fuzzy locations
Ω	A universal set
Θ_s	Negative surface normal of a created line segment
Φ	Total degree of match between $\mathcal{M}$ and $\mathcal{G}$
Φ_d	Radial degree of match between $\mathcal{M}$ and $\mathcal{G}$
Φ_Θ	Angular degree of match between $\mathcal{M}$ and $\mathcal{G}$
Π	Possibility distribution
Π_X	Possibility distribution of the x component of a fuzzy location
Π_Y	Possibility distribution of the y component of a fuzzy location
Π_Θ	Possibility distribution of the θ component of a fuzzy location
Π_{xh}	Π of the x component of the hypothesized location
Π_{yh}	Π of the y component of the hypothesized location
$\Pi_{\theta h}$	Π of the θ component of the hypothesized location
$\Pi_{X_{od}}$	Π of the x component of the robot's location obtained from odometers
$\Pi_{Y_{od}}$	Π of the y component of the robot's location obtained from odometers
$\Pi_{\Theta_{od}}$	Π of the θ component of the robot's location obtained from odometers

$\Pi_{X_{so}}$	Π of the x component of the robot's location obtained from sonar
$\Pi_{Y_{so}}$	Π of the y component of the robot's location obtained from sonar
$\Pi_{\Theta_{so}}$	Π of the θ component of the robot's location obtained from sonar
Π_{X_f}	Π of the x component of the fused robot's location
Π_{Y_f}	Π of the y component of the fused robot's location
Π_{Θ_f}	Π of the θ component of the fused robot's location
$\Pi_{X\times Y}$	Cartesian product of Π_X and Π_Y
$\Pi_{\Lambda\|d}$	Angular uncertainty model at distance d
$\Pi_{d\|\gamma}$	Radial uncertainty model at angle γ
Π_{sd}	Possibility distribution of the shortest distance
α	Threshold value for $\pi_{\Gamma\|d_i}(\theta_s)$
β	Beam width of the sonar beam
δ	Angle between the sonar sensor and the surface normal
ϕ	Angular rotation of the robot
γ	Incidence angle of the sonar beam
λ	Wavelength of the sonar signal
$\bar{\theta}_f$	Defuzzified robot's θ coordinate
τ	Threshold value for the distance between (X_i, Y_i) and (X_s, Y_s)
σ_s	Standard deviation of a surface irregularities
ζ_1	Threshold for D
ζ_2	Threshold for V
μ_A	Membership value of fuzzy set A
λ^*	Ratio determines if there is an intersection between L and O_j
μ^*	Ratio determines if (X_i, Y_i) is within the coordinates of a line segment
$\forall$	'for all'
$\neq$	'not equal to'
$\subseteq$	'subset or equal to'
sup	Supremum

$\cap$	Set intersection
$\cup$	Set union

Chapter 1

Introduction

The study of robotics has evolved as a result of the industrial need of achieving accuracy and speed for different industrial applications. During the last two decades these needs have encouraged researchers to focus on the design and control of armed robots (robot manipulators) which can efficiently replace human operators. The results of this research have led to advances in industrial applications for automotives, manufacturing, inspection, material handling and vision systems, among many others [1, 2, 3, 4, 5].

The key issue for the success of armed robots in industrial applications is that the industrial environments of the armed robots are structured so that the uncertainty (noise and errors) in its all levels (modeling, actuating, and sensing) is reduced to a negligible level. For example, in an environment where the robot has to grasp a certain part from a specific location there are special feeders that are designed to precisely locate the parts in the location from where the robot must grasp them. Moreover, there exists different kinds of grippers that are connected to the end effector of the robot to make sure that the parts are securely grasped. In such structured environments, the robots rarely rely on their sensing abilities to reason about the actions that must be taken in each situation. The more structured the

environment, the less sensing and reasoning are needed. Most industrial environments where robot manipulators are needed are structured so they do not require external sensing, and robots perform repetitive motions to accomplish certain tasks.

During the last decade, researchers have been trying to find solutions for industrial applications where the robots must work in unstructured environments. The tasks of the robots require that they leave their locations to accomplish their tasks. Moving from one location to another requires sensing and reasoning so that the robots can take the appropriate actions to accomplish their tasks. This requirement has led to the design of mobile robots, and has added more challenges for robotics researchers where there is uncertainty at all levels. Mobile robots have many applications such as transferring materials in a factory, fire fighting, cleaning, painting, maintaining nuclear plants and helping handicapped people [6, 7, 8, 9, 10, 11, 12].

Mobile robots operating in such environments must be able to cope with significant uncertainty in their location. Traveling between two locations, simply going from location A to B (navigation) without artificial guiding aids (magnetic strips, artificial beacons, etc.), is a challenging task. On the other hand, this task is considered trivial compared to industrial manipulators.

For mobile robot applications, sensing and reasoning are considered to be the two primary elements for performing tasks successfully without the interference of humans. By sensing, the robot can estimate its location inside its environment, identify different environmental features, avoid obstacles while approaching its goal, and follow different paths to achieve its tasks. There are different types of sensors available for mobile robots: ultrasonic (Sonar), odometry, infrared, laser range finders, and cameras. The difficulty with any sensing methodology is accurate data results and interpreting these data. In reasoning, the robot makes use of the sensory information to reason about its state and then to determine what actions must be taken to achieve a certain task. For a mobile robot, most reasoning problems are

geometric in nature, such as determining its current location in a certain environment, i.e., localization, determining the path that has to be followed to reach its goal location, and avoiding obstacles while approaching its goal. These tasks become more challenging with the presence of uncertainty in the robot's sensors.

1.1 Problem Definition

For a mobile robot to navigate an environment, it must have the answers to the following questions [13]:

- What is my current location?
- What is my current map?

Providing an answer to the first question requires designing localization algorithms that rely on sensing the robot's environment and then reasoning and estimating its current position and orientation, i.e., location. The second question is answered by providing map updating algorithms that update the robot's map based on the sensory data provided by the robot's sensors.

To localize and update its map, the mobile robot relies on the data provided by two types of its devices: proprioceptive and exteroceptive. Odometers are proprioceptive devices (or internal sensors) that can provide reliable location information over short distances. Sonar sensors, laser range finders, and cameras are exteroceptive devices (or external sensors) that can be used for mobile robot localization and map updating.

There is no perfect sensor that can provide accurate location information for mobile robots. Each sensor has drawbacks that prevent it from being a perfect candidate for mobile robot localization and map updating. Odometers suffer from two types of errors: systematic and non-systematic [14]. The source of the first type of error is the robot's parameters which can have differences in the wheel dimensions

and alignment. In addition, there is uncertainty about the contact point between the robot's wheels and the floor. The source of the second type of error comes from the robot's movements, such as wheel slippage and the floor's characteristics. Most of the exteroceptive devices have drawbacks that result from their design, the interaction of their signals with the objects of the working environment, and their sensitivity to environmental phenomena. These drawbacks introduce uncertainty in the information provided by these sensors. Furthermore, some of these sensors are too expensive to be used on mobile used in low cost applications. This is the case with laser range finders and cameras. Alternately, sonar sensors are inexpensive and are often used for mobile robot localization, navigation and map updating [15, 16, 17, 18, 19, 20, 21, 22].

There are two main drawbacks that affect sonar based localization and map updating algorithms: the beam width of the sonar sensor and false reflections. The beam width introduces uncertainty in the position and orientation (*radial* and *angular* uncertainty, respectively) of the detected objects and it therefore affects the quality of the location information provided by the localization algorithms. False reflections provide inaccurate information about the robot's surroundings and this is in turn affects the functionality of the localization and map updating algorithms. Therefore, a modeling of the uncertainty associated with these sensors is needed so that they can be used effectively to solve mobile robot localization and map updating problems.

Localization algorithms are divided into two types. The first type provides algorithms to solve the problem of estimating the robot's location in its navigation environment given that the map of the environment is known and the robot has a complete lack of knowledge about its current location. This problem is known as the *Global Localization* [23], *First Localization* [24], or *Getting Lost* problem [25]. The robot faces this problem when it is activated without knowledge of its initial location. The solution to this problem depends on providing localization algorithms

that match the information provided by the robot's sensors, usually represented by a local composite map of the robot's environment, and the global map which is provided for the robot. As a result of this matching, the localization algorithms can provide a unique candidate location or multiple candidate locations. Further movements by the robot can help in collecting and accumulating sensory information to reduce the number of candidate locations until there is one unique location. In this thesis, this algorithm is referred to as the global localization algorithm. The second type of localization algorithms deals with the problem of providing an estimate of the robot's current location given that its initial location is known. In other words, this type of algorithms updates or maintains the robot's location based on its sensory data while it is moving. The current location of the robot is estimated based on the fusion of sensory information obtained by the robot's proximity sensors and odometers; this estimate is used to update the robot's odometers. In this thesis, this algorithm is referred to as the location updating algorithm.

For a mobile robot to be able to adapt to the changes in its environment, map updating algorithms are necessary to update the robot's map based on the recognition of new objects. The current location of the robot is estimated using the location updating algorithm and is used along with the current sonar data to recognize new objects. These objects are extracted in the form of line segments and added to the robot's map to update it. Updating the robot's map requires a reliable estimation of the robot's current location. Therefore, location updating is needed concurrently with map updating.

This thesis can be considered as one of the research projects carried out to provide solutions for localization and map updating problems for mobile robots equipped with low cost sensors, namely sonar sensors. We have constructed models that represent the uncertainty associated with the readings provided by these sensors. These models are used to construct a fuzzy local composite map which represents the robot's surroundings. This map is used along with the robot's global

map to estimate the robot's location and update its map.

Provided next is a literature review of the research projects concerned with mobile robot localization and map updating.

1.2 Literature Review

A variety of mobile robot localization and map updating algorithms have been developed in order to reliably estimate the robot's location and update its map while achieving its tasks. Given in this section is an overview of research projects that deal with the localization and map updating problems of mobile robots. This section is divided into three parts. Since any sonar based localization or map updating algorithm must be able to deal with the uncertainty associated with sonar sensors, the first part of this section reviews review research projects related to the modeling of uncertainty in sonar data. The second part deals with research projects related to the problem of global localization. The last part reviews different projects related to location and map updating problems.

1.2.1 Modeling Uncertainty in Sonar Sensors

Sonar sensors are widely used in mobile robot applications primerly for their low cost and the ease with which the sonar data can be processed to provide range information. Furthermore, sonar sensors have a better range compared to infrared sensors, and a lower cost compared to laser range finders.

There are two major drawbacks to sonar sensors: beam width and false reflections. The beam width causes uncertainty when measuring the position and direction of the detected objects. In addition to the beam width, some environmental factors may cause uncertainty in the measured distances, such as temperature and humidity. False reflections cause the sonar sensors to detect objects at distances farther away than their actual distances.

The presence of the beam width has a noticeable effect on the certainty of the data obtained by sonar sensors. First, the beam width causes uncertainty in the measured distances. This uncertainty results from the fact that the beam is reflected from the portion of the target closest to the sensor and not at the direct line of sight of the sonar sensor. Second, when there is an object detected by the sensor, there is uncertainty in the direction of the detected object. In this thesis, these two types of uncertainty related to sonar sensors are referred to as *radial* and *angular* uncertainty, respectively. Chapter 2 introduces more details about these two types of uncertainty.

In the literature regarding the above mentioned uncertainties, there are several proposed methods for modeling the uncertainty in sonar readings. Crowley [26] considers that the echo received by a sonar sensor comes from an arc shaped region. In this region, the length of the arc represents the angular uncertainty while the width of this region represents the radial uncertainty. Gasós and Martín [27] model the errors in sonar readings by using trapezoidal fuzzy sets. However, their model does not take into account the effect of the beam's width. Demirli and Türkşen [28, 29] model the angular and then the radial uncertainty in sonar readings by using trapezoidal membership functions which are constructed from empirical studies. Elfes [30] and Cho and Lim [31] model the angular and radial uncertainty in sonar sensors by using Gaussian probability density functions. These functions are proposed based on the shape of the sonar beam and not on its actual behavior. Kleeman and Kuc [32] introduce statistical models of the angular and radial uncertainty of sonar sensors. These models are limited to an array of only two sonar sensors separated by a known distance.

1.2.2 Global Localization

Guibas *et al.* [33] introduce a theoretical solution for the global localization problem by dealing with it as a geometric problem. The map of the robot's environment is

represented as polygon P and the data obtained from a range finder is represented as a star-shaped polygon V. In addition, the robot's orientation in its environment is assumed to be known by reading the compass on the robot. The localization problem is then solved by finding a point in P (or a set of points) for which the portion of P that is visible is a translation congruent to V. The authors assume that the robot's environment, the range finder, and the compass are all perfect, i.e., that they do not have any noise, and they use simulation to demonstrate their results. In an attempt to make this method applicable in practice, Karch and Noltemeier [34] introduce a description of a distance function that models the resemblance between the noisy range data and the noisy robot's environment. However, calculating such a distance function is time consuming and restricts the implementation of the localization algorithm in practice. As a result, the authors introduce a simplified simulation of their findings but no experimental results are reported.

The two methods mentioned above result in more than one candidate location of the robot in its environment when there are identical features at different places in the robot's environment. However, no additional steps are taken to reduce these locations or to obtain one unique location. A theoretical work introduced by Dudek *et al.* [35] deals with this situation. Dudek and his colleagues try to find the optimal path that the robot follows so that it can, at the end of the path, uniquely identify its location. Using its range finder, the robot probes the environment at different locations on this path. In addition, the robot's range finder is switched off while the robot is traveling from one probing location to another. The authors show that finding this path is NP-hard. Therefore, they introduce a greedy strategy by which the robot will travel a predetermined distance to uniquely localize itself. The authors assume that the robot's orientation is known and that the robot has a perfect range finder.

Drumheller [36] introduces a practical method for mobile robot localization. His approach is based on a 360^o scan of the environment while the robot is stationary.

In this approach, the possible matches between the environment model and the sonar contour obtained from the scan are determined. Then, possibilities that are inconsistent with the fact that the beam can not penetrate solid objects are excluded. This is referred to as a sonar barrier test. Based on these matches, the stationary location of the robot is obtained.

Crowley *et.al* [37] introduce a practical approach to solving the global localization problem. This approach is based on a principal component analysis of laser readings. The robot's environment is represented as a family of surfaces in the eigen space which is built from the principal components of the laser readings. Consecutive laser reading sets obtained from the environment are projected as points in the map of the environment. Each point is associated with a family of surfaces in the robot's environment which results in a candidate location (position and orientation). A Kalman filter is used to reduce the number of these locations and to select the most likely location consistent with the small movements of the robot.

Ducket and Nehmzow [38] introduce another practical approach for the global localization problem. They introduce a localization method that is based on evidence accumulated from odometric readings and both sonar and infrared readings. Information collected from different iterations is combined to reduce the number of candidate locations using the Bayes rule. In this study the uncertainty in sonar readings is not taken into account.

A dynamic localization method is introduced by Crowley [26] for a mobile robot navigating in a known environment. In this method, the robot navigates its environment and stores a large amount of data used to extract line segments. These segments are extracted using Kalman filtering. The line segments are matched to the given global map to estimate the robot's location.

Demirli and Türkşen [28, 29] introduce a global fuzzy logic based localization algorithm. The algorithm consists of two parts, the first one is called initial localization and the main issue here is to determine an approximate location of the robot

in the environment after matching the sonar readings to a real map of the environment given to the robot. The second part is called detailed localization where the uncertainty in the robot's location is reduced to a fuzzy region. This fuzzy region identifies a collection of the robot's locations, each with a degree of certainty or confidence. This region is determined based on the combination of two fuzzy sets representing the location of the robot from a different wall in the environment. The proposed algorithm relies only on sonar readings obtained from the walls of the robot's environment to estimate the robot's location. However, readings obtained from other environmental features such as corners are not taken into account. The proposed algorithm may provide more than one candidate location of the robot in its environment. However, no further steps are taken to reduce the number of candidate locations. The proposed algorithm relies on the sonar readings obtained from one place in the robot's environment while the robot is stationary.

Mota and Ribeiro [39] introduce a mobile robot localization algorithm based on a 2D laser image obtained from a laser range scanner and a reconstructed 3D model obtained from a video image. This algorithm consists of two layers. In the first layer a coarse estimate of the robot's location is obtained based on a 2D laser scanner and a 3D reconstructed map of the robot's environment. This is achieved by matching the information obtained from the 2D laser scanner with the 3D reconstructed map. The result of this matching process is a set of candidate locations for the robot in its environment. In the second layer, the set of candidate locations is analysed and clustered to obtain a reduced set of candidate locations. The most likely solution is then obtained by using a weighted clustering algorithm.

Wijk and Christensen [40] introduce a localization algorithm that depends on naturally selected localization points in the robot's environment. The robot's environment is given in the form of pairs of x and y coordinates that represent the features in the map; these features are called reference features. The reference features are extracted based on a triangulation based fusion algorithm (TBF). In TBF,

the robot is trained to extract these features from its environment. It is assumed that the robot always has full knowledge of its orientation in the environment. Once the robot has the map of its environment, it can navigate to extract current features from the sonar readings. A simple graph matching algorithm is used to make the match between reference and current features. The result of this matching is a linear transformation that can be used to estimate the global location of the robot. It is important to mention that if the robot does not know its orientation, the obtained transformation will be non-linear and requires more processing steps.

1.2.3 Concurrent Localization and Map Updating

Saffiotti and Wesley [41] introduce a perception-based self-localization method using fuzzy sets. It is important to mention that in their method, the authors assume that the robot has an approximate hypothesis of its own location in the environment, i.e, they do not solve the global localization problem. The perceptual-based localization technique depends on matching fuzzy perceptual clues included in the map and current clues extracted by the robot's sonar sensors. The results of the matching process are represented by fuzzy sets, and the robot's approximate location is determined. This matching process relies on collecting information while the robot is moving to decide what type of clue is current. For example, if there is evidence that there is a wall in the proximity of the robot, a segment must be established to be used in updating the robot's position. The authors do not introduce models for angular and radial uncertainty for constructing the current obtained features by sonar. However, they assume that the measured sonar traces have arbitrary fuzzy sets. This method is applied in long scale environments such as corridors.

A similar approach is presented by Gasós and Martín [27]. In their approach the robot describes an object in the environment based on four sonar readings obtained from this object. The uncertainty in the measured distances is represented by using trapezoidal fuzzy sets which are constructed based on confidence intervals.

These fuzzy sets are established without experimentally studying the relationship between the sonar readings obtained from an object and the actual distance to the object. In this study, the angular uncertainty in sonar readings is not considered. In their work, Gasós and Martín propose a method for updating the current location of the robot. This method depends on constructing a partial map of the robot's environment by using sonar traces and matching this map to the global map. The partial map is constructed in the form of fuzzy line segments. Constructing line segments to be used in the location updating process has a significant effect on the location updating frequency. This creates the need to rely on the odometers for longer traveled distances.

Cox [42] introduces a localization algorithm that updates the robot's location in a known map. The algorithm depends on optical range data that are matched to the robot's environment in an attempt to update the odometers. The matching algorithm finds an optimal linear transformation that provides the best match between the range data and the environmental model. This transformation is obtained by using the least square algorithm. The obtained transformation is then used to obtain the robot's location in the environment. This location is combined with the information provided by the robot's odometers to provide an update to its current location.

Hoppenot and Colle [43] introduce a localization algorithm that depends on Cox's idea. In their localization method, the sonar measurement impact points are estimated based on the robot's current position as obtained by the odometers. These points of impact are then matched to the nearest segment of the robot's environment. The authors use only seven sonar sensors distributed on half ring. The authors completely ignore the angular and radial uncertainty associated with sonar sensors.

A fusion algorithm is proposed by Neira *et al.* [44] to update the robot's location while traveling. This method relies on fusing two types of complementary

sensory information obtained from a laser sensor. The first type of information is range images which are used to determine the locations of walls in front of the robot, and the second type is intensity images which are processed to determine the locations of vertical edges which represent door and window frames. An extended Kalman filtering algorithm is used to fuse the two types of sensory information. The proposed algorithm is implemented and satisfactory localization errors are reported.

Boem and Cho [45] include two cylinders of different diameters in the robot's environment to determine its location based on triangulation. The sonar readings obtained from scanning the environment are used to detect the presence of the cylinders. From the position of each cylinder, the robot can determine its location. For this algorithm to work, these two cylinders must be present in the robot's environment.

Updating the map of the environment where the robot navigates has become an important direction for research in today's robotics community. Some authors face the problem by assuming that the robot's location is accurately estimated based on the robot's encoders (odometers) [46, 47].

Crowley [26] uses a recursive line fitting algorithm to build a line-based model of the robot's map from the robot's sonar readings. This approach does not take into account the uncertainty associated with sonar readings.

Using the probabilistic modeling of uncertainty in sonar readings, Elfes [30] introduces the Certainty Grid approach for map building. In the Certainty Grid approach, sonar readings are placed in the grid by using probability profiles that describe the certainty about the existence of objects at individual grid cells. The grid based approach does not take into account the false reflections of sonar readings. The Certainty Grid approach requires large amounts of sonar data to build the robot's map. This approach requires the robot to stop periodically to take sensor readings.

Poloni *et.al.* [48] introduce a fuzzy logic based Certainty Grid approach for

mobile robot map updating. In this approach, the robot's map is represented in terms of two fuzzy sets. The first fuzzy set represents the empty grids, and the second fuzzy set represents the occupied grids. The proposed approach requires collecting large amounts of sonar data to update the robot's map. Therefore, the robot is required to stop at different locations to collect sufficient sonar data. During its stop, the robot is rotated in certain degrees to explore its surroundings.

1.3 Motivations

Modeling uncertainty in sonar readings using the probability theory is achieved based on the assumption that this uncertainty can be described by a normal probability distribution and that it is small enough, that linear approximations can be correctly used [30]. These assumptions are provided to justify the use of Kalman filtering in solving mobile robot localization and map updating problems.

Modeling uncertainty in sonar readings requires taking into account the effect of the beam's width and false reflections. The effect of the beam width can be captured by modeling the angular and radial uncertainty. False reflections can be avoided by combining information from adjacent sensors.

Fuzzy sets are able to capture the uncertainty in sonar readings [27], however, building fuzzy models requires interpreting the behavior of sonar sensors using well established theoretical tools.

Modeling uncertainty in sonar readings based on one sonar sensor may result in poor uncertainty models. To overcome this problem, sonar readings provided by adjacent sonar sensors are combined to reduce uncertainty associated with only one sensor and for filtering false reflections.

Sonar uncertainty models should be constructed based on a general configuration of these sensors used on mobile robots. In other words, constructing these models for a specific configuration is not feasible [32].

Global localization algorithms provide either one candidate location or multiple candidate locations. Therefore, dynamic global localization algorithms are needed so that the robot can make use of the newly accumulated range information about its surroundings to reduce the multiple candidate locations to one location. However, this reduction is not possible in the case of the static global localization algorithms [28, 36]. In addition, global localization algorithms that depend on probing the robot's environment at different locations [38, 35] are not efficient since the robot is not able to make use of the information that can be obtained between any two probing locations.

Localization requires practical real time approaches that enable the robot to reason about and estimate its location. Theoretical localization algorithms [33, 34], which assume perfect sensing, do not represent practical solutions. This is due to the fact that sensor uncertainty is not avoidable.

Sensors for mobile robots are required to be capable of providing real time signals that can be interpreted on-line with low-cost processing. This opens the door to the design of localization algorithms that do not depend on storing large amount of sensory data [27]. Storing raw sensory data results in a large database. The size of the database depends on the length of the path that the robot follows.

To make the use of mobile robots feasible in practical applications, it is necessary to reach a trade off between costs and benefits. Often this prevents the use of expensive sensors [44, 43, 42, 37] in favor of inexpensive devices such as sonar sensors.

Because they are inexpensive, most mobile robots have a ring of sonar sensors. These sensors are arranged around the robot so that more range information about the robot's surroundings can be obtained. Therefore, localization algorithms should be designed in a general fashion for a class of robots with the ring configuration.

The ring of sonar sensors provides information about the nature of the objects in the robot's environment. Natural landmarks such as walls and corners can

be recognized and their global coordinates can be used for localization. However, structuring the robot's environment with artificial landmarks for the purpose of localization is not a practical approach and is not considered in this thesis [45].

Sonar based localization algorithms must take into account the uncertainty associated with sonar sensors. It is impractical to introduce sonar based localization algorithms based on the assumption that these sensors are precise [43]. It is necessary that sonar based localization algorithms provide correct location information to the robot so that it can achieve its tasks effectively. This location information can be obtained by providing suitable uncertainty models of sonar readings.

Map updating algorithms need to be dynamic so the robot does not have to stop to collect sensory data used to update the map [48]. Sonar based map updating algorithms must take into account the uncertainty associated with sonar readings. Relying on the robot's odometers to update the map is not a practical solution since odometer errors accumulate while the robot is navigating [46, 47]. Therefore, map updating algorithms must be designed to work with sensor based location updating algorithms to make sure that the robot's location is updated while the map updating process is taking place.

1.4 Objectives, Methodology and Contributions

1.4.1 Objectives

This thesis aims to provide sonar based dynamic algorithms for global localization, and concurrent localization and map updating problems. These algorithms rely on sonar sensors which are inexpensive. However, these sensors have drawbacks that introduce uncertainty to the readings provided by the sensors. Therefore, appropriate uncertainty models are introduced to represent the uncertainty associated with sonar readings. These models are used in the proposed algorithms to estimate the robot's location and update its map.

The objectives of this thesis are to:

- Develop uncertainty models for sonar readings. These models represent the angular and radial uncertainty in sonar readings.
- Develop a global localization algorithm.
- Develop concurrent localization and map updating algorithms.
- Verify and implement the proposed algorithms in a real environment.

1.4.2 Methodology

To overcome the beam width effect of sonar sensors, the behavior of these sensors is studied when they detect objects in the robot's environment. This is achieved by providing an appropriate experimental set-up and carrying out sets of experiments that enable us to understand the behavior of the sonar sensors. The experiments study the behavior of the sonar readings when they are coming from walls and corners since these two objects are available in the environment of any mobile robot. Based on the experimental results, fuzzy logic based models (possibility distributions) are constructed to represent the angular and radial uncertainty in sonar readings obtained by one sensor.

A solution is introduced for the false reflections problem based on combining range information from adjacent sensors. Adjacent sonar sensors with small differences in the range readings are considered to be reflected from the same objects.

Localization is accomplished by matching the sonar readings obtained from the robot's environment, i.e., a local map, with the robot's global map that is given in the form of walls and corners. The sonar readings are associated with the appropriate uncertainty models which are given in the form of possibility distributions (fuzzy sets). This results in constructing a fuzzy local composite map which represents the current proximity of the robot. This map consists of a set of components, each

representing the shortest distance between the robot and a detected object, and the orientation of the detected object with respect to the robot. These components are represented by possibility distributions (fuzzy sets).

In the proposed global localization algorithm, a matching algorithm is developed to match the obtained fuzzy local composite map and the robot's global map to obtain all of the robot's possible locations in the global map. For the matching process to be successful, at least two non-parallel components of the fuzzy local composite map must be associated with objects in the robot's global map. Generally, the result of the matching process is either one candidate location or a number of candidate locations of the robot in the global map. In the case of multiple candidate locations, the robot moves to accumulate range information in the form of a new fuzzy local composite map. A new set of fuzzy locations is identified from this map and a new hypothesized set of candidate locations is constructed based on the old set of candidate locations. This is achieved by taking into account the traveled distance of the robot obtained by the robot's odometers. A fuzzy pattern matching technique is used to match the hypothesized set of locations with the new set of candidate locations. Then, the new candidate locations with a lower degree of match are eliminated. This process is continued until a unique location is obtained.

The proposed fuzzy logic based location updating algorithm relies on the principle of fusing sensor information to estimate the current location of the robot. The current location of the robot is obtained by combining the location of the robot obtained by the odometers over short traveled distances and the location of the robot obtained based on the sonar readings. To estimate the robot's location based on sonar readings, the components of the fuzzy local composite map are transformed into the global coordinates. As a result of this transformation, two sets of the fuzzy local composite map components are identified. The first set consists of the components that have matching components in the global map. The second set consists of

non-matching components. Fuzzy triangulation technique is applied to each component of the first set to estimate either the x or the y coordinates of the robot's location. As a result of this triangulation technique, more than one component may describe the x or the y coordinate. Then, the principle of combining information from different sources is applied to obtain one x and one y coordinate. The result of this combination is the robot's location based on sonar readings. The robot's location is also estimated based on the odometer readings by taking into account the robot's previous location and the distance traveled. Then, a fuzzy logic based fusion technique is applied to the location obtained from the sonar readings and the odometers. The result of the fusion operation is the current location of the robot. This location is obtained in the form of possibility distributions (fuzzy sets). A defuzzification technique is applied on these distributions to obtain crisp values that can be used to update the robot's odometers.

Our proposed map updating algorithm is used to update the robot's map by adding new line segments. This is achieved by relying on the set of non-matching components to identify new objects in the robot's environment. The process of updating the robot's environment consists of three parts: the first part is responsible for initializing new line segments, the second part is responsible for creating new line segments from initialized segments, and the third part is responsible for updating the created line segments. Updating the robot's map requires that the current robot's location is reliable. Therefore, the location updating algorithm is implemented concurrently with the map updating algorithm.

1.4.3 Contributions

This thesis introduces models for angular and radial uncertainty of sonar readings reflected from walls and corners; It shows how to select the appropriate uncertainty models based on the range information and the number of adjacent sensors detecting the same object. Then, these models are used to obtain the shortest distances

between the robot and the detected objects in the robot's environment. These short distances are used in the proposed fuzzy logic based dynamic localization and map updating algorithms to obtain the robot's location and update the robot's map. The method used to construct the uncertainty models can be generalized for any robot with a ring configuration.

Combining information from adjacent sensors solves the false reflection problem of the sonar readings. In addition, the thesis introduces reduced models of uncertainty in sonar readings when they are reflected from the same walls and corners. The reduced models are derived based on the knowledge of the angle between any two adjacent sensors in the sonar ring and the number of the adjacent sensors detecting the same object.

The concept of the fuzzy local composite map is introduced. This map is constructed based on the sonar readings and their associated models of angular and radial uncertainty. The fuzzy local composite map is used in the localization and map updating algorithms to estimate the robot's location and to update its map.

A dynamic fuzzy logic based global localization algorithm is proposed to solve the mobile robot global localization problem where the location information is accumulated while the robot is exploring its map. In this algorithm, the robot makes use of the range information obtained while it is exploring its environment and locates itself in a known environment. The algorithm can be implemented on any mobile robot with a ring of sonar sensors. Using this algorithm, natural landmarks such as walls and corners are identified and their coordinates are used to estimate the robot's location. In addition, identifying corners has an effect on the number of steps needed to obtain a unique location. The proposed algorithm is implemented on a Nomad 200 robot in a real environment. The implementation shows how the robot can identify its location when it is lost in its environment. In addition, the obtained location has a small degree of error when compared to the real location of the robot. This is due to modeling the uncertainty of sonar readings based on the

actual behavior of sonar.

A dynamic fuzzy logic based location updating algorithm is proposed to enable the robot to update its location while navigating its environment. This algorithm does not rely on artificial landmarks either. The proposed algorithm takes into account the false reflections and the uncertainty associated with sonar readings, and it is generalized for robots with a ring configuration. Moreover, the algorithm does not depend on large amounts of sonar data to be used in the location updating process. The proposed location updating algorithm is tested on a Nomad 200 robot in a real environment. Experimental results are compared with the results obtained by relying only on odometers to estimate the robot's location. These experiments show that the proposed algorithm has a small degree of error in the estimation of the robot's location.

A map updating algorithm is proposed to enable the robot to update its global map while navigating. The proposed algorithm does not wait to obtain large amounts of sonar data in order to establish line segments. It is a real-time algorithm where sonar readings reflected from new objects are used immediately to initialize, create and update line segments that represent the new objects in the environment. In addition, the algorithm is able to handle the uncertainty associated with sonar readings. The proposed algorithm is implemented on a Nomad 200 mobile robot and the effectiveness of the algorithm is demonstrated experimentally.

1.5 Thesis Organization

The thesis is organized as follows:

- Chapter 2 deals with sonar sensors, their operation principles, uncertainty, and the factors that affect their performance.
- Chapter 3 reviews different concepts of uncertainty, different methods to model uncertainty, fuzzy logic, fuzzy sets, the operations of fuzzy sets, possibility

theory, and the construction of possibility distributions. These concepts are necessary for modeling sonar sensors' uncertainty.

- Chapter 4 is based on the possibilistic approach, and models of angular and radial uncertainty of sonar sensors are constructed. These models are obtained in the form of possibility distributions. These distributions are used to identify the detected objects. This is achieved by estimating the position and orientation of the detected objects.

- Chapter 5 includes a description of the proposed fuzzy logic based localization algorithms. The first section of this chapter proposes a fuzzy logic based localization algorithm as a solution for the global localization problem. In the second section algorithms for the location and map updating problems are proposed. The location updating algorithm is implemented concurrently with the map updating algorithm.

- Chapter 6 implements the proposed localization and map updating algorithms on the Nomad 200. The experimental results and a discussion of the these results are reported in this chapter.

- Chapter 7 concludes the thesis and introduces guidelines for future work.

Chapter 2

Sonar Sensors

2.1 Introduction

This chapter introduces different aspects related to sonar sensors. Sonar physical principle of operation is explained, the design of sonar sensors is introduced, different factors that affect the performance of sonar sensors are discussed, and different types of uncertainty resulting from the effect of these factors are identified.

Exteroceptive sensors mounted on any mobile robot are used to enable the robot to sense and explore its surroundings. Undoubtedly, the most popular exteroceptive sensors used on mobile robots are sonar sensors. This is mainly due to their low cost and their capability of providing real time range data. Their operation is based on the time-of-flight (TOF) principle using the properties of sound waves. Understanding the behavior of sonar sensors is very important to engineer models that can deal with the errors obtained when we use these sensors for mobile robot applications. This will enable us to avoid using expensive sensors, yet still achieve a high level of performance. In mobile robot applications, it is important to keep the cost of the mobile robot as low as possible so it is affordable for practical applications such as cleaning, mail delivery, painting, and material handling.

2.2 Time of Flight Measurement (TOF)

Time-of flight (TOF) range finders measure the round-trip time needed by a pulse of emitted energy to reach a reflecting object and echo back to a receiver. Time of flight measurements provide an easy and direct way of obtaining range data without expensive processing.

An ultrasonic range finder is an example of a sensor that uses the time of flight measurement principle. This type of sensor is known as Sonar, which stands for SOund Navigation and Range. Sonar was initially developed to be used in underwater applications [49]. However, these sensors, after modification, are used for airborne applications such as in the case of mobile robots. Most conventional sonar ranging systems employ a single transducer that acts as both a transmitter and receiver. This is called a monostatic transceiver. After the sonar sensor emits sound waves, a void period follows during which the internal circuitry is reset. The transducer then becomes a receiver, receiving the detected echos in a time variable gain amplifier. This amplifier has a gain factor that increases with time to compensate for the attenuation of sound in air. The output of the amplifier is then sent to a thresholding circuit as shown in Figure 2.1. The time-of-flight (TOF) measurement is obtained by measuring the difference in time from the beginning of the pulse transmission to the first time the threshold exceeded. The traveled distance d is obtained as [50]:

$$d = \frac{vt}{2}$$

where v is the speed of sound in air (343 m/s) and t is the round-trip time of the sound wave. The minimum range of the transducer is determined by the time required for the transducer to switch from transmitter to receiver.

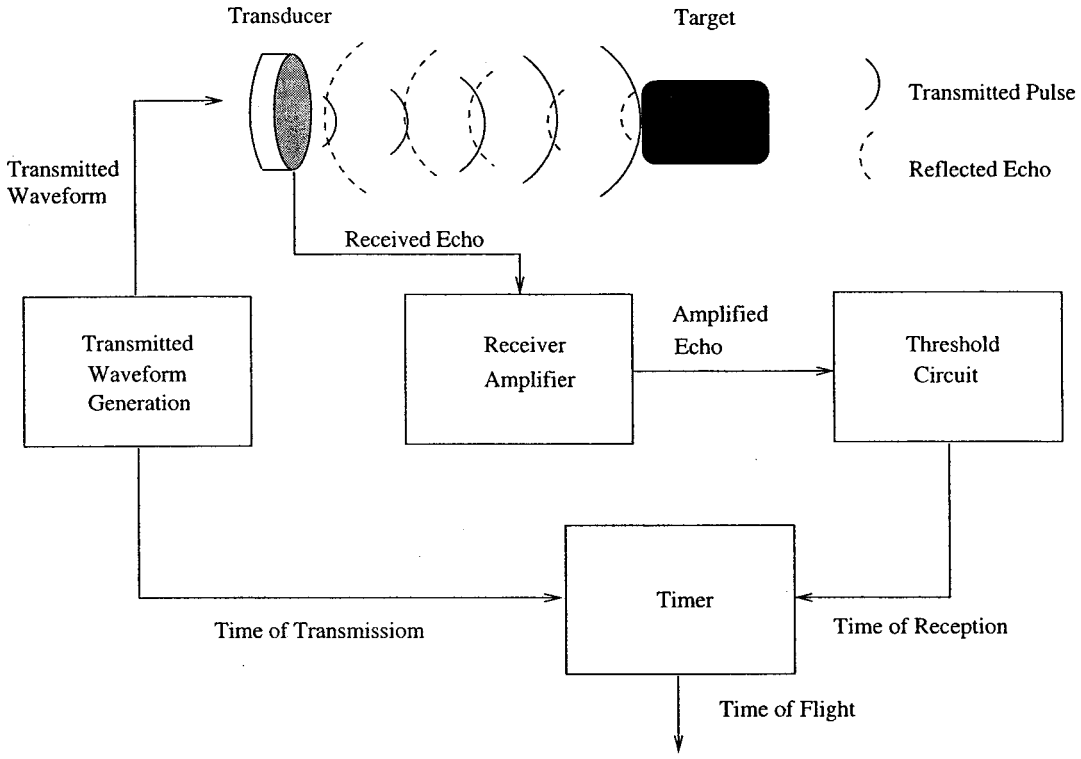

Figure 2.1: The Polaroid ultrasonic ranging system [51]

2.3 Sonar Sensor Design

Sonar transducers are usually modeled as a flat piston of radius a in an infinite baffle. The piston is vibrating at a certain frequency f and yielding acoustical energy with a wave length λ. The wave length is directly proportional to the speed of sound as follows:

$$\lambda = \frac{v}{f}$$

When the radius of the transmitting aperture a is much larger than the acoustic wavelength λ, the acoustic waves propagate in the form of a beam as shown in Figure 2.2. The obtained beam has two different regions, the first of which starts at the surface of the sensor and ends at the range approximately equal to $\frac{a^2}{\lambda}$; this region is called the *near zone*. The second region is called the *far zone* and starts just after the *near zone*. In the *far zone* region, the beam diverges with half-angle β_o which is obtained as:

$$\beta_o = \sin^{-1}(\frac{0.61\lambda}{a})$$

From this equation it is clear that the beam width is a function of the wavelength of the acoustic pulse. Since the wavelength depends on the frequency, so does the beam width. This means that a narrow beam width can be obtained with a high frequency of emitted acoustic energy. However, practically it is impossible to eliminate the presence of this beam width. An ideal range sensor is one that has no beam width and has a high range accuracy independent of the surface characteristics of targeted objects. This type of sensor is called a *ray-trace scanner* [51]. Many mobile robot researchers deal with sonar as a *ray-trace scanner* [35, 34, 36, 41] which does not represent the actual behavior of sonar sensors.

2.4 Performance of Sonar Sensors

The performance of a sonar sensor is affected by the following factors:

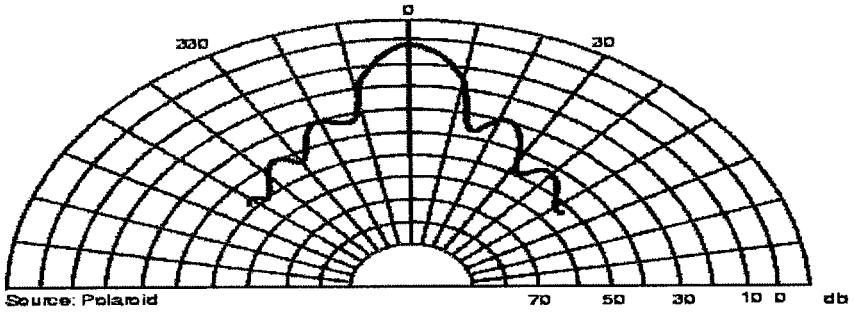

Figure 2.2: Radial beam pattern of the sonar transducer.

- **Beam Width**

  The presence of the beam width has an effect on the reliability of data obtained by a sonar sensor. The beam width is responsible for two major types of uncertainty in sonar readings. The first type results from the fact that when the sonar sensor is used to measure the distance of a certain object from the sensor, it is assumed that the sonar beam detects the portion of the object that is along the line of sight of the sensor. However, according to the presence of the beam width, the portion of the object closest to the beam is detected. Therefore, the reading provided by the sensor may not represent the actual distance between the sensor and the object. The second type of uncertainty is related to the direction of the detected objects with respect to the line of sight of the sensor. It is assumed that the direction of the detected object is the same as the incidence angle of the sensor. However, since the presence of the beam width causes detection of the portion of the object that is not along the

line of sight of the sensor, the direction of the detected portion of the object is within the beam width of the sensor. Therefore, we can define two types of uncertainty related to sonar sensors; *angular* and *radial* uncertainty. Certainty refers to the degree of possibility that the value of a physical parameter belongs to a certain interval. In the case of sonar sensors, the direction of the detected object belongs to the interval that represents the beam width with different degrees of possibility. Similarly, the set of possible values of the position of the detected object is represented by an interval where each element belonging to this interval has a certain possibility of being the actual position of the object. Chapter 4 demonstrates we show how to construct the angular and radial uncertainty models associated with sonar readings.

1. **Radial Uncertainty**

   When a sonar sensor is pointing in a normal direction at a wall, the error in the readings obtained by the sensor is mainly due to environmental factors (temperature, humidity, etc.) discussed later in this chapter. However, when the sensor is directed at a certain angle from the surface normal of the wall, the effect of the beam width starts to contribute to the error in the sonar readings. Consider the sonar sensor in Figure 2.3 which has a beam width described by the angle β. If the sonar beam is directed at a certain incidence angle γ from the surface normal of the wall, then the expected reading is the measurement of the distance along the line of sight of the sensor. However, due to the fact that the beam is reflected from the portion of the target closest to the sensor, the reading obtained by the sensor is the measurement of the distance between the sensor and the first detected part of the object. The difference between the expected reading and the reading given by the sensor is defined as the *radial uncertainty.* The radial uncertainty is affected by the value of the incidence angle γ and the beam width β. The radial uncertainty has a

noticeable effect on the location information provided by a mobile robot that is relying on the sonar to estimate its position.

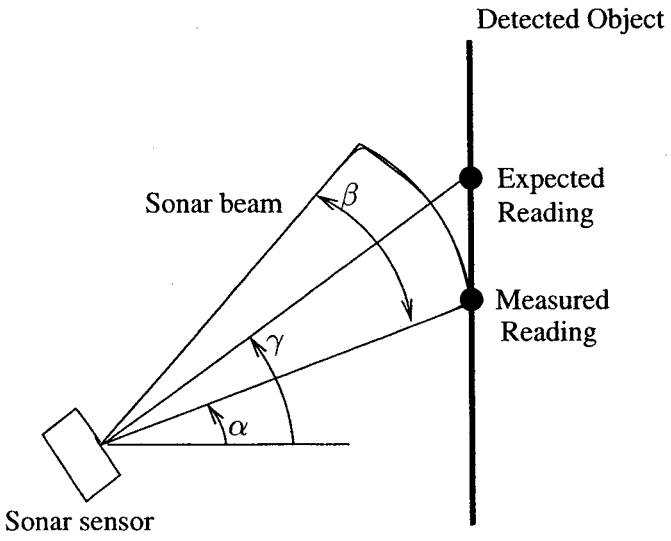

Figure 2.3: The effect of the beam width on the sonar readings.

2. **Angular Uncertainty**

As the beam width contributes to the error in the readings obtained by the sonar sensor, it also contributes to the measurement error in the direction of the detected objects. Due to the nature of the beam of the sonar, it can not be considered as a ray-trace scanner. The direction of a detected object can be described as within the beam width of the sensor. In other words, it is impossible to describe the direction of the detected object by using crisp values. For example, in Figure 2.3 we can not say that the direction of the detected object is γ, however, we can say that the direction of the detected object belongs to the interval $[\gamma + \frac{\beta}{2}, \gamma - \frac{\beta}{2}]$. This interval represents the angular uncertainty of the sonar sensor. The angular uncertainty affects the performance of sonar based localization and navigation algorithms. In localization, the robot orientation which is basically estimated from the direction of the objects detected by sonar

will have errors. In navigation, the beam width can make the robot view small objects as wider, and openings as closed passages.

- **Target Characteristics**

  Kleeman and Kuc [32] introduce a classification of the types of surfaces included in any mobile robot's environment. The classification is introduced for two reasons: the first factor is surface irregularities, and the second factor is the wavelength of the acoustic signal λ. Surface irregularities are said to have Gaussian distribution with a zero mean and a standard deviation of σ_s. According to these factors, there are three types of surfaces. The first type is a smooth surface where $\sigma_s << \lambda$. When an acoustic pulse detects a smooth surface it echos back with the same incidence angle. The detection of the reflected pulse occurs when it falls on the receiver element and produces a signal with an amplitude greater than the threshold value. This kind of reflection is called specular reflection or mirror-like reflection. In a mobile robot's environment, most of the objects can be classified as smooth surfaces and can include: metallic desks, painted walls, and doors. The second and third types are moderately rough and rough surfaces, where $\sigma_s \approx \lambda$ and $\sigma_s >> \lambda$ respectively. For rough and moderately rough surfaces, part of the echo energy is scattered in different directions due to surface irregularities. The energy of the echo pulse reflected from these surfaces is less than that of a smooth surface. The reflection of the acoustic pulse from rough or moderately rough surfaces is called diffused reflection. Outdoor environmental objects such as concrete and textured walls are classified as rough surfaces.

  Each surface has a certain angle after which the echo of the directed sonar beam is not reflected to the receiver. This is due to the fact that the surface normal of the object comes out of the beam boundaries as the incidence angle of the sonar beam becomes shallow as illustrated in Figure 2.4. This angle

is called the *critical angle* and it is a function of the operating frequency and surface roughness. If the incidence angle is more than the critical angle of the surface the reflected pulse may not be detected or it will be detected after being bounced off some objects in the environment as shown in Figure 2.5. The latter phenomenon is called *false reflection.* False reflection occurs when an object is detected far from its real location; they can be eliminated by combining readings from consecutive sensors. If a set of adjacent sensors provides close readings, this means their readings are not false reflections. This is explained in more detail in Chapter 4.

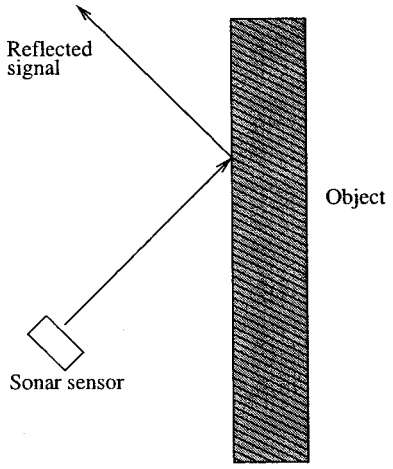

Figure 2.4: The incidence angle increases above a certain critical angle and reflected waves are no longer detected by the sonar sensor

- **Environmental Phenomena**

  Sonar readings are affected by the following environmental phenomena:

  1. **Atmospheric Attenuation**

     The power of the acoustic wave depends on the traveled distance. The

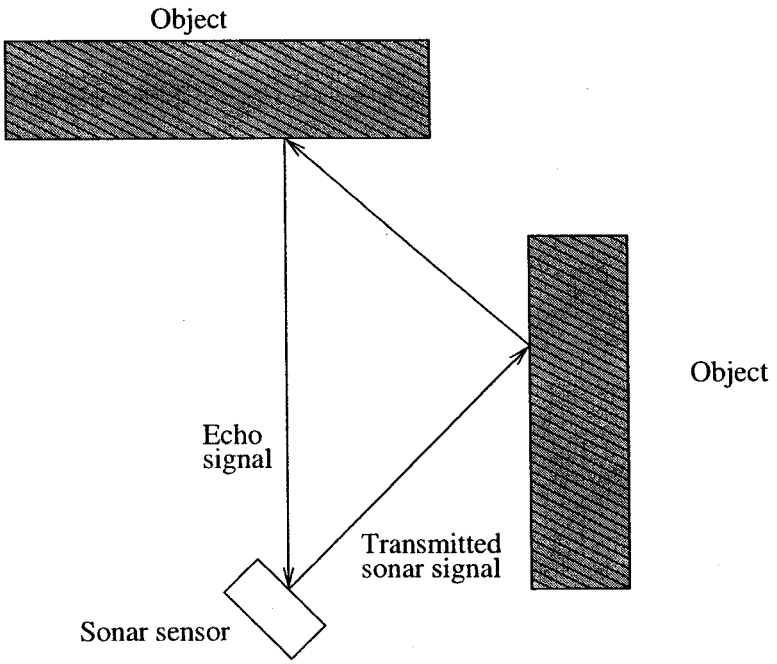

Figure 2.5: False reflections.

following equation describes this relation:

$$P = \frac{P_o}{4\pi R^2} \tag{2.1}$$

where P is the intensity (power per unit area) at distance R, and P_0 is the maximum (initial) intensity. The medium in which the sound waves travel also affects the power of the acoustic wave. The following equation describes this effect:

$$P = P_o e^{-2kR} \tag{2.2}$$

where k is the attenuation coefficient for the medium. The variable k is affected by the humidity and dust existing in the air, and is also affected by the operating frequency. To obtain the governing equation for the two effects, the above two equations are combined:

$$P = \frac{P_o e^{-2kR}}{4\pi R^2} \tag{2.3}$$

This equation shows that the intensity is inversely proportional to the square of the traveled distance. The farther the distance traveled, the weaker the power of the acoustic wave which means the weaker the echo. This will affect the reliability of the measured distance obtained by the sonar in terms of radial uncertainty.

2. **Temperature**

   Temperature affects the speed of sound in the air. This will directly affect the data obtained by sonar. However, this effect can be eliminated by using a correction factor based on the ambient temperature, which can be measured by an external sensor mounted on the robot.

   The correction of range is based on the ambient temperature in the proximity of the sensor. However, there is a possibility of a temperature gradient between the sensor and the target which will affect the reliability of the sonar readings in terms of radial uncertainty. This uncertainty can not be eliminated.

The next chapter reviews different approaches for uncertainty modeling. Adopted is one of the approaches developed by Molhim [52] for modeling the radial and angular uncertainty in sonar readings. These models are used to correct sonar readings when used for mobile robot localization.

Chapter 3

Fuzzy Logic Based Uncertainty Modeling

3.1 Introduction

This chapter addresses different definitions of uncertainty. In addition, there are reviews of traditional and new approaches to modeling uncertainty. We focus on the new approaches that belong to "General Information Theory", which includes mainly fuzzy logic and possibility theory. Then, a review of the different aspects associated with fuzzy logic theory such as fuzzy sets and their basic operations is discussed. Different concepts related to possibility theory such as possibilistic measures and their distributions are also investigated. We explain how to construct possibilistic histograms based on interval values set statistics obtained from experimental data and their empirical random sets. Demonstrated next is how continuous approximation between the candidate points of possibilistic histograms can be used to obtain possibility distributions (fuzzy sets).

Next, we review different points of view about the definition of uncertainty, its types, and causes according to Zimmerman [53], Klir [54], and Dubois and Prade [55].

3.1.1 Zimmerman's Point of View

Zimmerman [53] defines the "certainty" as "the case when one has the appropriate quantitative and qualitative information to describe, prescribe or predict deterministically and numerically a system, its behavior or other phenomena". Anything not described by this definition shall be called "uncertain". Furthermore, Zimmerman introduces a classification of uncertainty causes based on the quality and quantity of the available information. He classifies the causes of uncertainty as follows:

- **Lack of Information**:

  Lack of information may be considered the most frequently occurring type of uncertainty. For example, in decision logic one calls "decision under uncertainty" the case in which a decision making process lacks information about the possible states of nature that may occur. This kind of unavailable information can be considered a quantitative lack of information. The counterpart of this kind of information lack is qualitative. With qualitative, the decision making process has information about the probabilities of the occurrence of various states but is not sure which state will occur; this is called "decision making under risk". Another situation that can be described by the lack of information is "Approximation". This depends on the situation presented. For instance, one can decide that the available information is sufficient for the situation and he/she may not be able to or does not want to gather more information to make an exact description. Transition from a situation of "uncertainty" caused by a lack of information to a situation of "certainty" can be achieved by increasing the available information or collecting higher quality information; the ability to make the transition depends on the situation.

  This study faces this type of uncertainty when dealing with the global localization problem. Initially the robot does not have information about its location in the global map. To overcome the lack of information, the robot then starts

collecting more sensory information so that it can find its location in the map.

- **Abundance of Information**:

  This is due to the capability of a system to process large amounts of data at the same time. To reduce complexity, people tend to classify the available data in understandable forms by using a coarser grid or rougher "granularity", or by concentrating on the most important features while neglecting the least useful information for that situation. To do so, especially in scientific activities, some kind of "scaling" is used.

  An example of abundance of information exists in our proposed concurrent localization and map updating algorithm. The readings obtained from the sonar sensors are classified into two types: those reflected from features of the global map and those reflected from new features added to the global map. The first group of sonar readings are used to update the current location of the robot. The second group of sonar data is used to update the global map in terms of new line segments.

- **Conflicting Evidence**:

  This situation occurs when the available information describing two different behaviors of a system conflicts. The reason for this conflict may be erroneous available information, it may also be information concerning irrelevant features of the system being used, or the model which the observer has of the system is wrong. In this situation, correcting the available information can initiate the transition from "uncertain" to the state of "certain".

  The false reflection phenomenon of sonar readings is a good example of conflicting pieces of evidence. When a sonar sensor is used to measure the distance between the robot and any object in the environment, the readings obtained by the sonar may not represent the actual distance between the robot and the object due to the false reflection phenomenon. To overcome this type of

uncertainty, the readings obtained from consecutive sensors are considered to be able to estimate the actual distance between the robot and the object.

- **Ambiguity**:

  Ambiguity is a situation in which certain information has a different meaning based on the situation. From a mathematical point of view, it is a situation in which we have a one-to-many mapping. This type of uncertainty can be classified under lack of information because adding more information about the situation may put us in a situation closer to certainty.

  This type of uncertainty is common in the global localization problem; it exists in situations where the robot matches its local map to the global map and more than one match is obtained. In this case, the robot attempts to reduce the number of candidate locations by collecting more information through the exploration of its environment.

- **Measurement**:

  Measurement means describing the physical properties of a system or object; these may include weight, temperature, length etc. The precision of the measured quantity depends on the accuracy of the used tools. The quality of measuring technology has increased with time but it has not achieved perfection. In this situation there is uncertainty about real measures and the only available information is the indicated measurements.

  This is a typical example of the accuracy of sonar readings when used to estimate the distance between the robot and any object in the environment. Due to the factors mentioned in Chapter 2, the measured distances by sonar are different from actual distances.

- **Belief**:

  This cause of uncertainty appears when subjective information is available as a kind of belief in a certain situation. This belief is built by an observer (expert)

from past subjective information about the system or by statistical data about the system.

3.1.2 Klir's Point of View

Klir [54] found that there are six definitions of "uncertain" in the dictionary:

- not certainly known, questionable, problematical.
- vague, not definite or determined.
- doubtful, not having certain knowledge, not sure.
- ambiguous.
- not steady or constant, varying.
- liable to change or vary, not dependable or reliable.

When the definitions underwent a more detailed investigation, Klir found that uncertainty can be captured by two classes; vagueness and ambiguity. The former is related to the difficulty of making sharp or precise distinctions in the world. The latter is associated with one-to-many relations which means situations with two or more alternatives where the choice between them is left unspecified. In addition, Klir introduced a recent definition of uncertainty based on its connection to information theory. The most fundamental aspect of this connection is that uncertainty included in any situation is a result of an information deficiency. Information may be incomplete, imprecise, fragmentary, not fully reliable, vague, contradictory, or deficient in some other way.

3.1.3 Dubois and Prade's Point of View

Dubois and Prade state that imprecision and uncertainty can be considered as two complementary aspects of a single reality; the reality of imperfect information. It

has been observed that much of this information often cannot be obtained as precise and definite for various reasons; imperfect measuring instruments, the fact that the sole source of information is a human being, and information that is imprecise, incoherent, and in many cases incomplete. Dubois and Prade clearly distinguish between the concepts of imprecision and uncertainty: imprecision is associated with the contents of a piece of information, while uncertainty is associated with its truth. Imprecision refers to a lack of knowledge about the value of a physical parameter. The possible values of the parameter are represented by a certain interval obtained experimentally or from an expert. This interval represents the imprecision in the physical parameter. Certainty refers to the degree of truth that the value of the physical parameter belongs to a certain interval. In other words, each element belonging to this interval has a certain possibility to be the actual value of the physical parameter. This possibility is associated with a weight that is derived from the available knowledge about the physical parameter. When there are different imprecision intervals representing the value of the physical parameter, these intervals are used to construct a new interval without sharp boundaries. This interval is represented by a fuzzy set as is explained later in this chapter. Each element belonging to this interval has a degree of truth for being the actual value of the physical parameter. Therefore, this new interval represents the uncertainty of the physical parameter.

Uncertainty can be judged by means of different qualifiers such as probable, possible, or necessary. Probable has two different meanings: one is related to statistical experiments and the other is related to subjective judgment. Like probable, possible has two interpretations; physical (as a measure of material difficulty of performing an action), and subjective judgment. On the other hand, necessary has a much stronger notion, in either the physical or the subjective sense. A piece of information will be called precise when the subset associated with its value or component cannot be subdivided.

There are different qualifiers associated with imprecision, for example, vague,

fuzzy, or ambiguous. Ambiguity is allied with language. But vagueness or fuzziness in a piece of information resides in the absence of a clear boundary for the set of values attached to this piece of information.

From the above overview about uncertainty and its causes, it is our opinion that Dubois and Prade's definition of uncertainty is more comprehensive and practical than the others. The readings obtained from sonar sensors contain uncertainty in their values and directions. This uncertainty is captured using sonar data which is imprecise due to the factors that affect the behavior of sound waves in the environment. The direction from which the sonar readings are obtained belongs to the field of view of the sensor but with a degree of truth. Similarly, there is uncertainty in the distance of the detected objects. Chapter 4 establishes models of uncertainty for the distance of the detected objects (radial uncertainty) and their directions (angular uncertainty) based on the imprecise sonar data collected through our experimentation.

3.2 Modeling Uncertainty

3.2.1 Traditional Models for Uncertainty

Traditionally, two methods of representing imperfect information were used: probability theory and what is known as interval analysis. Probability theory is a tested mathematical theory that has a clear set of axioms and has been developed extensively. The basic axioms in probability is that the probability of disjoint events can be added. There are three schools that interpret probability theory in different ways. The first school's interpretation is based on the "Calculus of Chance" in games of chance where the probability of an event is defined as proportional between the number of favorable cases and the total number of possible cases. The second interpretation belongs to what is known as the "Frequencies School" in which the

probability of an event is defined as the limit of the frequency of this event's appearance. The third school is called the "Subjective School", by which the probability is defined as proportional to the sum an individual would like to pay if a proposition that he asserts prove false. In mobile robot applications, the "Frequencies School" is used for interpretation, the modeling of sensory data and making decisions about the robot's environment, and the actions taken to achieve certain tasks [56, 57, 58].

Interval analysis, used extensively by physicists tends to represent the inaccuracy in a measuring instrument in the form of interval through the measured quantity. Mathematically, one evaluates the image of a function whose arguments are subsets. Interval analysis has no gradation; while one does not know the exact value of a parameter, one does know the exact limits of its domain of variation.

It commonly occurs that imprecision of the error-of-measurement kind is present at the heart of a series of trials intended to exhibit a random phenomenon. In such cases, it can be observed that one can hardly represent the information in a purely probabilistic form without introducing further hypothesis. In fact, a hypothesis fundamental to the applicability of probability to statistics is that there should be a relation between the sample space and the event space; to every event there is an associated set of sample points that realizes the event (which is nonempty if the event is not impossible), and for every pair of distinct events there is at least one sample point that realizes one but not the other. This hypothesis therefore allows the sure event to be partitioned into elementary events, each corresponding to a specific sample point. In the case of the collection of statistical data, this amounts to supposing that the result of each experiment can be associated with one and only one element of this partition.

A probabilistic model is suitable for the expression of precise but dispersed information. Once the precision is lacking, one tends to question the validity of the model.

3.2.2 New Methods for Modeling Uncertainty

Nowadays, non-probabilistic mathematical methods for representation of uncertainty are developed. Klir [59] calls these methods "General Information Theory (GIT)". GIT consists of fuzzy sets, systems, and logic [60]; fuzzy measures [61]; random set [62] and Dempester-Shafer evidence theory [63]; possibility theory [64]; and others. The importance of such theories become evident when used in engineering applications. Fuzzy systems theory is the most prevalent component of GIT. Traditional fuzzy semantics is based on the interpretation of fuzzy sets as representations of human and cognitive categories. The other components of GIT are measurement methods other than cognitive modeling.

In this thesis we model the uncertainties associated with sonar readings using possibility distributions. These distributions are obtained based on possibilistic measures which are defined based on evidence theory. In addition, these distributions are fuzzy sets. Therefore, next we introduce the concept of fuzzy logic and fuzzy sets. In addition, we introduce two different forms to represent fuzzy sets. Then, basic operations on fuzzy sets are reviewed.

3.3 Fuzzy Sets and Logic

Fuzzy sets were introduced in 1965 by Dr. Lotfi Zadeh [65], a professor at the University of California in Berkeley, as a means to model the uncertainty of the real world. They are used to represent imprecise, ambiguous, or vague information. Fuzzy logic which was introduced in 1973 by the same professor [66], is a superset of conventional Boolean logic that has been extended to handle intermediate values between "completely true" and "completely false".

Boolean logic has two values often defined as true or false, on or off, black or white. However, in the real world there are many situations where events are not black or white but some shade of gray. Fuzzy logic is a continuous form of logic

that allows us to describe the shades of gray. If you are asked to describe your day in Boolean logic it would be good or bad. Fuzzy logic might recognize the day as being very bad, bad, poor, average, better than average, good, very good.

Zadeh defines the process of "fuzzification" as a methodology to generalize any specific theory from a crisp to a fuzzy form. This is achieved by applying the "extension principle" [65]. Researchers have applied this principle on many areas such as control, reasoning, mathematical programming, decision making, pattern recognition, and many others.

In addition to its role in modeling and processing imprecise or ambiguous information, fuzzy logic is used to model complex systems. These systems are difficult to be described using mathematical relations. In addition, mathematical modeling becomes more difficult when there are uncertainties and ambiguities in the systems to be modeled. The ideas of fuzzy modeling are found in the early papers of Zadeh. Zadeh's approach was later expanded into fuzzy systems modeling by Sugeno and Yasukawa [67], Bezdek [68] and Chiu [69]. Fuzzy modeling is a qualitative modeling scheme by which we qualitatively describe system behavior using natural language. The relation between the inputs and outputs of the system is given in the form of IF-THEN rules. There are two approaches of fuzzy systems modeling: one is subjective where the system behavior is established based on the knowledge of an expert [70] and the other is objective where the system behavior is established from input-output data via fuzzy clustering algorithms [71, 72, 73].

3.4 Classical and Fuzzy Sets

Let U be the universe of discourse which consists of all possible elements that are associated with a particular context or application. A crisp set A defined on U may be represented by listing all the elements that satisfy the definition of A in the case that A is finite (the list method). If A is infinite, it can represented by specifying

the rules that must be satisfied by elements of U to be considered elements of A (rule method). The former method is limited. On the other hand, the later method is more general. The membership function $\mu_A(x)$ of a classical set A defined on U by using the rule method is defined by:

$$\mu_A(u) = \begin{cases} 1, & \text{if} \quad u \in A \\ 0, & \text{if} \quad u \notin A \end{cases}$$

This means that an element u is either a member of set A (with $\mu_A(u) = 1$) or not a member (with $\mu_A(u) = 0$). In classical logic, the membership value of u can be taken as the truth value of the proposition "*u belongs to A*". In this situation there is only one possible truth value of this proposition: *false* or *true*.

A fuzzy set, introduced by Zadeh [65], is a set with graded membership. In a fuzzy set each element of U belongs to the set A with a membership degree characterized by a real number in the closed interval $[0, 1]$ (i.e., $\mu_A(u) \in [0, 1]$). An element may belong to the fuzzy set with lesser degree than another element, however, they both belong to the same fuzzy set. In fuzzy logic, the membership value of u represents the degree of truth of the proposition "*u is A*".

Since a fuzzy set may contain elements with zero degree membership and elements with one degree membership, then we can consider the concept of a crisp set to be a special case of the more general concept of a fuzzy set.

3.4.1 Basic Characteristics of Fuzzy Sets

We now introduce some important characteristics that are linked to fuzzy sets. These characteristics are shown in Figure 3.1 along with the following explanation:

1. The support of a fuzzy set A within a universal set U, is the crisp set that contains all elements of U that have nonzero degree membership in A, that is:

$$\text{supp}(A) = \{u \in U \quad | \, \mu_A(u) > 0\}$$

2. The core of a fuzzy set A within a universal set U, is the crisp set that contains all elements of U that have one degree membership in A, that is:

$$\text{core}(A) = \{u \in U \quad | \, \mu_A(u) = 1\}$$

Note that the core of a fuzzy set is a subset of its support.

3. The height of a fuzzy set A is the largest membership grade obtained by any element in that set, that is :

$$h(A) = \sup_{u \in U} \mu_A(u)$$

A fuzzy set with a height equal to 1 is called normal and with $h(A) < 1$ subnormal.

4. An α-cut of a fuzzy set is a crisp set A_α that contains all the elements in U that have membership values in A greater than or equal to α, that is:

$$\alpha - \text{cut}(A) = \{u \in U \quad | \, \mu_A(u) \geq \alpha\}$$

The core of a fuzzy set is an α-cut with $\alpha = 1$.

3.4.2 Representation of a Fuzzy Set

There are two methods to represent fuzzy sets:

1. Set of ordered pairs representation [65]: a fuzzy set A in U may be represented as a set of ordered pairs of a generic element u and its membership value, that is:

$$A = \{(u, \mu_A(u)) \quad | \, u \in U\}$$

When U is discrete A is commonly written as:

$$A = \sum_{i=1}^{m} \mu_A(u_i)/u_i = \mu_A(u_1)/u_1 + \cdots + \mu_A(u_m)/u_m$$

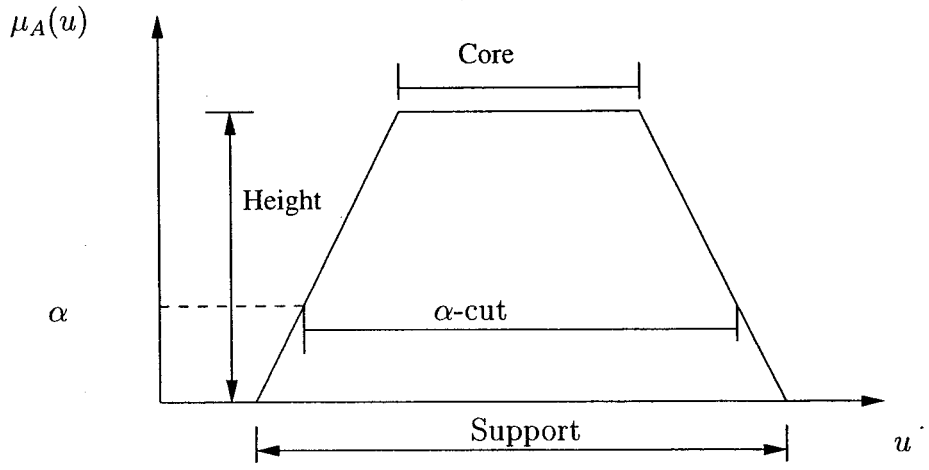

Figure 3.1: The support, core, *alpha*-cut and height of a fuzzy set

In this equation the summation sign does not represent arithmetic addition, it represents the collection of all points $u \in U$ with the associated membership function $\mu_A(u)$.

When U is continuous (for example, $U = \Re$), A is commonly written as:

$$A = \int_u \mu_A(u)/u$$

where the integral sign does not represent integration; it represents the collection of all points $u \in U$ with the associated membership function $\mu_A(u)$.

Example: Let A = integer close to 10, then:

$A = .1/7 + .5/8 + .8/9 + 1/10 + .8/11 + .5/12 + .1/13$

Three points to note from A:

- The integers not explicitly shown all have membership values equal to zero.
- The membership values were chosen by a specific individual, except for the unity membership value when $x = 10$, they can be modified based on our own personal interpretation of the phrase "close."

- The membership function is symmetric about $x = 10$, because there is no reason to believe that integers to the left of 10 are close to 10 in a different way than are integers to the right of 10. But again, we are free to make other interpretations.

2. Functional representation: In this representation functional description is used to represent fuzzy sets. An example is the functional description of a trapezoidal-shaped fuzzy set shown in Figure 3.2:

$$\mu_A(u) = \begin{cases} \frac{u-a_1}{a_2-a_1} & \text{If} \quad a_1 \leq u \leq a_2 \\ 1 & \text{If} \quad a_2 < u \leq a_3 \\ 1 - \frac{a_3-u}{a_3-a_4} & \text{If} \quad a_3 < u \leq a_4 \end{cases}$$

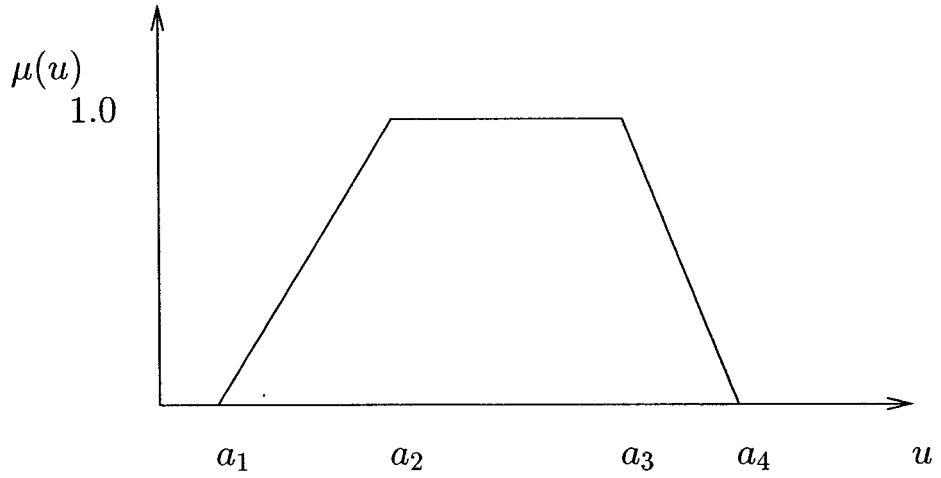

Figure 3.2: Trapezoidal fuzzy set

Comparing the above two types of a fuzzy set representation, it is obvious that the ordered pairs representation will be chosen for computer implementation. Due to complexity of the operations when using functional representation discretizations are necessary in practical applications.

3.5 Classical Set Operators

In classical set theory there are three main operations that are defined on classical sets; intersection, union and complement. These operations are defined by the two-valued logical operators *and*, *or* and *not*, respectively. They are defined for the two sets A and B which are defined on U as follows :

- The union of A and B, represented as $A \cup B$, is a new set that contains all of the elements in either A or B. The membership value of any element belonging to this new set is given as $\mu_{A \cup B}(u) = \max(\mu_A(u), \mu_B(u))$. For example, if $u \in A$ $(\mu_A(u) = 1)$ or $u \in B$ $(\mu_B(u) = 1)$, then $\mu_{A \cup B}(u) = 1$. Similarly, $\mu_{A \cup B}(u) = 0$ if $u \notin A$ $(\mu_A(u) = 0)$ or $u \notin B$ $(\mu_B(u) = 0)$. The union operation can be defined as:

$$A \cup B = \{u \mid u \in A \quad \text{OR} \quad u \in B\}$$

- The intersection of A and B, denoted $A \cap B$, contains all the elements that are simultaneously in A and B. The membership value of any element belonging to this new set is given as $\mu_{A \cap B} = \min(\mu_A(u), \mu_B(u))$. For example, if $u \in A$ and $u \in B$, then $\mu_{A \cap B} = 1$. Similarly, $\mu_{A \cap B} = 0$ if $u \notin A$ and $u \notin B$. The intersection operation can be defined as :

$$A \cap B = \{u \mid u \in A \quad \text{AND} \quad u \in B\}$$

- The complement $\bar{A}$ is a new set contains all the elements that are not in A. The membership value of any element belonging to this new set is given as $\mu_{\bar{A}}(u) = 1 - \mu_A(u)$. For example, if $u \in A$, then $\mu_{\bar{A}}(u) = 0$. Similarly, $\mu_{\bar{A}}(u) = 1$ if $u \notin A$. The complement operation can be defined as:

$$\bar{A} = \{u \mid \ u \notin A\}$$

In classical logic, the logical operators *and*, *or* and *not* are used to evaluate the truth value of different propositions. The truth tables for these logical operators are given as follows:

A	B	$A \cap B$
0	0	0
1	0	0
0	1	0
1	1	1

Table 3.1: The truth table of the logical operator AND

A	B	$A \cup B$
0	0	0
1	0	1
0	1	1
1	1	1

Table 3.2: The truth table of the logical operator OR

A	$\bar{A}$
1	0
0	1

Table 3.3: The truth table of the logical operator NOT

In the next section, we extend the operators of classical set theory to fuzzy sets operators. In Chapter 5, the operators of fuzzy sets are used in our fuzzy logic based localization algorithms to combine shortest distance information provided by the sonar sensors. This information is used to estimate the robot's location. In addition, fuzzy operators are used in the fusion process of the fuzzy location information provided by the sonar sensors and the odometers to update the current location of the robot. The shortest distance information takes into account the uncertainties in sonar readings which are modeled by possibility distributions (fuzzy sets) as shown in Chapter 4. Therefore, the shortest distance information is given

in the form of possibility distributions (fuzzy sets) and so is the estimated robot's location.

3.6 Basic Operations on Fuzzy Sets

The extension of standard operators of classical set theory such as union, intersection, and complement to the fuzzy sets operators is not unique, due to the extension of the range of membership function to the interval $[0, 1]$ instead of the restricted set of $\{0, 1\}$. The following are some examples of the these operations.

Consider the two fuzzy sets A and B defined on U:

- The union of A and B is a fuzzy set in U denoted by $A \cup B$, whose membership function is defined as:

$$\mu_{A \cup B}(u) = \max[\mu_A(u), \mu_B(u)]$$

  This is a natural extension of the crisp union operator defined on classical sets. Note that $\forall u \in A, 0 \leq \mu_A(u) \leq 1$. Similarly, $\forall u \in B, 0 \leq \mu_B(u) \leq 1$. Consequently, $0 \leq \mu_{A \cup B}(u) \leq 1$.

- The intersection of A and B is a fuzzy set $A \cap B$ in U with membership function defined as:

$$\mu_{A \cap B}(u) = \min[\mu_A(u), \mu_B(u)]$$

- The complement of A is a fuzzy set in U denoted by $\bar{A}$, whose membership function defined as

$$\mu_{\bar{A}} = 1 - \mu_A(u)$$

  These basic operations are shown in Figure 3.3.

In fuzzy logic, the linguistic operators *and*, *or* and *not* are modeled through the use of fuzzy set operators: intersection, union and complementation, respectively. Intersection, union and complementation are also interchangeably used with

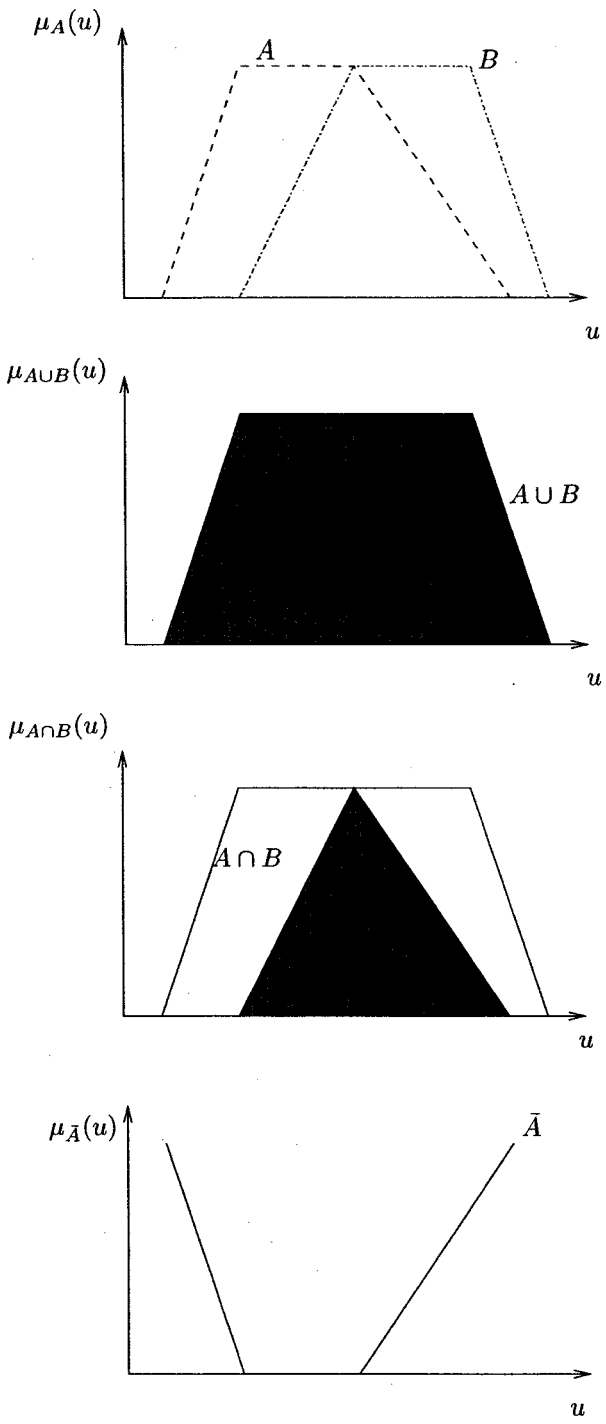

Figure 3.3: Basic operations on fuzzy sets

conjunction, disjunction and negation, respectively. These operators are used to evaluate the truth value of fuzzy set propositions such as " X is A *AND* Y is B", or "X is A *OR* Y is NOT B", where A and B are fuzzy sets.

In the classical set theory there is only one unique definition for each operation. However, there are number of possible definitions that can be chosen to implement intersection, union and complementation in fuzzy set theory. Triangular norms (t-norms) and triangular (t-conorms), developed by Schweizer and Sklar [74] in the context of statistical metric spaces, are adopted and used as fuzzy set intersection and union operators. A significant body of literature has appeared concerning the appropriate definitions for intersection and union of fuzzy sets [65, 75, 76, 77, 78, 79]. Zadeh [65] has stated that the selection of fuzzy operators depend on the situation. For example, when we take the intersection of two fuzzy sets, we may want the larger fuzzy set to have an impact on on the result. However, if we apply the intersection operator as defined above this objective will not be achieved. Complementation can also be defined using different functions. These functions are called negation functions.

In the following three subsections we introduce the definitions of negation functions, t-norms and t-conorms, respectively.

3.6.1 Negation Functions

The complement $\bar{A}$ of a fuzzy set A can be defined point-wise by a mapping n: $[0,1] \rightarrow [0,1]$ as

$$\mu_{\bar{A}}(u) = n(\mu_A(u)), \qquad \text{for all } u \in U \tag{3.1}$$

where $\bar{A}$ denotes the complement of A.

Bellman and Giertz [80] suggest the following axioms as being natural for a negation operation n:

N1. $n(0) = 1; \quad n(1) = 0;$

N2. n is strictly decreasing and continuous mapping;

N3. n is involutive, i.e., $n(n(a)) = a$ for all $a \in [0, 1]$.

Axiom N1 is obviously for recovering crisp complementation.

It is natural to expect $n(a) > n(a')$ when $a < a'$ and this is assured by N2.

Finally, the involution property N3 preserves the well-known property of complementation $\bar{\bar{A}} = A$.

Negation functions can be formally defined as follows:

Definition 1 *A function n, as defined in* (3.1)*, is called a* negation function *if it is non-increasing and satisfies axiom N1.*

Definition 2 *A negation function is called* strict *if it satisfies N2.*

Definition 3 *A strict negation function is called* strong *if it also satisfies N3.*

Examples of negations

Example 1 *The standard negation:*

$$n(a) = (1 - a).$$

Example 2 *Another strong negation, different from the standard one, is defined by Yager [81] as:*

$$n(a) = (1 - a^p)^{\frac{1}{p}} \quad p > 0.$$

Example 3 *The negation function introduced by Dubois and Prade [82] does also satisfy N1-N3.*

$$n_\lambda(a) = \frac{1 - a}{1 + \lambda a}, \qquad \lambda > -1.$$

3.6.2 Triangular Norms (t-norms)

let $t : [0,1] \times [0,1] \rightarrow [0,1]$ be a function that transforms the membership functions of fuzzy sets A and B into the membership function of the intersection of A and B, that is

$$t[\mu_A(u), \mu_B(u)] = \mu_{A \cap B}(u) \tag{3.2}$$

For the function t to be qualified as an intersection operator it must satisfy the following axioms:

t1. Boundary condition:

$$t(0,0) = 0; t(a,1) = t(1,a) = a$$

t2. Monotonicity

$$t(a,c) \leq t(b,d) \quad \text{when} \quad a \leq b, \text{ and } \quad c \leq d$$

Which means that the value of the conjunction should not decrease when the value of at least one proposition increased. We should be more willing to accept "b and d" than "a and c."

t3. Associativity

$$t(a, t(b,c)) = t(t(a,b), c)$$

This means that the order of conjunction is not important.

t4. Commutativity

$$t(a,b) = t(b,a)$$

This means that conjunction does not depend on the order of a, and b. This is expected since there is no reason to assign different truth values to $t(a,b)$, and $t(b,a)$.

3.6.3 Triangular Conorms (t-conorms, s-norms)

In the case of classical sets, intersection and union are related via complements by DeMorgan laws:

$$A \cap B = (\overline{\bar{A} \cup \bar{B}})$$

$$A \cup B = (\overline{\bar{A} \cap \bar{B}})$$

In the case of fuzzy sets DeMorgan laws are also applied to establish a relationship between conjunction and disjunction via a negation function n.

For a t-norm t, we can define its (*conjugate pair*) with respect to any strong negation n as:

$$t(a, b) = n(s(n(a), n(b))), \tag{3.3}$$

since n is involutive, this holds if and only if,

$$s(a, b) = n(t(n(a), n(b))), \tag{3.4}$$

where s is called a *t-conorm* and it is the n-dual of a t-norm t with respect to a negation function n.

t-conorm $s : [0, 1] \times [0, 1] \rightarrow [0, 1]$ is a function that transforms the membership functions of fuzzy sets A and B into the membership function of the union of A and B, that is

$$s[\mu_A(u), \mu_B(u)] = \mu_{A \cup B}(u) \tag{3.5}$$

For the function s to be qualified as a union operator it must satisfy the following axioms :

s1. Boundary condition

$$s(1, 1) = 1, s(0, a) = s(a, 0) = a$$

s2. Monotonicity

$$s(a, c) \leq s(b, d) \quad \text{when} \quad a \leq b, \text{ and } \quad c \leq d$$

Which means that the value of the disjunction should not decrease when the value of at least one proposition increased. We should be more willing to accept "b or d" than "a or c."

s3. Associativity

$$s(a, s(b, c)) = s(s(a, b), c)$$

This means that the order of disjunction is not important.

s4. Commutativity

$$s(a, b) = s(b, a)$$

This means that disjunction does not depend on the order of a and b. This is expected since there is no reason to assign different truth values to $s(a, b)$, and $s(b, a)$.

3.6.4 Fuzzy Sets Intersection and Union: Examples

There are several examples of t-norms and t-conorms. We list here the most frequently used, and important ones.

Example 4 *Zadeh [65] proposes to use:*
$t_{\min}(a, b) = \min(a, b)$, *as a conjunction. (minimum)*
$s_{\max}(a, b) = \max(a, b)$, *as a disjunction. (maximum)*

Min-max are the most popular in fuzzy literature. They are described as non-interactive operators. It means that if A is modified, it is not necessary that the results of the above operations change.

Example 5 *One pair of the probabilistic like operators is:*
$t_{prod.}(a, b) = ab$, *as a conjunction. (algebraic product)*
$s_{sum}(a, b) = a + b - ab$, *as a disjunction. (algebraic sum)*

Prod-sum operators reflect a trade-off between A and B, they are described as interactive operators, because the outcome of the combination using one of these operators depends on A as well as B, this means that any modification of A or B will change the result of these operators.

Example 6 *Bold intersection and union:*
$t_{bold}(a,b) = \max(0, a+b-1)$, *as a conjunction (bold intersection).*
$s_{bold}(a,b) = \min(1, a+b)$, *as a disjunction (bold union).*

Example 7 *Drastic product and sum:*

$$t_w(a,b) = \begin{cases} a & \text{if} \quad b = 1 \\ b & \text{if} \quad a = 1 \\ 0 & \text{otherwise} \end{cases}$$

where t_w is a conjunction operator (Drastic product).

$$s_w(a,b) = \begin{cases} a & \text{if} \quad b = 0 \\ b & \text{if} \quad a = 0 \\ 1 & \text{otherwise} \end{cases}$$

where s_w is a disjunction operator (Drastic sum).

Next, we review the possibilistic approach for modeling uncertainty.

3.7 Possibility Theory Approaches

Possibility theory is a component of "General Information Theory (GIT)". Probability and possibility are logically independent, they exist in parallel and are related within GIT in a formally analogous manner [59]: probability and possibility measures arise in Dempster-Shafer evidence theory as fuzzy measures defined on random

sets; possibility and their dual necessity measures represent extreme ranges of probability intervals; and the distributions of all these generally non-additive measures are fuzzy sets.

3.8 Two Approaches for Possibility theory

There are two approaches to possibility theory; the first one is introduced by Zadeh [83] as an extension of fuzzy set theory. The second approach is introduced by Klir and Folger [84] based on Dempster-Shafer's theory of evidence. Zadeh's approach is plausible and it deals with possibility theory as a tool for representing information. However, the second approach introduces the possibility theory in an axiomatic way.

3.8.1 Zadeh's Approach

This approach depends on the concept of fuzzy sets theory. Let x be a variable that takes values in the universe of discourse U and let A be a fuzzy set in U. The proposition " x is A" can be interpreted as putting a fuzzy restriction on x and this restriction is characterized by the membership function $\mu_A(u)$. $\mu_A(u)$ is interpreted as the degree of possibility that $x = u$. If, for example, x represents a person's height and A is the fuzzy set " tall" given that the only knowledge available is that the person is tall " x is A", but we do not know exactly his height, then $\mu_A(180(cm))$, where $180 \in \text{supp}(A)$, could be interpreted as the degree of possibility that the person's height is 180 cm. Then, the possibility distribution associated with x, denoted as Π_x, is defined in terms of the membership function of A as:

$$\Pi_x(u) = \mu_A(u)$$

3.8.2 The Axiomatic Approach

Klir and Folger [84] and Klir and Yuan [60] develop the possibility theory within the framework of Dempster-Shafer's evidence theory. Since this approach was proposed based on axiomatic basis, this enables the researchers to derive possibility distributions, that represent the uncertainty in a certain phenomenon, based on mathematical properties that are associated with the possibility theory. This approach is adopted in this thesis to represent radial imprecision and angular uncertainty in sonar readings.

Next, we review the basic theories that are used to develop possibility theory. We review fuzzy measures and evidence theory. Then, we show how possibility measures, used to construct possibility distributions, are derived based on evidence theory.

3.9 Fuzzy Measures

A fuzzy measure assigns a value to each possible crisp set to which the element in question might belong. This value indicates the degree of evidence or certainty of the element's membership in the set. This is different from the assignment of membership grades in fuzzy sets. In the later case, a value is assigned to each element in universe of discourse, signifying its degree of membership in a particular set with unsharp boundaries. Fuzzy measure theory is not of interest of this thesis, however, we need to introduce the concept of fuzzy measure theory to understand its special branches; evidence theory and possibility theory.

Definition 4 *(Fuzzy measures)*
Given a universal set Ω and the set of all its crisp subsets (power set) $\mathcal{P}(\Omega)$, a function

$$g\colon \mathcal{P}(\Omega) \rightarrow [0,1]$$

is defined such that $g(A)$ indicates the degree of certainty that an element of Ω belongs to a certain crisp set A. In order to achieve this purpose, function g must meet the following requirements:

g1. $g(\phi) = 0$ and $g(\Omega) = 1$

g2. $\forall A, B \in \mathcal{P}(\Omega)$, if $A \subseteq B$, then $g(A) \leq g(B)$

The first requirement is called boundary requirement and it says that, the empty set does not contain any element, therefore, it cannot contain the element of our interest, either. On the contrary, the universal set, contains all elements, therefore, the presence of our element in the universal set is sure. The second requirement is called the monotonicity requirement, which states that the evidence of the membership of an element is a subset of another set must be smaller or equal to the evidence that the element belongs to the big set itself. Since both $A \cap B \subseteq A$ and $A \cap B \subseteq B$ for any two sets A and B, it follows from the monotonocity requirement of fuzzy measures that the inequality:

$$g(A \cap B) \leq \min[g(A), g(B)] \tag{3.6}$$

is satisfied for any three sets A, B, $A \cap B \in \mathcal{P}$. Similarly, since both $A \subseteq A \cup B$ and $B \subseteq A \cup B$ for any two sets, the monotonocity of fuzzy measures implies that the inequality

$$g(A \cup B) \geq \max[g(A), g(B)] \tag{3.7}$$

is satisfied for any three sets A, B, $A \cup B \in \mathcal{P}$.

3.10 Evidence Theory

Evidence theory is based on two dual non additive measures: *belief* and *plausibility* measures. Given a universal set Ω, assumed here to be finite, a belief measure is a function:

$$Bel\colon \mathcal{P}(\Omega) \rightarrow [0,1]$$

such that $Bel(\phi) = 0, Bel(\Omega) = 1$ and

$$Bel(A_1 \cup A_2 \cup \ldots \cup A_n) \geq \sum_j Bel(A_j) - \sum_{j<k} Bel(A_j \cap A_k) + \ldots + (-1)^{n+1} Bel(A_1 \cap A_2 \cap \ldots \cap A_n) \tag{3.8}$$

For each $A \in \mathcal{P}(\Omega)$, $Bel(A)$ is interpreted as the degree of belief that a given element of Ω belongs to the set A.

When the sets $A_1, A_2, \ldots, A_n$, in Equation (3.8) are pair-wise disjoint, the inequality requires that the degree of belief associated with the union of the sets is not smaller than the sum of the degrees of belief pertaining to the individual sets. This basic property of belief measures is thus weaker version of additivity property of probability measures. This implies that the probability measures are special cases of belief measures for which the equality in (3.8) is always satisfied.

We can show that (3.8) implies the monotonicity requirement (**g2**) of fuzzy measures. Let $A \subseteq B$ ($A,\ B \in \mathcal{P}(\Omega)$) and let $C = B - A$. Then, $A \cup C = B$ and $A \cap C = \phi$. Applying now A and C to (3.8) for $n = 2$, we obtain

$$Bel(A \cup C) = Bel(A) \geq Bel(A) + Bel(C) - Bel(A \cap C).$$

Since $A \cap C = \phi$ and $Bel(\phi) = 0$, we have

$$Bel(B) \geq Bel(A) + Bel(C)$$

and, consequently, $Bel(B) \geq Bel(A)$.

Let $A_1 = A$ and $A_2 = \bar{A}$ in (3.8) for $n = 2$. Then, we can derive the following property of belief measures:

$$Bel(A) + Bel(\bar{A}) \leq 1 \tag{3.9}$$

Each belief measure is associated with a plausibility measure, PI, defined by:

$$PI(A) = 1 - Bel(\bar{A}) \tag{3.10}$$

for all $A \in \mathcal{P}(\Omega)$. Similarly,

$$Bel(A) = 1 - PI(\bar{A}) \tag{3.11}$$

Belief and plausibility measures are therefore mutually dual. However, plausibility measure can also be defined independent of belief measures.

A plausibility measure is a function:

$$PI\colon \mathcal{P}(\Omega) \rightarrow [0,1]$$

such that $PI(\phi) = 0$, $PI(\Omega) = 1$, and

$$PI(A_1 \cap A_2 \cap \ldots \cap A_n) \geq \sum_j PI(A_j) - \sum_{j<k} PI(A_j \cup A_k) + \ldots + (-1)^{n+1} PI(A_1 \cup A_2 \cup \ldots \cup A_n) \tag{3.12}$$

for all possible families of subsets of Ω.

Let $A_1 = A$ and $A_2 = \bar{A}$ in (3.12) for $n = 2$. Then, we can immediately derive the following fundamental property of plausibility measures:

$$PI(A) + PI(\bar{A}) \geq 1 \tag{3.13}$$

Belief and plausibility measures can conveniently be defined by a function

$$m : \mathcal{P}(\Omega) \rightarrow [0,1] \tag{3.14}$$

such that $m(\phi) = 0$ and

$$\sum_{A \in \mathcal{P}(\Omega)} m(A) = 1 \tag{3.15}$$

This function is called a basic probability assignment. For each set $A \in \mathcal{P}(\Omega)$, the value $m(A)$ express the degree to which all available and relevant evidence emphasizes the claim that a certain element of Ω belongs to set A. This value $m(A)$ associated with only one set A does not represent any additional claim regarding subsets of A. If there is some additional information strengthening the claim that

the element belongs to a subset of A, say $B \subseteq A$, it must be expressed by another value $m(B)$.

Even though there is a similarity between Equation (3.15) and the equation for probability distribution function, there is a fundamental difference between them. The latter is defined on Ω, while the former is defined on $\mathcal{P}(\Omega)$.

Basic probability assignment has the following properties:

- it is not required that $m(\Omega) = 1$;
- it is not required that $m(A) \leq m(B)$ when $A \subseteq B$; and
- no relationship between $m(A)$ and $m(\bar{A})$ is required

It follows from these properties that the basic assignments are not fuzzy measures. However, given a basic probability assignment m, a belief measure and a plausibility measure are uniquely determined for all set $A \in \mathcal{P}(\Omega)$ by the formulas :

$$Bel(A) = \sum_{B|B \subseteq A} m(B) \tag{3.16}$$

$$PI(A) = \sum_{B|B \cap A \neq \phi} m(B) \tag{3.17}$$

From Equation (3.16), $m(A)$ and $Bel(A)$ has the following meaning: $m(A)$ represents the degree of evidence or belief that an element belongs to the set A alone, and $Bel(A)$ represents the total evidence or belief that the element belongs to A as well as to the various special subsets of A. The plausibility measure $PI(A)$, as defined in (3.17), has different meaning: it represents not only the total evidence or belief that an element belongs to A or to any of its subsets, but also the additional evidence associated with sets that overlap with A. Hence,

$$PI(A) \geq Bel(A) \tag{3.18}$$

for all $A \in \mathcal{P}(\Omega)$.

Every set $A \in \mathcal{P}(\Omega)$ for which $m(A) \geq 0$ is usually called a focal element of m. Focal elements are subsets of Ω on which the available evidence focus. When Ω is finite, m can be fully characterized by a list of its focal elements A with the corresponding values $m(A)$. The pair $\langle \mathcal{F}, m \rangle$, where $\mathcal{F}$ and m denote a set of focal elements and associated basic assignment, respectively, is often called a body of evidence.

Total ignorance is expressed in terms of the basic assignment by $m(\Omega) = 1$ and $m(A) = 0$ for all $A \neq \Omega$. That is, we know that the element is in the universal set, but we have no evidence about its location in any subset of Ω. It follows from (3.16) that the expression of total ignorance in terms of the corresponding belief measure is exactly the same: $Bel(\Omega) = 1$ and $Bel(A) = 0$ for all $A \neq \Omega$. However, the expression of total ignorance in terms of the associated plausibility measure quite different: $PI(\phi) = 0$ and $PI(A) = 1$ for all $A \neq \phi$. This expression follows directly from (3.17).

3.11 Possibility and Necessity Measures

Possibility theory is a special branch of evidence theory that deals with bodies of evidence whose focal elements are nested. In this case, the plausibility measure is a *possibility* measure $Poss$ and the belief measure is a *necessity* measure Nec. A possibility measure $Poss$ is a mapping from $\mathcal{P}(\Omega)$ to $[0, 1]$.

The necessity and possibility measures have the following properties for all A, $B \in \mathcal{P}(\Omega)$:

$$Nec(A \cap B) = \min[Nec(A), Nec(B)] \tag{3.19}$$

$$Poss(A \cup B) = \max[Poss(A), Poss(B)] \tag{3.20}$$

When we compare the above two equations with the general properties (3.6)

and (3.7) of fuzzy measures, we can see that possibility theory is based on the extreme values of fuzzy measures. From this point of view, necessity and possibility measures are sometimes defined axiomatically by (3.19) and (3.20).

Since necessity measures are special belief measures and possibility measures are special plausibility measures, they satisfy equations (3.9)-(3.11) and (3.13). Hence,

$$Nec(A) + Nec(\bar{A}) \leq 1 \tag{3.21}$$

$$Poss(A) + Poss(\bar{A}) \geq 1 \tag{3.22}$$

$$Nec(A) = 1 - Poss(\bar{A}) \tag{3.23}$$

Furthermore, it follows immediately from (3.19) and (3.20)

$$\min[Nec(A), Nec(\bar{A})] = 0 \tag{3.24}$$

$$\max[Poss(A), Poss(\bar{A})] = 1 \tag{3.25}$$

The possibility measure can be built from a possibility distribution, i.e., a function Π from Ω to $[0, 1]$ such that $\sup_{\omega \in \Omega} \Pi(\omega) = 1$. More specifically we have

$$\forall A, Poss(A) = \sup_{\omega \in A} \Pi(\omega)$$

Finding a possibility distribution from the knowledge of $Poss$ can be achieved by stating

$$\Pi(\omega) = Poss(\{\omega\})$$

In this chapter the possibility measure is used to establish possibility distributions based on interval valued set statistics and their random sets. In Chapter 5, the possibility measure is used to perform fuzzy pattern matching between the

robot's fuzzy locations in an attempt to reduce the number of candidate locations into one unique location.

We are now sufficiently equipped to discuss a methodology for constructing possibility distributions from experimental data. This methodology is explained next.

3.12 Possibilistic Approach for Modeling Uncertainty in Physical Measurements

When we need possibilistic data, it is almost always preferable to collect them in a form similar to their possibilistic representation. Thus objective empirical measurement procedures are required that yield data in accordance with semantic aspects of possibility theory. The additivity of frequency data results from the specificity of observations of singleton. Therefore, we need non-specific data which are possibility non-disjoint, and thus not yielding traditional frequency distributions. This is the concept of set statistics originally advanced by Wang and Liu [85], and developed more by Dubois and Prade [86, 87]. Joslyn Cliff used interval valued set statistics, obtained from studying a certain physical phenomenon, and then their empirical random sets, to develop a method for constructing possibility distributions in the form of possibilistic histograms [88, 89, 90, 91, 64, 92].

In this thesis we use interval valued sets collected experimentally to construct possibility distributions that represent the radial imprecision and angular uncertainty of sonar readings.

3.12.1 Possibilistic Measurement

In this section we introduce some of the basic definitions that are necessary to understand the methodology of constructing possibility distributions from experimental

data.

To derive a possibility distribution from an empirical source, it is necessary to observe subsets $B_s \subseteq \Omega$. These subsets are called general measuring record as defined below:

Definition 5 *(Measuring Record)*
A general measuring record is a vector $\vec{B} := \langle B_s \rangle = \langle B_1, B_2, \ldots, B_M \rangle$, *where* s *is counter on* M, M *is the number of elements of* $\vec{B}$, $1 \leq s \leq M$, *and* B_s*'s are subsets of* Ω.

Definition 6 *(Empirical Focal Set)*
Given a general measuring record $\vec{B}$, *let* $\mathcal{F}^E := \{B_j\} = \{B_1, B_2, \ldots, B_N\}$ *be an empirical focal set derived by eliminating the duplicates from* $\vec{B}$, *where* j *is counter on* N, N *is the number of elements of* B_j, $1 \leq j \leq N$, $N \leq M$, $\forall B_j \in \mathcal{F}^E, \exists B_s \in \vec{B}, B_s = B_j$.

Definition 7 *(Set-Frequency Distribution)*
Given a general measurement record $\vec{B}$ *and empirical focal set* $\mathcal{F}^E$, $C_j := C(B_j)$ *is the number of occurrences of* B_j *in* $\vec{B}$ $\forall B_j \in \mathcal{F}^E$. *Then, a set-frequency distribution is a function* $m^E : \mathcal{F}^E \rightarrow [0, 1]$ *where:*

$$m^E(B_j) := \frac{C_j}{\sum_{B_j \in \mathcal{F}^E} C_j}, m_j^E := m^E(B_j), \tag{3.26}$$

and from (3.15) it follows that:

$$\sum_{\forall B_j \in \mathcal{F}^E} m(B_j) = 1$$

This means that the set-frequency distribution is a basic probability assignment function (Section 3.10).

Definition 8 *(Random Set)*
Given an evidence function m, $\mathcal{S} := \{\langle B_j, m_j \rangle : m_j > 0\}$ *is a finite random set where* $B_j \subseteq \Omega$ *and* $m_j := m(B_j)$

The mathematics of the random sets is more detailed, but for our purposes, and especially in the finite case, they can be seen simply as random variables taking values on subsets of Ω

Next, we show how possibilistic histograms are formed based on random sets.

3.12.2 Possibilistic Histograms

Possibility distributions derived from consistent empirical random sets can be properly described as possibilistic histograms, similar to ordinary (stochastic) histograms, but resulting from overlapping interval observations, and thus governed by the mathematics of random sets.

Definition 9 *(Possibilistic histograms)*
Assume $\mathcal{S}^E$ is consistent, then a possibilistic histogram is the possibility distribution Π determined from the plausibility assignment formula (3.17).

The possibilistic histogram can be obtained as follows:

$$\Pi(\omega) = \sum_{\omega \in B_j} m_j^E = \frac{\sum_{\omega \in B_j} C_j}{M} \tag{3.27}$$

3.12.3 The form of Possibilistic Histograms

In order to analyze the properties of possibilistic histograms it is necessary to mathematically describe their components. The following definitions show these components.

Definition 10 *(Empirical focal set components and requirements)*
Let $\Omega = \Re$, and assume a random set $\mathcal{S}^E$. Then

1. *Let each observed subset $B_j \in \mathcal{F}^E$ be closed interval denoted by its endpoints $B_j := [l_j, r_j]$*

2. *Let $l_{(j)}$ and $r_{(j)}$ be the order and "reverse order" statistics of the left and right end points, so that*

   $l_{(1)} \leq l_{(2)} \leq \ldots \leq l_{(N)}, r_{(N)} \leq r_{(N-1)} \leq \ldots \leq r_{(1)}$ *are permutation of the l_j, r_j.*

3. *Denote the vectors of endpoints and ordered endpoints as:*
   $\vec{E} := \langle l_1, l_2, \ldots, l_N, r_1, r_2, \ldots, r_N \rangle$, $\vec{E}^l := \langle l_1, l_2, \ldots, l_N \rangle$, $\vec{E}^r := \langle r_1, r_2, \ldots, r_N \rangle$, $\hat{E} := \langle l_{(1)}, l_{(2)}, \ldots, l_{(N)}, r_{(N)}, r_{(N-1)}, \ldots, r_{(1)} \rangle$, *where $\vec{E}$ is the vector of endpoints, $\vec{E}^l$ is the left endpoints vector, $\vec{E}^r$ is the right endpoints vector, and $\hat{E}$ is the ordered endpoints vector.*

4. *consistency requirement: if $\mathcal{F}^E$ is consistent then*

   - $\max_j l_j = l_{(N)} \leq r_{(N)} = \min_j r_j$, *so that $C(\Pi) = [l_{(N)}, r_{(N)}]$, where l_j is the j^{th} element of E^l, r_j is the j^{th} element of E^r, and $C(\Pi)$ is the core of the poossibility distribution.*
   - *the joint linear order on $\hat{E}$ is $l_{(1)} \leq l_{(2)} \leq \ldots \leq l_{(N)} \leq r_{(N)} \leq r_{(N-1)} \leq \ldots \leq r_{(1)}$.*

Definition 11 *(Possibilistic histogram components)*
The following are the components of a possibilistic histogram:

- *$E := \{e_k\}$, $E^l := \{e^l_{k^l}\}$, $E^r := \{e^r_{k^r}\}$ are the sets of endpoints with duplicates omitted from $\vec{E}$, $\vec{E}^l$ and $\vec{E}^r$, respectively, where $\forall e_k \in \vec{E}$, $\forall e^r_{k^r} \in \vec{E}^r$, $\forall e^l_{k^l} \in \vec{E}^l$, $1 \leq k \leq Q := |E|$, $1 \leq k^l \leq Q^l := |E^l|$, $Q^r := |E^r| \geq k^r \geq 1$, so that $E = E^l \cup E^r$ and $Q^l + Q^r = Q$, where $\vec{E}$ is the endpoints vector, Q is the number of elements in E, Q^l is the number of elements in E^l, Q^r is the number of elements in E^r, k is counter on E to Q, k^r is the counter on E^r to Q^r, and k^l is the counter on E^l to Q^l.*

- $$G_k := \begin{cases} [e_k,\ e_{k+1}) & e_k,\ e_{k+1} \in E^l \\ [e_k,\ e_{k+1}] & e_k \in E^l,\ e_{k+1} \in E^r \\ (e_k,\ e_{k+1}] & e_k,\ e_{k+1} \in E^r. \end{cases}$$

  where $1 \leq k \leq Q-1$. *This is shown in Figure 4.9.*

- $$T_k := \{\langle x, y\rangle \in \Re \times [0,1] : x \in G_k, y = \Pi(x)\}$$

  where $1 \leq k \leq Q-1$, *where* $\Pi(x) = \sum_{x \in B_j} m^E(B_j)$, *and* $m^E(B_j)$ *is defined in Equation (3.26).*

Definition 12 *(Possibilistic histogram form)*
If Π *is a possibilistic histogram, then*

1. $core(\Pi)=[e^l_{Q^l},\ e^r_{Q^r}]$, *is the core of the possibility distribution.*
2. $supp(\Pi)=[e^l_1,e^r_1]=\cup_{k=1}^{Q-1}G_k$, *is the support of the possibility distribution.*
3. $\Pi([\ -\infty,\ e^l_1))=\Pi((e^r_1,\ \infty\ ])=0$. *This identifies the elements that do not belong to the support of the possibility distribution.*

The candidate points that can be used to construct possibility histograms are introduced next.

3.12.4 Candidate Points

Definition 13 *(Possibilistic histogram candidate points)*
Assume a possibilistic histogram considered as a set of points

$$\Pi := \{T_k\} = \{\langle e_k, \Pi(e_k)\rangle\} \subseteq \Re \times [0,1],$$

then the following points are the candidate points for a possibilistic histogram:

- *The left and right endpoints of each of the T_k, $1 \leq k \leq Q-1$:*

$$t_k^l := \begin{cases} \langle\ e_k,\ \Pi(e_k)\ \rangle, & e_k \in E^l \\ \langle\ e_k,\ \Pi(e_{k+1})\rangle, & e_k \in E^r. \end{cases}$$

$$t_k^r := \begin{cases} \langle\ e_{k+1},\ \Pi(e_k)\ \rangle, & e_k \in E^l \\ \langle\ e_{k+1},\ \Pi(e_{k+1})\rangle, & e_k \in E^r. \end{cases}$$

- *The midpoint of each of the T_k, $1 \leq k \leq Q-1$:*

$$h_k = \langle \frac{e_k + e_{k+1}}{2}, \Pi(e_k) \rangle$$

- *The midpoint of the core:*

$$c := h_{Q^l} = \left\langle \frac{l_{(N)} + r_{(N)}}{2}, 1 \right\rangle$$

- *The endpoints of the support on the axis:*
  $s_1 := t_1^l = \left\langle l_{(1)}, 0 \right\rangle, \quad s_2 := t_{Q-1}^r = \left\langle r_{(1)}, 0 \right\rangle.$

Next, we show how to construct a possibility distribution based on the points of its associated possibility histogram.

3.12.5 Continuous Approximation

A possibility distribution is represented by a continuous curve that passes through a selected set of the associated histogram candidate points. One of the most significant differences between possibilistic and stochastic histograms is that the former are collections of the intervals T_k, not discrete points. Therefore, normal interpolation or approximation methods (such as curve-fitting or maximum-likelihood estimation) are not appropriate. Instead, a representative set of points from the intervals T_k should be selected and a continuous curve is fitted to them. This curve represents the possibility distribution.

The points that can be selected for continuous approximation are:

1. The set of all the interval mid- and end-points to which a continuous curve may be fit:
   $K' := \{t_k^l, t_k^r, h_k\}$

2. The set of all the interval mid- and end-points to which a continuous curve actually will be fit:
   $K \subseteq K'$. K may be any selected subset from K' such that it doesn't contain two points have the same x but differ in Π.

3. The set of all these optional interval mid- and end-points to which the curve will be fit: $D := \{c, s_1, s_2\} \cup K \subseteq \Pi$ where K may be any subset of K'. Note that $K = \phi$ is allowed.

Once a set of points is selected, a variety of curve-fitting methods are available to determine Π. The simplest and most direct is to connect them with line segments, producing a piecewise linear, continuous distribution. An advantage of the line-segment method is that the approximated Π has the same form as the fuzzy sets.

3.12.6 A Numerical Example

Consider that we obtained experimentally the two intervals $B_1 = [x_1, x_2]$ and $B_2 = [x_3, x_4]$. Each interval is observed once. This means that $m(B_1) = 0.5$ and $m(B_2) = 0.5$. The components of the histograms constructed based on these intervals are shown in Figure 3.4(top). Note that $N = M = 2$ and $Q = 3$. The set of all the interval mid- and end-points to which a continuous curve may be fit is:

$$K' = \{h_1, t_1^r, t_2^l, t_3^l, h_3, t_3^r\}$$

Note that t_1^l and t_3^r are excluded from due to the conflict with s_1 and s_2.

The set of all the optional interval mid- and end-points to which the curve will be fit is:

$$D := \{c, s_1, s_2\} \cup K \subseteq \Pi$$

For continuous approximation, any subset $K \subseteq K'$ can be chosen as long as it does not contain either set of conflicts $\{t_1^r, t_2^l\}$ or $\{t_2^r, t_3^l\}$. The following are three possible candidates for K:

$$\{h_1, t_2^l, t_2^r, h_3\}, \{t_1^r, t_3^l\}, \phi$$

Based on these candidates, D has the following possiblities: $D_1 = \{c, s_1, s_2\} \cup \{h_1, t_2^l, t_2^r, h_3\}$, $D_2 = \{c, s_1, s_2\} \cup \{t_1^r, t_3^l\}$ and $D_3 = \{c, s_1, s_2\} \cup \phi$.

The three possibility distributions associated with these sets are shown in Figure 3.4(bottom).

3.13 Fuzzy Sets and Possibility Distributions

With respect to their representation, fuzzy sets and possibility distributions have the same mathematical description. Therefore, fuzzy sets operations can be transferred to possibility distributions without changes.

Using the above mentioned method for constructing possibility distributions from experimental data, possibility distributions that represent the radial imprecision and angular uncertainty in sonar readings are constructed in the next chapter.

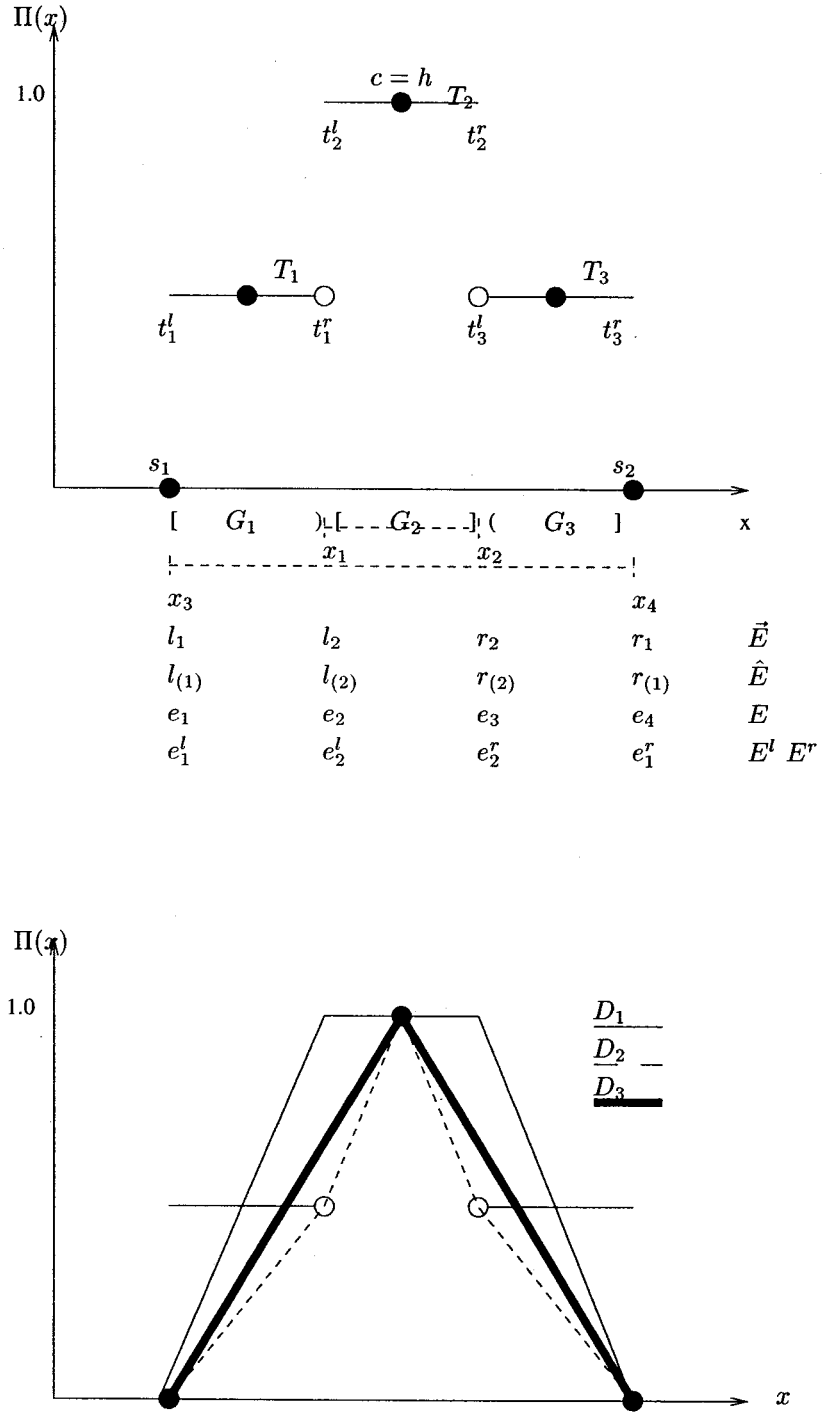

Figure 3.4: A simple possibilistic histogram with its candidate points (top). Three examples of piecewise linear continuous approximation (bottom)

Chapter 4

Modeling Uncertainty in Sonar Readings and Identifying the Objects in the Environment

4.1 Introduction

Our proposed localization algorithms are designed for mobile robots that are equipped with a ring of sonar sensors. The robot relies on its sonar sensors to identify objects in its environment and use the objects' location to localize itself.

In this chapter, our objective is to model the angular and radial uncertainty of sonar readings reflected from a wall and a 90^o corner by using possibility distributions. The obtained models are used to identify the objects in the robot's environment by estimating their position and orientation with respect to the robot. Then, the robot can use the identified objects to localize itself.

To model the angular and radial uncertainty of sonar readings, it is important to study their behavior when they are reflected from a wall and a 90^o corner, two common components of any indoor environment. In this chapter, a set of experiments is carried out to study this behavior. Then, the results of these experiments

are used to construct the possibility distributions that represent the angular and radial uncertainty in one sonar sensor. This is achieved using the method introduced in Chapter 3. Since we are dealing with a ring of sonar sensors, adjacent sensors that provide close readings are considered to be detecting the same object. In this chapter it is shown how this information is used to avoid false reflections and obtain reduced uncertainty models of sonar readings and how the shortest reading among the adjacent readings is used to estimate the position and orientation of the detected objects based on the reduced models.

4.2 The Nomad 200

The Nomad 200 (Figure 4.1) is a mobile robot produced by Nomadic Technologies Incorporation. The robot consists of two main parts: the base and turret. The base has three wheels that translate together (controlled by one motor) and rotate together (controlled by a second motor). The base has a third motor to rotate the turret. The robot has a zero-gyro radius, i.e., the robot can rotate around its center. The turret contains most of the sensing systems and the on-board computer. The Nomad 200 has four main sensing systems: the Sensus 100 Tactile System, the Sensus 200 Sonar Ranging System (Figure 4.2), the Sensus 300 Infrared Proximity System and the Sensus 400 Basic Vision System. The Sensus 100 consists of 20 pressure switches. This system is used to alarm the robot of contact with objects. The Sensus 200 consists of a ring of 16 sonar sensors mounted onto the robot's turret. The angle between any two adjacent sensors is 22.5^o. The sensors used in the Sensus 200 are standard Polaroid sensors controlled by the Polaroid 6500 board. The Sensus 300 consists of 16 infrared sensors. These sensors are used to detect objects within 60 cm of the robot. The distance to an object is estimated by the intensity of the light sent by the emitter and reflected to the detector from the object. The Sensus 400 system consists of a camera and a software interface library.

The camera is a Sony XC-75, a 450×512 black and white CCD camera. The Sensus 400 system is used for vision based applications.

The Nomad 200 has an on-board computer for sensor and motor control, and for host computer communication. It also has a complete software package for the host computer with a graphic interface and a robot simulator.

In this thesis, the Nomad 200 is used to implement our proposed fuzzy logic based localization algorithms (Chapter 6). In addition, we use the Sensus 200 system in our experiments to study the behavior of sonar readings when they are reflected from walls and corners. The results of these experiments are used to construct the possibility distributions that represent the angular and radial uncertainty in the sonar readings as shown next.

4.3 Experimental Setup

Our experimental setup consists of the Nomad 200 and a host computer connected through wireless Ethernet. The robot is placed in front of a dry-wall at distance d and at an initial direction perpendicular to the wall, i.e., $\gamma = 0$. A command is issued from the computer to the robot to fire only the sensor that is at $\gamma = 0$. After the sensor detects the echo received from the wall, the reading that represents the distance to the wall is sent directly to the computer through the Ethernet. This reading represents the measured distance to the wall. The direction of the robot is increased in a 1^o step by commanding the turret of the robot to rotate counter-clockwise one step as shown in Figure 4.3(top). The sensor is then fired and the measured distance and the direction γ are registered. This procedure is continued until no readings are received from the wall. The direction γ is then decreased in 1^o step by rotating the turret clockwise; the measured distances and direction are registered until no echo is received. This experiment is then repeated at different distances; $d = 50$, 75, 100, 125, 150, 175, 200, 225, 250, 275, 300, 325, 350, and 375

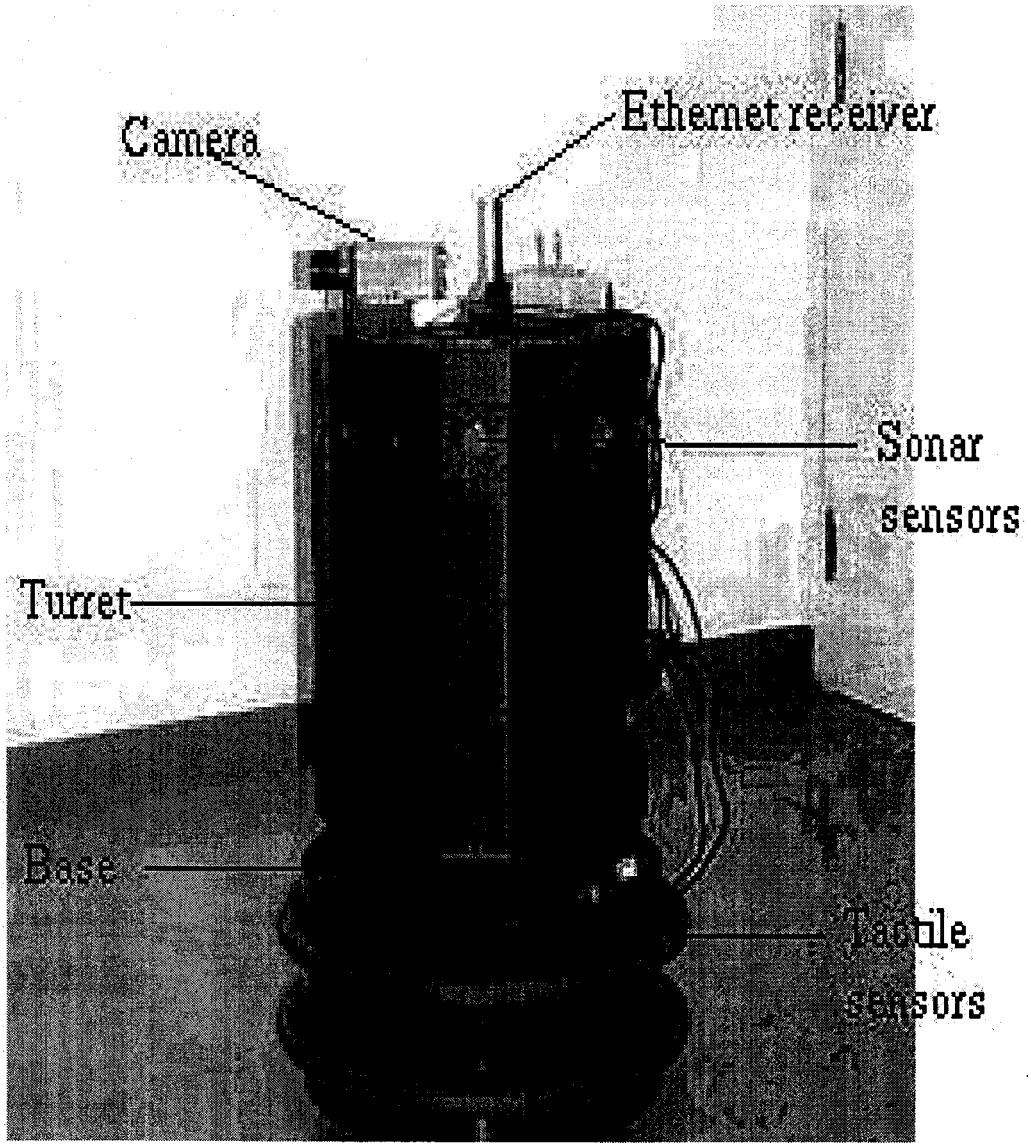

Figure 4.1: The Nomad 200.

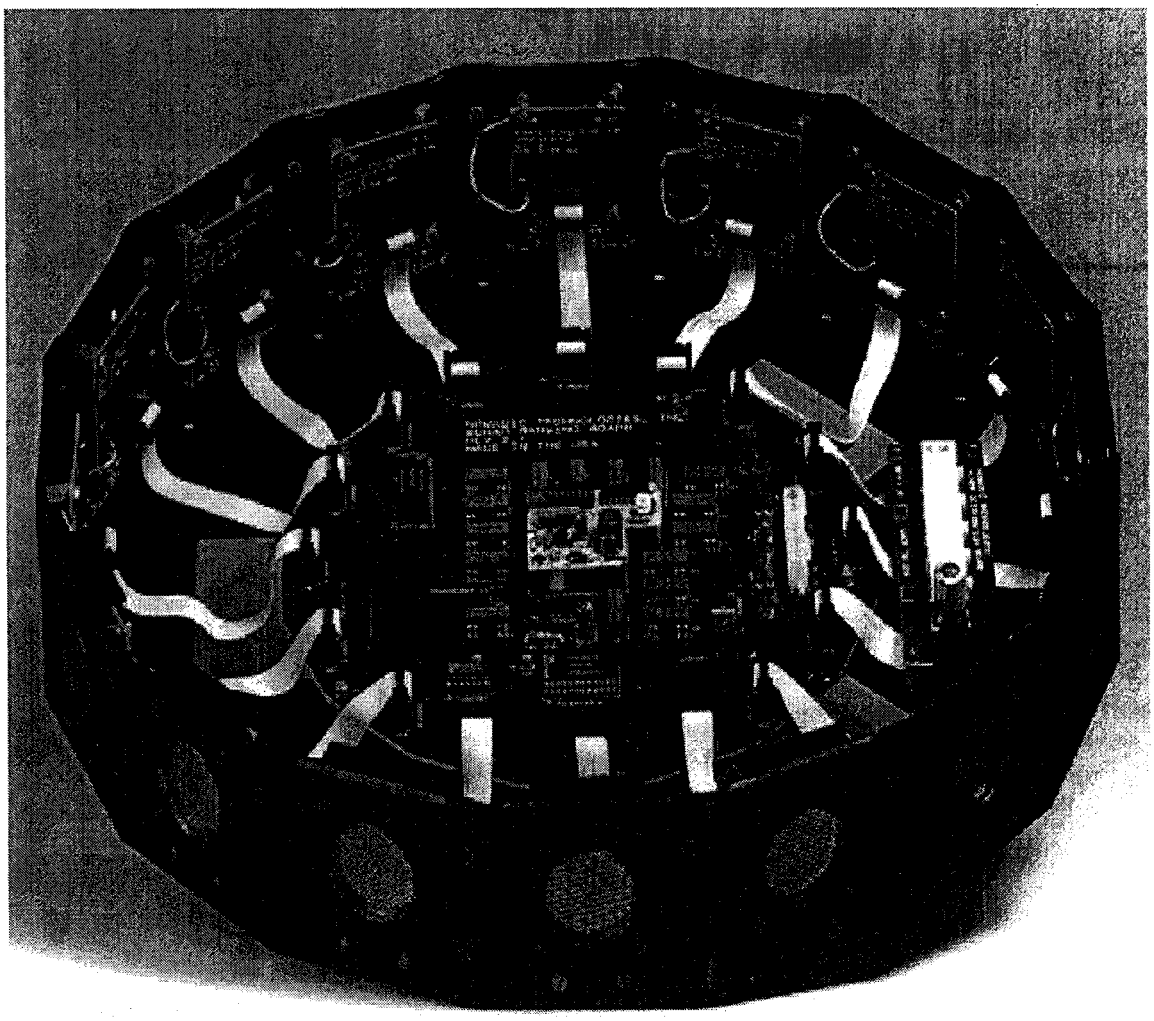

Figure 4.2: The Sensus 200 sonar ranging system.

cm. A similar set of experiments is done while the sensor is facing a 90^o corner as shown in Figure 4.3(bottom).

Radial imprecision is defined as the actual distance minus the measured one (the reading from the sensor). For the wall case, the radial imprecision can be calculated as follows:

$$e = r - OB = r - \frac{OA}{\cos(\gamma)} \tag{4.1}$$

where, OB is the actual distance between the sensor and the wall as shown in Figure 4.4, and r is the distance detected by the sensor.

For the corner case, the radial imprecision is calculated based on Figure 4.5 as:

$$e = X_{sonar} - X \ = X_{sonar} - \frac{d}{\cos(45 - \gamma)\sqrt{(2)}} \tag{4.2}$$

Tables A.1 and A.2 show an example of the experimental results for a wall when d is approximately 50 cm with different values of γ. These data are represented in the polar coordinates as shown in Figure 4.6. Tables A.3 and A.4 show an example of the experimental results for a corner when d is approximately 100 cm with different values of γ. These data are represented in the polar coordinates as shown in Figure 4.7.

The most significant issue for representing the angular uncertainty in sonar sensors is the *field of view* of these sensors when the readings of these sensors are reflected from walls and corners. The *field of view* can be defined as the interval of angles which contains the sensor direction when an object is detected.

Next, the experimental data are used to model the angular and radial uncertainty of sonar readings based on possibility theory.

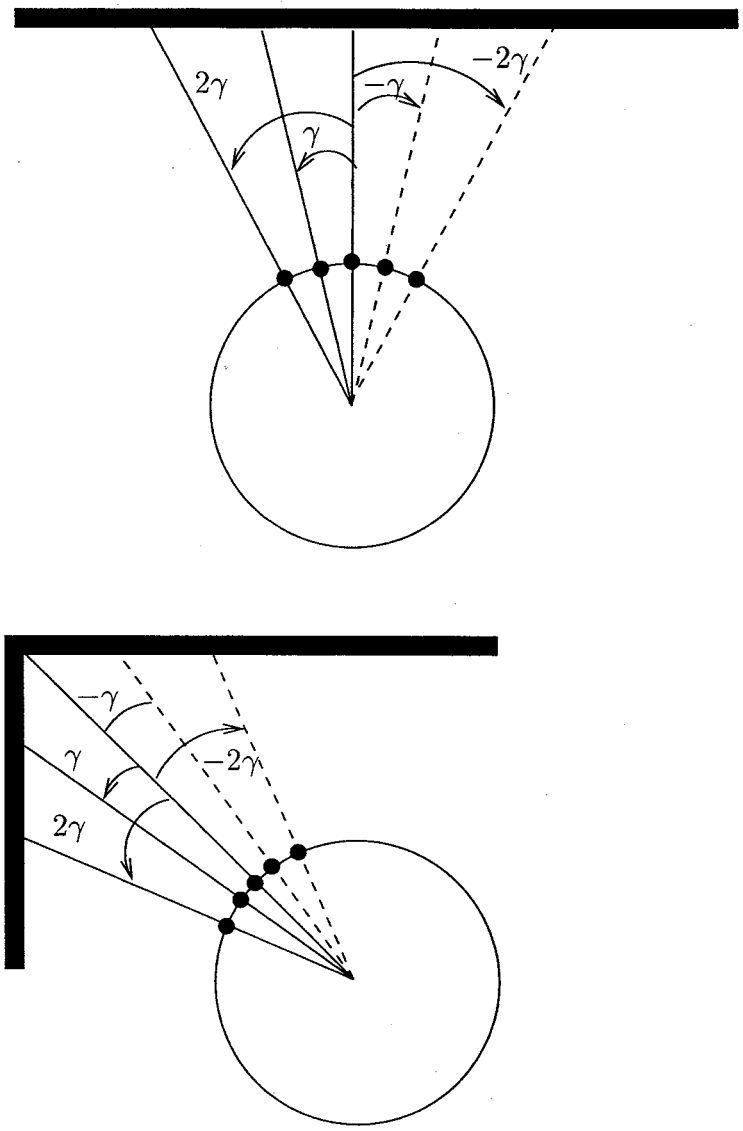

Figure 4.3: Experiments for studying the behavior of the sonar sensor when it is in front of a wall (top) and a corner (bottom).

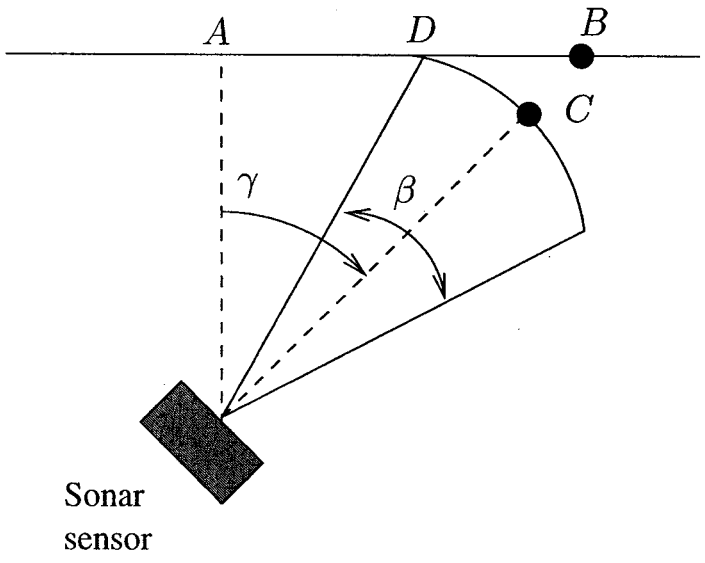

Figure 4.4: Error calculation for a sonar reading coming from a wall at a certain distance d and incidence angle γ.

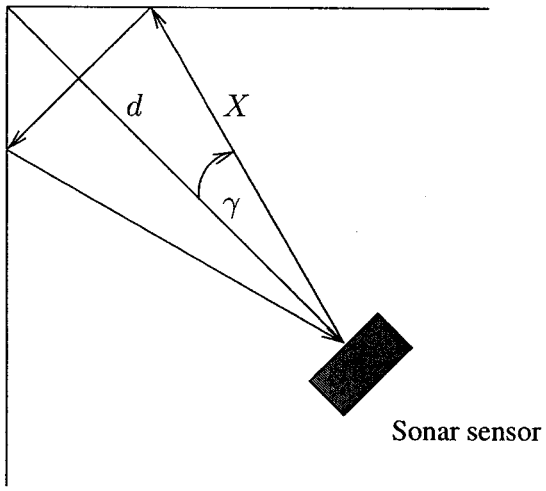

Figure 4.5: Error calculation for a sonar reading coming from a corner at a certain distance d and incidence angle γ.

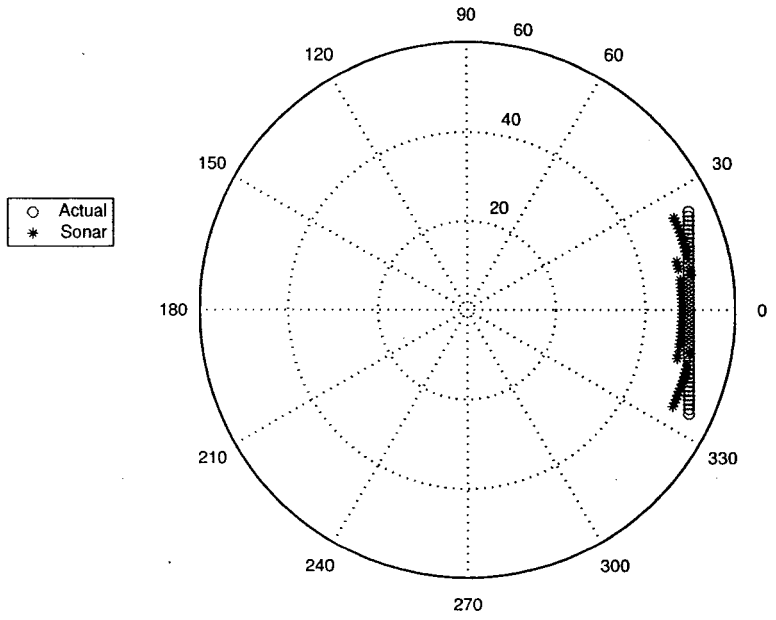

Figure 4.6: Polar coordinates for actual and sonar measured distances at different angles from a wall.

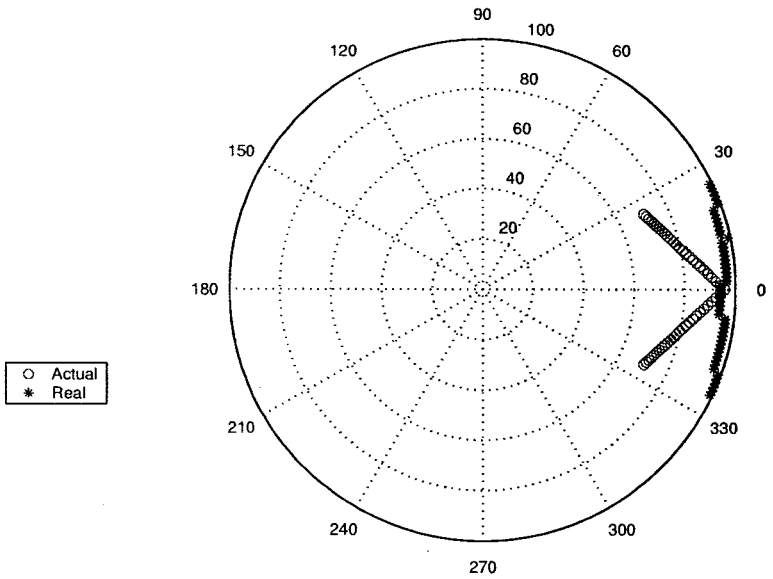

Figure 4.7: Polar coordinates for actual and sonar measured distances at different angles from a corner.

4.4 Modeling Angular and Radial Uncertainty of Sonar Readings Reflected From a Wall

In this section, the angular and radial uncertainties of sonar sensors are represented by possibility distributions. According to the empirical results presented in Tables A.1 and A.2, we observe that when the sensor is approximately 50 cm away from a dry-wall surface, the incidence angle has a range of $[-25^o,25^o]$ and the distance readings has the radial imprecision interval[1] [−5,0] cm in the direction of the sonar sensor. In the case of the corner, as Tables A.3 and A.4 show, the radial imprecision interval is [0, 28] cm when the sensor is approximately 100 cm from the corner.

The radial imprecision intervals of the sonar sensor used in the experiments can be considered random sets obtained from an empirical source (Section 3.12). The possibility distributions that represent the radial uncertainty for the readings obtained from a dry-wall and a corner can then be constructed.

The following steps show how to use the method introduced in Section 3.12 to establish the radial uncertainty models for the readings obtained from a wall. The method is applied to the data shown in Table 4.1 which represents the radial imprecision intervals of the sonar readings obtained at different distances from a wall.

Distance from a wall (cm)	Radial Imprecision (cm)
50	[-5,0]
75	[-5, 1]
100	[-8,1]

Table 4.1: Radial imprecision intervals when the sensor is at different values of d from a wall.

- Measuring record

[1]See Section 3.1.3 for the difference between imprecision and uncertainty.

The general record is represented by the vector $\vec{B} := \Big\langle [-5,0],[-5,1],[-8,1] \Big\rangle$, where the number of elements is $M = 3$.

- Empirical focal set

  The empirical focal set is derived by eliminating the duplicates from $\vec{B}$. Since there are no duplicates in $\vec{B}$, the empirical focal set for our example is given by: $\mathcal{F}$:={ [-5, 0], [-5, 1] , [-8,1]}. The number of elements in this empirical focal set is $N = 3$.

- Set-Frequency distribution

  Using Equation (3.26) obtains the set frequency distribution as follows: $m(B_1 = [-5,0]) = 1/3$, $m(B_2 = [-5,1]) = 1/3$ and $m(B_3 = [-8,1]) = 1/3$.

- Random set

  The random set obtained based on the values of m_j and B_J is:

$$\mathcal{S} := \{\langle [-5,0], 1/3\rangle, \langle [-5,1], 1/3\rangle, \langle [-8,1], 1/3\rangle\}$$

  .

- Empirical focal set components and requirements

  Let $\Omega = \Re$, and assume a random set $\mathcal{S}^E$ as shown above, then:

  1. The order and reverse order statistics of the left and right endpoints are: $-8 \leq -5 \leq -5$, $0 \leq 1 \leq 1$.
  2. The vectors of endpoints and ordered endpoints are: $\vec{E} := \langle -8,-5,-5,0,1\rangle$, $\vec{E}^l := \langle -8,-5,-5\rangle$, $\vec{E}^r := \langle 0,1,1\rangle$, and $\hat{E} := \langle -8,-5,-5,0,1\rangle$.
  3. Consistency requirement: If $\mathcal{F}^E$ is consistent then:

     $\star$ $\max_j l_j = l_{(N)} \leq r_{(N)} = \min_j r_j$, so that $C(\pi) = [l_{(N)}, r_{(N)}]$. Which in this case $l_{(N)} = -5$, and $r_{(N)} = 0$. The core of the possibility distribution is [-5, 0].

$\star$ The joint linear order on $\hat{E}$ is $-8 \leq -5 \leq 0 \leq 1$.

The two requirements are met which mean that $\mathcal{F}^E$ is consistent.

- Possibilistic histogram components

  The components of the possibilistic histogram are shown graphically in Figure 4.9 and are given as follows:

  1. The sets of endpoints with duplicates omitted from $\vec{E}, \vec{E}^l, \vec{E}^r$ are: $E := \{-8, -5, 0, 1\}$, $E^l = \{-8, -5\}$, $E^r = \{0, 1\}$, where $\vec{E}$ is the endpoints vector. Note that $1 \leq k \leq Q = 4$, and $1 \leq k^l \leq Q^l = 2$, $1 \leq k^r \leq Q^r = 2$.
  2. $G_k = \{[-8, -5), [-5, 0], (0, 1]\}$, where $1 \leq k \leq 3$.
  3. $T_k := \{\langle -8, 1/3\rangle, \langle -5, 1\rangle, \langle -1, 2/3\rangle\}$, where $1 \leq k \leq 3$.

- Possibilistic histogram form

  If Π [2] is a possibilistic histogram, then:

  1. The core of the possibility distribution is $\mathbf{C}(\Pi)$= [-5, 0].
  2. The support of the possibility distribution is $\mathbf{U}(\Pi)$=[-8,1].
  3. $\Pi([-\infty, -8))=\Pi((1, \infty])=0$.

- Possibilistic histogram candidate points

  Assume a possibilistic histogram considered as a set of points:

  $$\pi := \{\langle e_k, \pi(e_k)\rangle\} \subseteq \Re \times [0, 1]$$

  then the possibilistic histogram candidate points are:

  $\star$ The left and right endpoints of each of the T_k are:

  $t_k^l :=$ { ⟨ -8, 1/3 ⟩, ⟨ -5, 1 ⟩ } $t_k^r :=$ { ⟨ 0, 1 ⟩, ⟨ 1, 2/3 ⟩ }

[2] We assign the same symbol for both the possibility distribution and its associated possibilistic histogram. This is due to the fact that the former is obtained by a continuous approximate between the points of the latter.

⋆ The midpoint of the core: $c := \langle -2.5, 1 \rangle$

⋆ The endpoints of the support on the axis:
$s_1 := \langle -8, 0 \rangle$, $s_2 := \langle 1, 0 \rangle$

⋆ The midpoints of each of the T_k are:
h_k : { ⟨ -3.5,1/3 ⟩, ⟨ -2.5, 1 ⟩, ⟨ 0.5, 2/3 ⟩ }

- Continuous approximation

  To obtain the possibility distribution, a continuous curve may be fitted to the following points:

  1. The set of all interval mid and endpoints to which a continuous curve may fit:
     $K' := \{-5, 0, -6.5, -2.5, 0.5\}$
  2. The set of all interval mid and endpoints to which a continuous curve actually will fit: $K = \{-5, -2.5, 0\}$.
  3. The set of all of these optional interval mid and endpoints to which the curve will fit $D := \{-2.5, -8, 1\} \cup \{-5, -2.5, 0\}$.

In Figure 4.9, the possibility distribution of the radial uncertainty of the sonar sensor facing a wall is presented. The information that can be obtained from this distribution is that when the distance reading obtained from the sonar sensor is about 50 cm then there is a possibility of 1 that the error in this reading belongs to the interval $[-5, 1]cm$. Moreover, there is a varying possibility of the error in the sonar reading belonging to the intervals $[-8, -5]$ and $[0, 1]$. This possibility distribution of the radial uncertainty is valid for any incidence angle where the sonar sensor detects a wall.

It is found experimentally that the sonar sensor can give readings when its incidence angle belongs to the interval $[-25^o, 25^o]$. This means that if one sonar

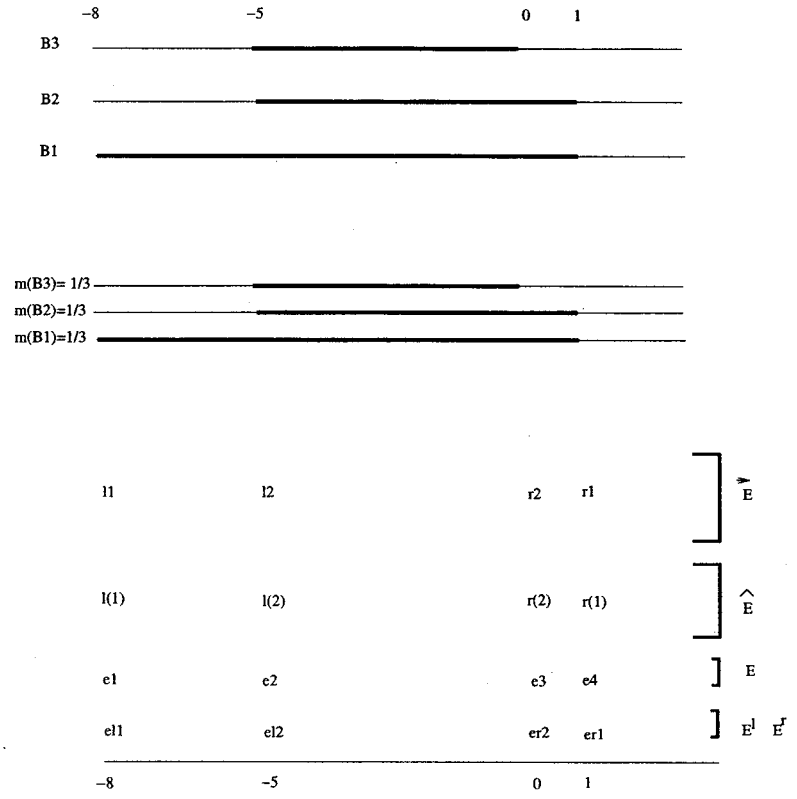

Figure 4.8: A measurement record (top), focal set (middle), and components of possibilistic histogram (bottom).

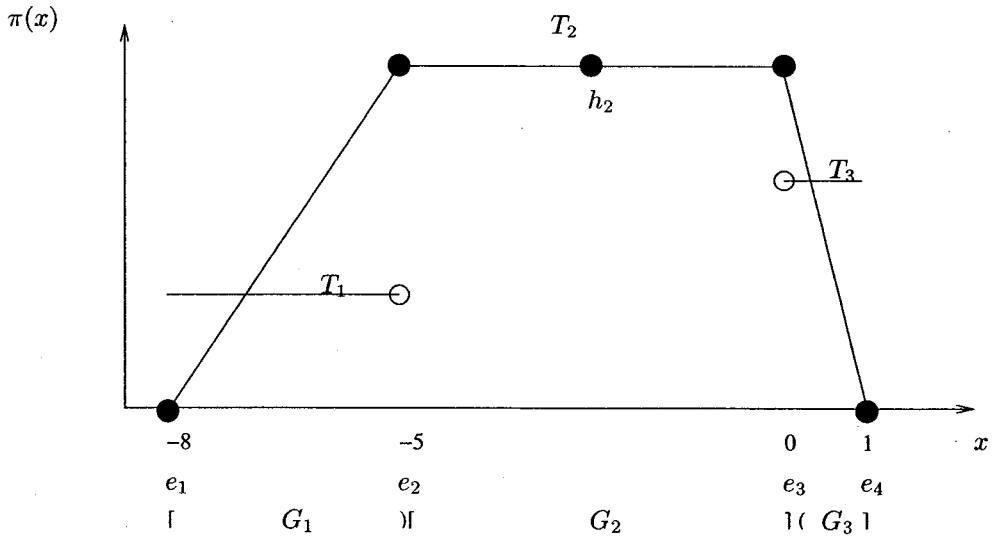

Figure 4.9: Possibility distribution for the radial uncertainty of sonar readings when the sensor is at distances between 50 cm and 100 cm.

sensor detects an object when the incidence angle of the sensor is γ, then the direction of the object with respect to the sensor belongs to the interval $[\gamma - 25^o, \gamma + 25^o]$. Similar observations are made in the case of corners. Thus, the angular uncertainty of the sonar sensor is high when it is facing a wall or a corner.

In the next section, the angular and radial uncertainty in sonar readings obtained from a wall are reduced based on the new information.

4.5 Reduction of Angular and Radial Uncertainty in The Wall Case

One sensor reading is not reliable to be used in localization because of two main reasons. The first reason is due to the fact that this reading may be a false reflection, the second is that one sonar sensor has a high angular and radial uncertainty as discussed in the previous section. To overcome false reflections, we combine range information obtained from adjacent sonar sensors. The readings obtained from any set of adjacent sensors are considered to be reflected from the same object if these readings are within a predefined tolerance [36, 26, 29, 28]. When adjacent sonar readings are combined, the fields of view of their associated sonar sensors overlap. The shared part of their fields of view is used to construct the reduced angular uncertainty model. This results in the reduction of radial uncertainty models since it depends on angular uncertainty. For example, if two sonar sensors are detecting the same wall, the readings coming from the two sensors may vary in their values, but not too much according to the direction of each sensor. As remarked by Demirli and Türkşen [28, 29], the shortest reading is the one that comes from the sensor with the smallest incidence angle from the surface normal of the wall. This piece of information is used to reduce the angular and radial uncertainty in sonar sensors. In other words, the lack of information in the beginning (Section 3.1.1) prevented the reduction of the angular and radial uncertainty. Now, we can obtain new possibility

distributions based on this reduction as shown next.

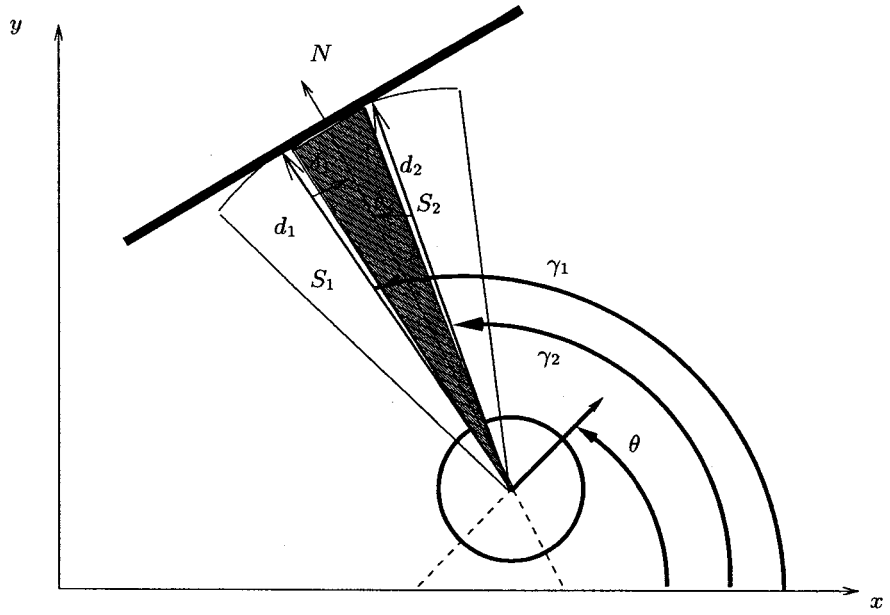

Figure 4.10: Two sonar sensors detecting the same wall.

Consider the case where we have two readings from two sensors as shown in Figure 4.10, denoted (d_1, γ_1) and (d_2, γ_2) where d_1 is the reading obtained from first sensor, d_2 is the reading obtained from the second sensor, γ_1 is the orientation of sensor one with respect to the robot's coordinate system, and γ_2 is the orientation of sensor two with respect to the robot's coordinate system. Furthermore, δ_1 and δ_2 denote the angle between the first sensor and the surface normal, and the second sensor and the surface normal, respectively. Then, from a field of view of an interval of [-25, 25], the following three cases can be identified and studied [93]:

1. Case I: $\delta_1 = 25^o$ and $\delta_2 = 2.5^o$

   In this case d_1 is on the left boundary of the field of view and it is shown in Figure 4.11 (top). Due to the fact that the angle between the two sensors is 22.5^o, $\gamma_2 = 2.5^o$. Since $S2$ has a smaller incidence angle, d_2 is expected to be the minimum distance reading between the two, i.e., $d_2 < d_1$, and the

incidence angle $\gamma = \gamma_2 - 2.5^o$.

2. Case II: $\delta_1 = 11.25^o$ and $\delta_2 = -11.25^o$

   In this case $d_1 = d_2$ and the incidence angle is $\gamma = \gamma_1 - 11.25^o$ or $\gamma = \gamma_2 + 11.25^o$. This is shown in Figure 4.11 (middle).

3. Case III: $\delta_2 = -25^o$ and $\delta_1 = -2.5^o$

   This case is shown in Figure 4.11 (bottom). The shortest distance is d_1, i.e., $d_1 < d_2$, and the incidence angle is $\gamma = \gamma_1 + 2.5^o$.

Based on this analysis, we have the following possibilities for the incidence angle:

- When $d_1 < d_2$, from cases 2 and 3:

  $\Pi_{\Gamma|d}(\gamma) = 0.0, \forall\gamma \in [\gamma_1 + 2.5, \infty) \cup (-\infty, \gamma_1 - 25]$; $\Pi_{\Gamma|d}(\gamma) = 1.0, \forall\gamma \in [\gamma_1 + 2.5, \gamma_1 - 11.5])$; and $\Pi_{\Gamma|d}(\gamma)$, $\forall\gamma \in]\gamma_1 - 25, \gamma - 11.5[$ is obtained by continuous approximation (Section 3.12) as shown in Figure 4.12 (top), where $\Pi_{\Gamma|d}(\gamma)$ is the angular uncertainty for γ.

- When $d_2 < d_1$, from cases 1 and 2:

  $\Pi_{\Gamma|d}(\gamma) = 1.0, \forall\gamma \in [\gamma_2 - 2.5, \gamma_2 + 11.5]$; and $\Pi_{\Gamma|d}(\gamma) = 0.0, \forall\gamma \in [\gamma_2 + 25, \infty) \cup (-\infty, \gamma_2 - 2.5]$, and $\Pi_{\Gamma|d}(\gamma)$, $\forall\gamma \in]\gamma_2 + 11.5, \gamma_2 + 25[$, is obtained by continuous approximation as shown in Figure 4.12 (middle).

- When $d_1 = d_2$:

  $\Pi_{\Gamma|d}(\gamma) = 0.0, \forall\gamma \in [\gamma_1 + 2.5, \infty) \cup (-\infty, \gamma_1 - 25]$; $\Pi_{\Gamma|d}(\gamma) = 1.0$, for $\gamma = \gamma_1 - 11.25$; and $\Pi_{\Gamma|d}(\gamma)$, $\forall\gamma \in]\gamma_1 - 11.5, \gamma_1 - 25[\cup]\gamma_1 - 11.5, \gamma_1 + 2.5[$, is obtained by continuous approximation as shown in Figure 4.12 (bottom) or

  $\Pi_{\Gamma|d}(\gamma) = 0.0, \forall\gamma \in (-\infty, \gamma_2 - 2.5] \cup [\gamma_2 + 25, \infty)$; $\Pi_{\Gamma|d}(\gamma) = 1.0$, for $\gamma = \gamma_2 + 11.5$; and $\Pi_{\Gamma|d}(\gamma)$, $\forall\gamma \in]\gamma_2 + 11.5, \gamma_2 + 25[\cup]\gamma_2 - 2.5, \gamma_2 + 11.5[$, is obtained by continuous approximation as shown in Figure 4.12 (bottom).

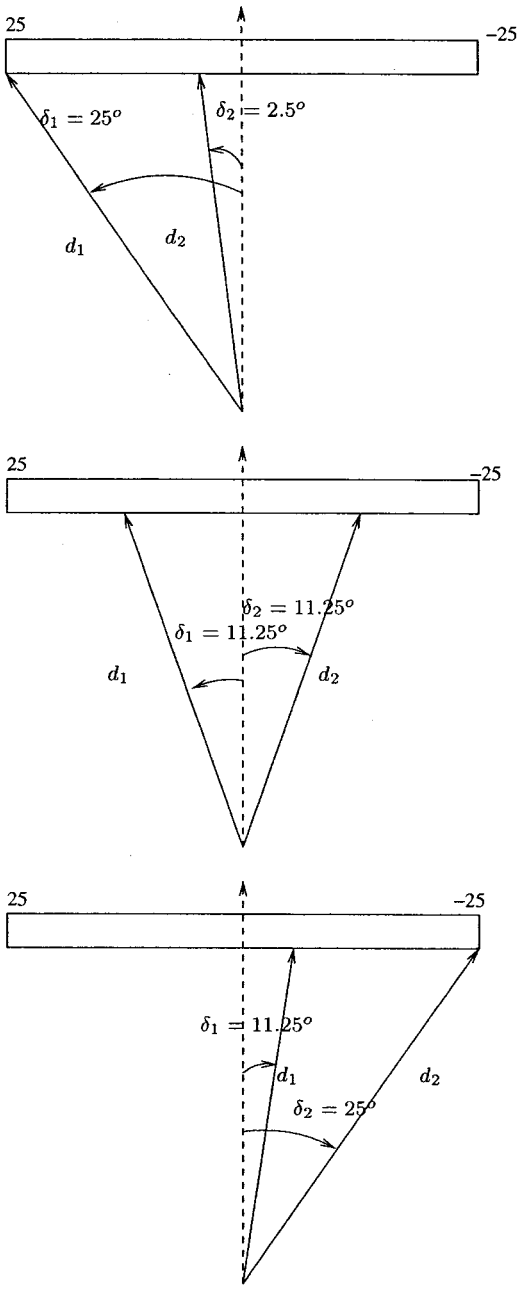

Figure 4.11: Three possible cases for the readings obtained from two sensors.

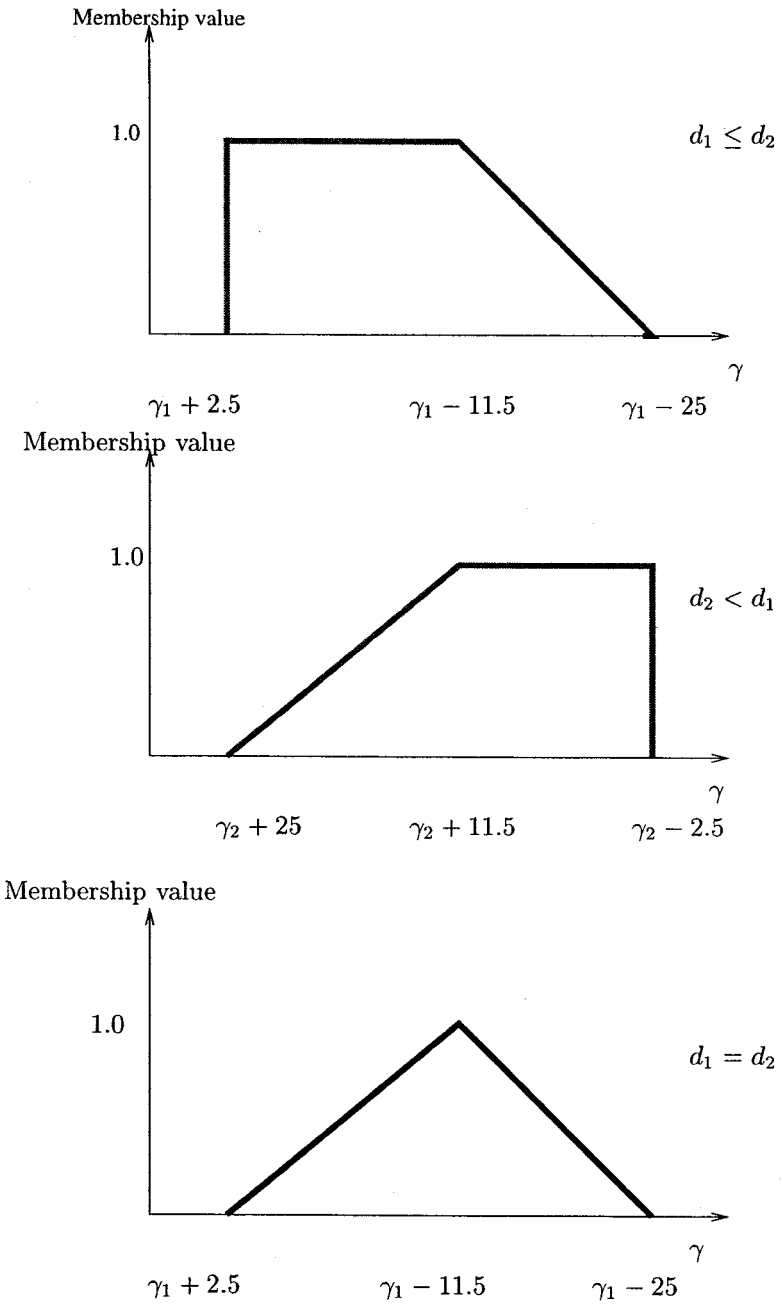

Figure 4.12: Reduced angular uncertainty for readings coming from a wall, $d_1 < d_2$ (top), $d_2 < d_1$ (middle), and $d_1 = d_2$ (bottom).

From these possibility values of the incidence angle, three possibility distributions are obtained and shown in Figure 4.12. These possibility distributions are considered to be the reduced models of angular uncertainty in sonar readings coming from a wall.

If we consider the case of three sensors (Figure 4.13) detecting the same wall, the angular uncertainty will be dramatically reduced. For example if we have (d_1, d_2, d_3) coming from the same wall where $d_2 < d_3$ and $d_2 < d_1$, then we will have the shortest reading from d_2 and therefore the angular uncertainty is given as :

$$\Pi_{\Gamma|d_2} = [\gamma_2 - 2.5, \gamma_2 + 2.5]$$

This uncertainty model indicates that the sensor incidence angle belongs to the interval $]-2.5^o, 2.5^o[$ with a possibility of 1.0.

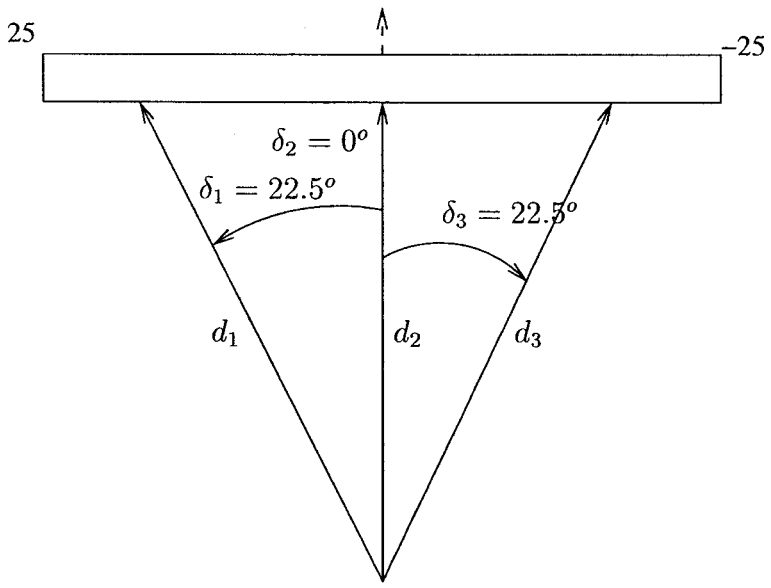

Figure 4.13: Three sensors detecting the same wall.

There are three questions to be answered at this point:

1. How can one decide which angular uncertainty model to select?

2. How can one use the selected angular uncertainty model to obtain the associated radial uncertainty model?

3. How can one use both angular and radial uncertainty models for identifying the detected objects, i.e., estimating their position and orientation with respect to the sensor?

To answer the first question, one can compare the magnitude of the reading obtained from the first sensor (d_1) and the reading obtained from the second sensor (d_2) to decide which angular uncertainty model to use from Figure 4.12. For example, if $d_1 < d_2$, the model shown in Figure 4.12 (top) is selected.

To answer the second question, for the selected angular uncertainty model we must first obtain a model for the radial uncertainty, $\Pi_{d|\gamma}$, at all angles belonging to the support of the selected angular uncertainty model, i.e.:

$$\Pi_{\Gamma|d} = \sum \pi_i/\epsilon_i, \quad \forall\gamma \in \text{ supp } \Pi_{\Gamma|d}$$

where $\Pi_{\Gamma|d}$ is the selected angular uncertainty model, ϵ_i is the radial uncertainty value and π_i is its possibility. To obtain $\Pi_{d|\gamma}$, we need to obtain the radial imprecision intervals associated with each incidence angle γ from our empirical results at each distance d. Then, we can obtain the possibility distribution that represents the radial uncertainty model at each incidence angle by following the same procedure for constructing possibility distributions from interval data as explained in Section 3.12.

Next, the radial uncertainty model $\Pi_{d|\gamma}$, is obtained by using the distance reading d as:

$$\Pi_{d|\gamma} = \sum \pi_i/(d + \epsilon_i)$$

However, the obtained possibility distribution for each γ does not take into account the reliability of this incidence angle, i.e., its possibility. Therefore, any

angle belonging to the support of the angular uncertainty model is considered a source of information with reliability equal to the possibility value of this incidence angle. By considering the reliability of the source (the possibility of the incidence angle) the possibility distribution of the radial uncertainty associated with each incidence angle is changed, as proposed by D. Dubois and H. Prade [94] as follows:

$$\Pi'_{d|\gamma} = \sum \pi'_i/(d + \epsilon_i) \tag{4.3}$$

where $\pi'_i = \min(\pi_i, \Pi_{\Gamma|d}(\gamma))$ and $\Pi_{\Gamma|d}(\gamma)$ is the reliability of the incidence angle γ (its possibility). Then $\Pi'_{d|\gamma}$ is the possibility distribution of the radial uncertainty after taking into account the reliability of the incidence angle.

For example, if we have a case where $d_1 < d_2$, the angular uncertainty model which is shown in Figure 4.12 (top) is selected. The next step is to construct the radial uncertainty model for each angle belonging to $[-11.5^o, 2.5^o]$. First, obtain the radial imprecision intervals for each incidence angle at each distance d from our empirical results obtained in Section 4.3.

For instance, with incidence angles of -11.5^o and 2.5^o if d_1 is approximately 50 cm, according to Tables A.1 and A.2, the incidence angle of $2.5^o \in [-3^o, 3^o]$ and the associated radial imprecision interval is [−1,0]. On the other hand, if the incidence angle is $-11.5^o \in [-12^o, 12^o]$, its associated radial imprecision interval is [−2, 0].

Tables 4.2 and 4.3 are obtained from the experimental data for different values of d at incidence angles 2.5^o and -11.5^o, respectively. By following the same procedure in Section 3.12 to build possibility distributions from interval data, the possibility distributions for radial uncertainty at 2.5^o and -11.5^o can be obtained as demonstrated in Figures 4.14 and 4.15, respectively. Note that the reliability of the incidence angles 2.5^o, and -11.5^o is one, and therefore no change will take place in their possibility distributions according to Equation (4.3). This is valid for the angles belonging to the interval [-11.5^o,2.5^o].

By combining information from adjacent sensors, the angular uncertainty in sonar readings is reduced from $[-25^o, 25^o]$ to $[2.5^o, -25^o]$ when two adjacent sensors

detect the same object, and from $[-25^o, 25^o]$ to $[-2.5^o, 2.5^o]$ with three adjacent sensors.

Finally, the last question is answered in Section 4.7 of this chapter.

Distance from a wall (cm)	Radial imprecision (cm)
50	[-1, 0]
75	[-1, 1]
100	[-1, 1]

Table 4.2: The reduced radial imprecision intervals when the incidence angle is 2.5^o for different values of d from a wall.

Distance from a wall (cm)	Radial imprecision (cm)
50	[-2,0]
75	[-2,0]
100	[-3,0]

Table 4.3: The reduced radial imprecision intervals when the incidence angle is -11.5^o for different values of d from a wall.

If one sonar sensor receives an echo and the other does not, no reduction in the angular and radial uncertainty is possible. In this case the possibility distributions obtained in the previous section represent the models for the angular and radial uncertainty of the reading obtained by this sensor.

4.6 Modeling Angular and Radial Uncertainty for Sonar Readings Reflected From a Corner

Following the same procedure used for the wall, we find that the field of view of the corner is the same as that of the wall, i.e., $[-25^o, 25^o]$. In Tables A.3 and A.4, the radial imprecision intervals of sonar data obtained from a corner at different incidence angles is obtained by using Equation (4.2). The reduced angular uncertainty

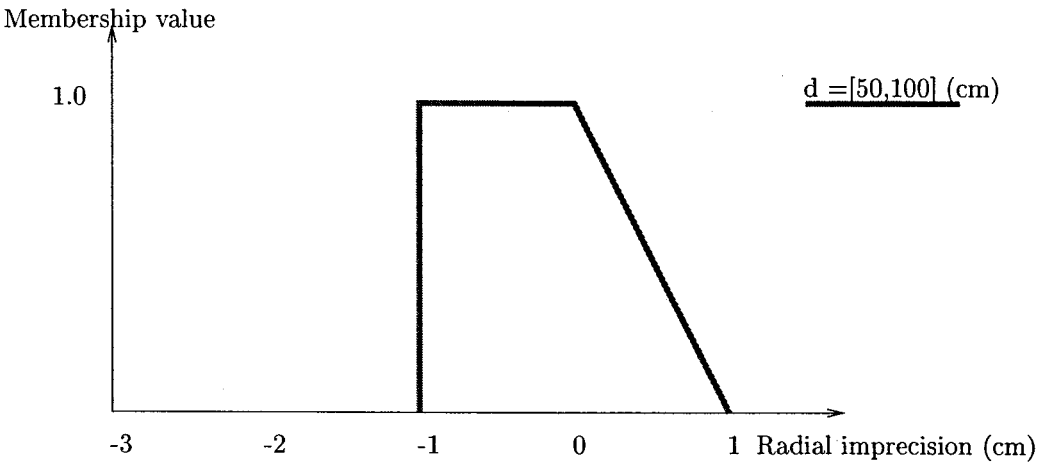

Figure 4.14: Reduced radial uncertainty model when the incidence angle is 2.5^o for different values of d from a wall.

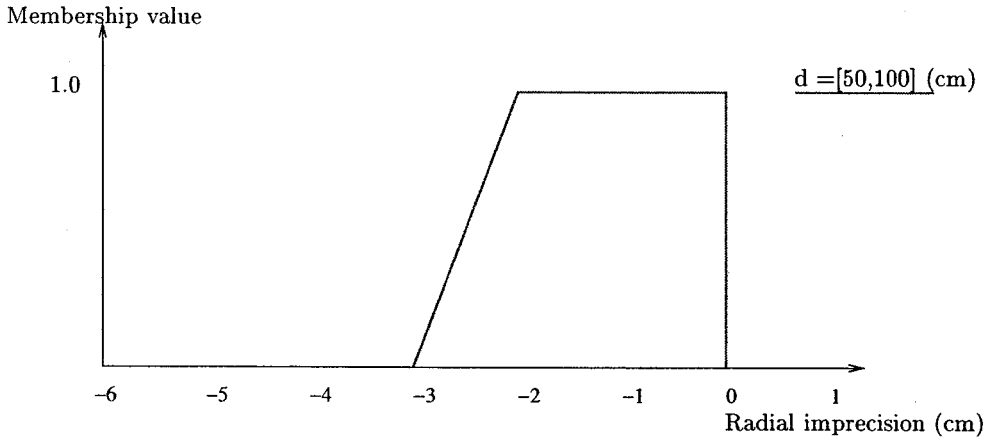

Figure 4.15: Reduced radial uncertainty model when the incidence angle is -11.5^o for different values of d from a wall.

models are similar to those obtained for the wall as shown in Figure 4.12.

Tables 4.4, 4.5 and 4.6 are constructed in a similar way to Tables 4.1, 4.2, and 4.3. These tables are used to obtain the radial uncertainty models and then the reduced radial uncertainty models when the sensor is facing a 90^o corner at different distances. These models are shown in Figures 4.16, 4.17 and 4.18.

Distance from a wall (cm)	Radial imprecision (cm)
100	[-2, 28]
125	[-1, 37]
150	[-1, 43]

Table 4.4: Radial imprecision intervals when the sensor is at different values of d from a corner.

Distance from a wall (cm)	Radial imprecision (cm)
100	[-2, 4]
125	[-2, 4]
150	[-1, 7]

Table 4.5: The reduced radial imprecision intervals when the incidence angle is 2.5^o for different values of d from a corner.

Distance from a wall (cm)	Radial imprecision (cm)
100	[-2, 19]
125	[0, 24]
150	[-1, 26]

Table 4.6: The reduced radial imprecision intervals when the incidence angle is -11.5^o for different values of d from a corner.

Next, we show how the uncertainty models of the sonar readings are used to identify the detected objects.

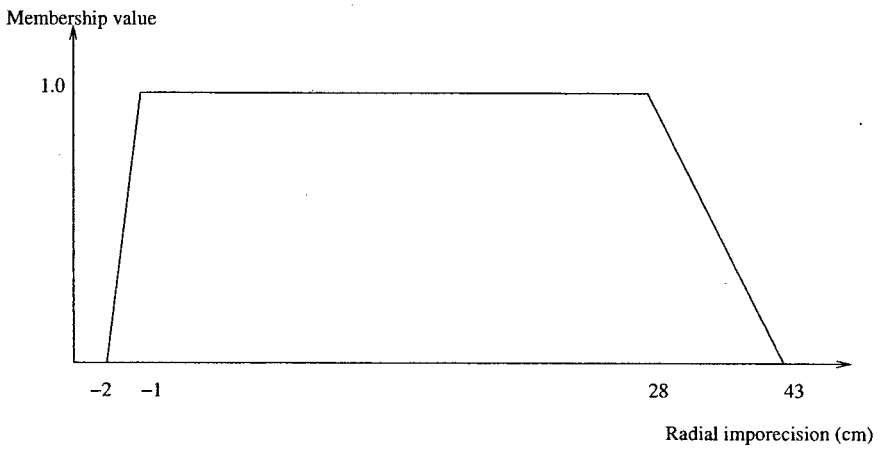

Figure 4.16: Radial uncertainty model when the sonar sensor is at different values of d from a corner.

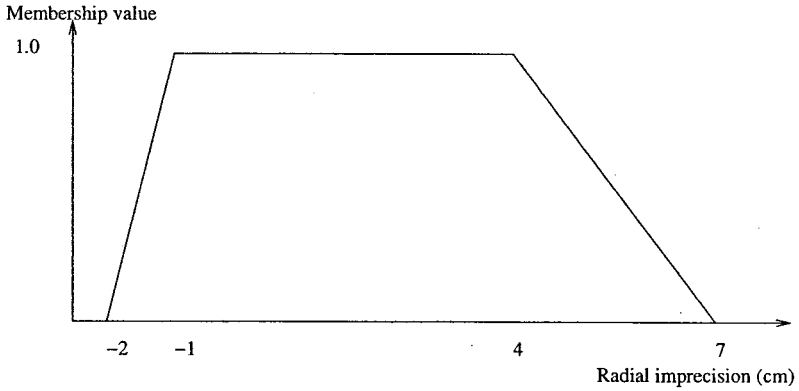

Figure 4.17: The reduced radial uncertainty model when the incidence angle is 2.5^o for different values of d from a corner.

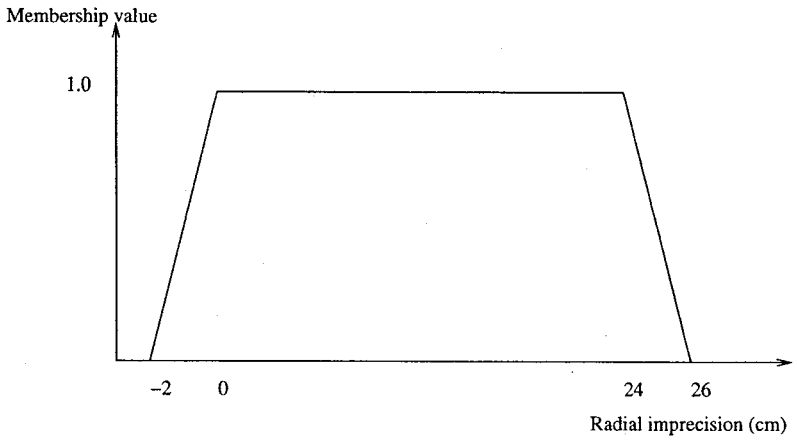

Figure 4.18: The reduced radial uncertainty model when the incidence angle is -11.5^o for different values of d from a corner.

4.7 Identifying The Objects in The Robot's Environment

Most existing mobile robots have many sonar sensors distributed on a ring around the robot (known as a ring configuration). If there is a set of consecutive sonar sensors giving close readings, i.e., the difference between these readings is less than a threshold determined experimentally, then this signifies that these sensors detect the same object in the environment. This object may be a corner or a wall. Since mobile robots, as mentioned earlier, have a ring of these sensors, then another set of the sensors may also give close readings and indicate that they detect another object. Given the orientation of sonar sensors with respect to the robot's coordinate system, and also given the map of the environment, it is possible to recognize which sensors are facing walls and which are facing corners if the angle between the two sets of sensors is approximately 45^o. Then, from this information one can select the appropriate uncertainty models to obtain the position and orientation of these objects with respect to the robot as shown next.

4.7.1 Orientation of The Detected Objects

The orientation of the detected object is obtained based on the angular uncertainty models which are selected based on the sonar readings reflected from the object. These models are shown in Figure 4.12. For example, if we have two sensors detecting the same object and the relation between their readings is $d_1 < d_2$, then the orientation of the detected object can be estimated based on Figure 4.12 (top). This figure shows that there is a possibility of one that the orientation of the detected object belongs to the interval $[\gamma - 11.25^o, \gamma + 2.5^o]$. Moreover, the orientation of the detected object belongs to the interval $]\gamma - 11.25^o, \gamma - 25^o[$ with a possibility value of less than one. Similarly, if we have three sensors detecting the same object when $d_2 < d_1$ and $d_2 < d_3$, then the orientation of the detected object belongs to the interval $[\gamma - 2.5^o, \gamma + 2.5^o]$.

4.7.2 Shortest Distance to The Detected Object

Our objective is to identify the shortest distance between the sensors and the detected object, i.e., the position of the detected object with respect to the sensor. One can use the reduced angular and radial uncertainty models obtained in the previous section to do this. Consider the case in Figure 4.10. When $d_1 < d_2$, we select the angular uncertainty model, $\Pi_{\Gamma|d_1}$, shown in Figure 4.12 (top). In addition, a radial uncertainty model $\Pi_{d_1|\gamma}$ for each angle γ belonging to the support of angular uncertainty model is obtained. The shortest distance between the sensor and the object can then be calculated as:

$$\Pi_{sd_1} = \bigcap_{\gamma \in supp\Pi_{\Gamma|d_1}} \Pi_{d_1 \cos\gamma}, \tag{4.4}$$

where:

$$\Pi_{d_1 \cos\gamma} = \sum_{r \in supp\Pi_{d_1|\gamma}} \pi_r/(r\cos(\gamma))$$

Equation (4.4) means that we rotate the radial uncertainty model for each angle in the support of the angular uncertainty model $\Pi_{d_1|\gamma}$ by its corresponding angle γ. For each angle, the obtained possibility distribution is represented by $\Pi_{d_1 \cos\gamma}$. We then combine the obtained possibility distributions conjunctively to get the shortest distance Π_{sd_1}. However, for simplicity, this rotation operation is performed only at the two limits of the core of the $\Pi_{\Gamma|d_1}$, as is shown in Figure 4.19. As a result, we obtain two possibility distributions that represent the two extreme shortest distances between the sensor and the wall. These distributions are combined to obtain one possibility distribution that represents the shortest distance between the sensor and the wall.

The above mentioned possibility distributions are combined by using the method of aggregation of information from different parallel sources as proposed by Dubois and Prade [94]. In this method, uncertain information from different sources can be combined by using a combination operator. However, there is no unique operator to perform the combination operation. The selection of this operator depends on the reliability and agreement of the sources. Since the shortest distance to an object is obtained by considering the two extreme points of the core, we can consider them to be coming from reliable sources with the same weight of 1.0. Therefore, the reliability factor is not relevant for selecting our fusion operator. Generally there are two types of fusion operators; the conjunctive operator is used when the sources agree (Section 3.6.2), and the disjunctive operator is used when the sources conflict (Section 3.6.3). The information from these two possibility distributions always agree. Therefore, we use the conjunctive operator (minimum)[3] to obtain the possibility distribution that represents the shortest distance between the sensor and the wall.

This also applicable for corners as demonstrated in Figure 4.20.

The fuzzy logic based localization algorithms are proposed in the next chapter. These algorithms rely on the angular and radial uncertainty models in estimating

[3]Any t-norm function that has the properties introduced in Section 3.6.2 can be used as well.

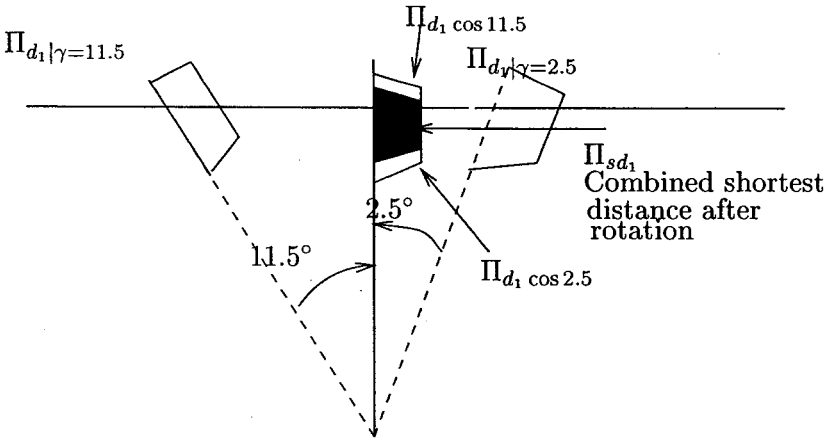

Figure 4.19: Conjunctive fusion of two pieces of information to obtain the shortest distance to a wall.

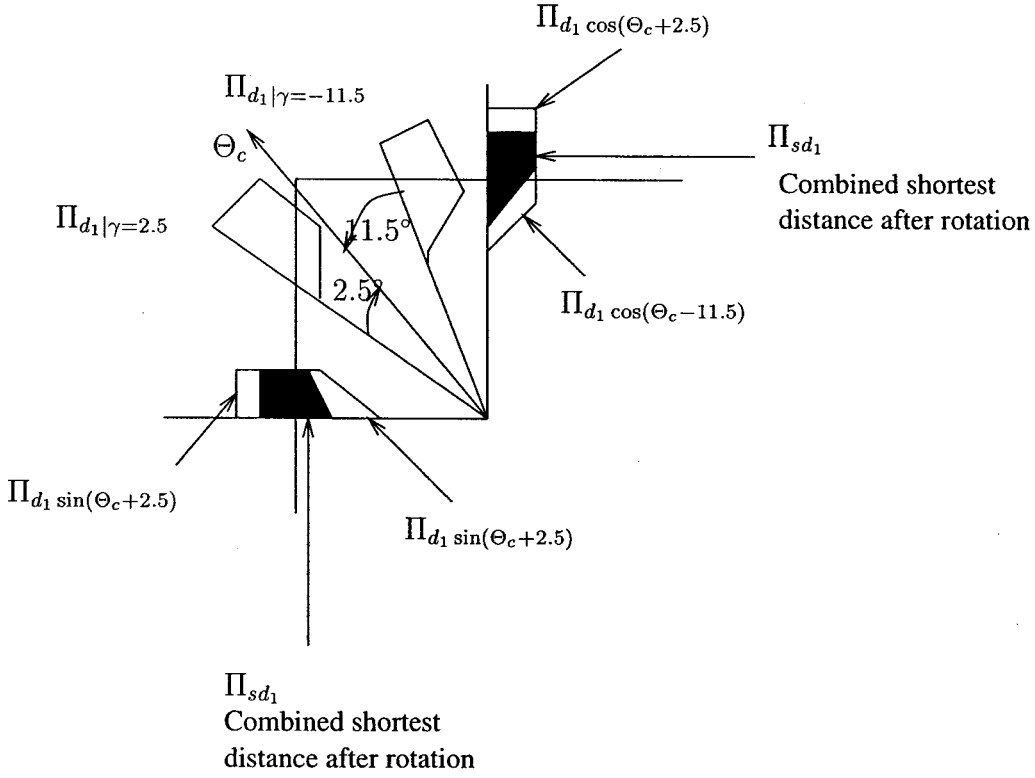

Figure 4.20: Conjunctive fusion of two pieces of information to obtain the shortest distance to a corner.

the location of the robot based on the odometers and the sonar sensors.

Chapter 5

Fuzzy Logic Based Localization

5.1 Introduction

In this chapter we propose three fuzzy logic based dynamic algorithms for mobile robots equipped with a ring of sonar sensors. The first algorithm is a global localization algorithm which is used to solve the global localization problem of mobile robots. The second algorithm is a location updating algorithm which is used to update the robot's current location while navigating its environment. The third algorithm is a map updating algorithm which is used to update the robot's map by extracting line segments from the sonar readings and adding them to the robot's map. The map updating algorithm requires that the current location used to extract the line segments is reliable. This is achieved by using the location updating algorithm concurrently with the map updating algorithm.

Mobile robot localization describes the task of driving a mobile robot to a known location in the robot's environment coordinates system. It inherently requires the process of location estimation in which a hypothesis for the robot's location is obtained from the interpretation of the readings obtained by the robot's sensors.

In the area of mobile robotics there are two well known localization problems; global localization, and concurrent localization and map updating. The objective

of the global localization algorithms is to initialize the robot's location given that no hypothesis is available. Due to the ambiguities of the data provided by the robot's sensors, global localization might require the integration of the sensors data collected while the robot is navigating its environment. Concurrent localization and map updating describe the process of updating both the robot's location and environment at each step along the robot's path by using the current sensory data and the previously available knowledge about the robot's environment.

5.2 Global Localization Problem

This section proposes a global localization algorithm to solve the global localization problem of mobile robots. The proposed algorithm depends on a collection of sonar readings obtained by the robot's sensor at each sonar scan. A sonar scan consists of the sonar readings at each localization cycle. The localization cycle consists of sensing, matching, and location estimation. In our approach, a fuzzy local composite map is constructed from sonar data and matched to the given global map of the environment to identify the robot's location. As a result of this matching process, either a unique fuzzy location or multiple candidate fuzzy locations are obtained. To reduce the multiple candidate locations, the robot moves to a new location and a new local fuzzy composite map is constructed. This results in a new set of candidate fuzzy locations. By considering the robot's movement, a set of hypothesized locations is identified from the old set of candidate locations. The hypothesized locations are matched with the new candidate locations and the candidates with a low degree of match are eliminated. The process continues until a unique location is obtained. The matching process is performed by using the fuzzy pattern matching technique. The proposed method is implemented on a Nomad 200 robot and the results are reported in Chapter 6.

Next, the global localization problem is formulated.

5.2.1 Formulation of The Global Localization Problem

Formulation of the global localization problem is solved like a matching problem in which the fuzzy local composite map, $\mathcal{M}^i$, obtained by the robot's sensors from the robot's working environment, is matched to the given global map $\mathcal{G}$ where i represents a sequential index ($i = 1$ in the beginning). Solving this matching problem consists of generating a set of fuzzy candidate location(s) $\mathcal{L}_k^i$, $k \in \{1 \ldots n\}$, where k is the index for the fuzzy candidate locations and n is the number of the fuzzy candidate locations. Each candidate location is obtained by identifying a correlation between the fuzzy local composite map and the global map. If there is only one correlation, then there is only one possible place in the robot's environment where the robot could have obtained this fuzzy local composite map, i.e., the robot has one unique location ($k = 1$). However, if there is more than one correlation, then there are different places in the environment where the robot could have obtained the same fuzzy local composite map, i.e., the robot has more than one candidate location in the environment ($k > 1$). In the latter case, the robot must move to obtain a new local fuzzy composite map, i.e., $i = i + 1$. This means that a new set of fuzzy candidate locations $\mathcal{L}_k^i$, where $k \in \{1 \ldots m\}$, is obtained based on the detection of new objects in the robot's environment. This assumes that the robot's odometers provide reliable location information when traveling short distances. By taking into account the distance traveled by the robot(obtained by the robot's odometers) the hypothesized set $\mathcal{L}_k^{(i-1)h}$ is formed from the first set of fuzzy candidate locations of $\mathcal{L}_k^{(i-1)}$. Then, the fuzzy candidate locations in $\mathcal{L}_k^{(i-1)h}$ and the fuzzy candidate locations in $\mathcal{L}_k^i$ are matched to reduce the number of candidate locations. This matching process is divided into three stages:

- The matching between the orientation of each candidate location belonging to the new set of the fuzzy candidate and the orientation of each fuzzy location belonging to the set of the hypothesized fuzzy locations. The resultant degree

of match is $\Lambda^i_{\Theta_{kj}}$, where $k = \{1, \ldots, n\}$ and $j = \{1, \ldots, m\}$.

- The matching between the x component of each candidate location belonging to the new set of the fuzzy candidate and the x component of each fuzzy location belonging to the set of the hypothesized fuzzy locations. The resultant degree of match is $\Lambda^i_{X_{kj}}$.

- The matching between the y component of each candidate location belonging to the new set of the fuzzy candidate and the y component of each fuzzy location belonging to the set of the hypothesized fuzzy locations. The resultant degree of match is $\Lambda^i_{Y_{kj}}$.

The above stages are followed in the given order. At any stage if the degree of match is less than the threshold, the associated new fuzzy location is disregarded. By the end of this matching process, if there is more than one candidate location a new fuzzy local composite map is constructed and the process continues until one unique location is obtained.

Next, we show how the objects of the global map are represented to be used in the matching process with the objects extracted by the sonar readings in the form of a fuzzy local composite map.

5.2.2 Global Map Representation

The global map of the robot's environment is given in terms of line segments and corners. Each line segment is represented by three attributes: the starting coordinates $(X_{s_{OL_j}}, Y_{s_{OL_j}})$, ending coordinates $(X_{e_{OL_j}}, Y_{e_{OL_j}})$, and the negative surface normal to the line segment NL_j, where j is the line segment index. The corner has two attributes; the corner coordinates (X_{OC_r}, Y_{OC_r}) and the corner angle NC_r, where r is the corner index. These attributes are shown in Figure 5.1. The global map can be represented using the attributes that follow:

$$\mathcal{G} = \{G_1, \ldots, G_k, \ldots, G_m\}$$

where G_k is either:

$$\mathcal{E}_j = \{(X_{s_{OL_j}}, Y_{s_{OL_j}}), (X_{e_{OL_j}}, Y_{e_{OL_j}}), NL_j\},$$

or:

$$\mathcal{C}_r = \{(X_{OC_r}, Y_{OC_r}), NC_r\},$$

and m is the number of the objects in the global map.

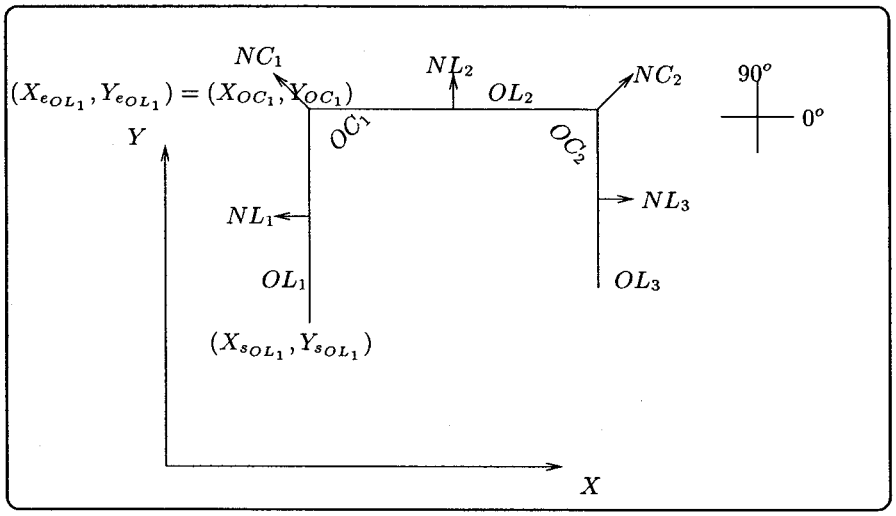

Figure 5.1: Elements of the global map.

As is explained later, the above elements of the global map are matched to the fuzzy local composite map to identify and estimate the robot's location in the environment.

Next, we show how a fuzzy local composite map is constructed based on the sonar readings obtained from the robot's environment.

5.2.3 Constructing a Fuzzy Local Composite Map

In the beginning of the global localization algorithm, the robot identifies a local composite map based on the sonar readings it obtains from its sensors. The local composite map consists of sonar readings obtained from adjacent sensors with close readings, i.e., the difference between the neighboring readings is within a predefined tolerance. This is done to filter out false reflections and to reduce angular and radial uncertainty. An example of a local composite map is shown in Figure 5.2 where the map is represented as:

$$\text{Local} = \{(d_{15}, d_0, d_1), (d_3, d_4), (d_6, d_7), (d_{11}, d_{12}, d_{13})\}$$

Then a simplified local composite map is represented as:

$$\text{sLocal} = \{\min(d_{15}, d_0, d_1), \min(d_3, d_4), \min(d_6, d_7), \min(d_{11}, d_{12}, d_{13})\}$$

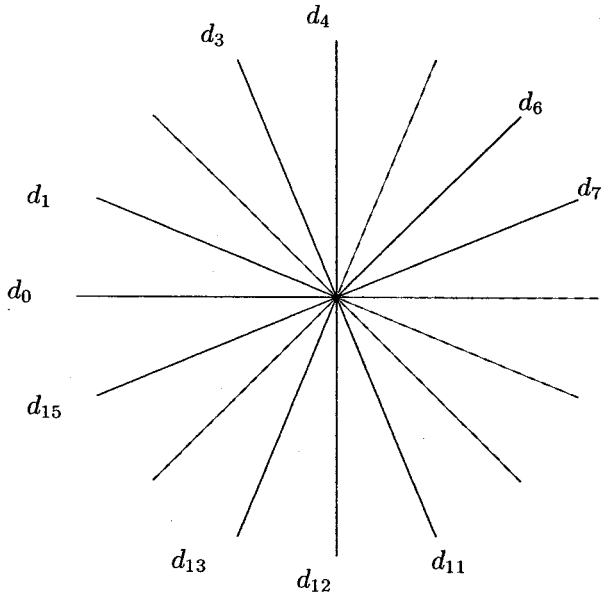

Figure 5.2: Local map.

This local composite map is transferred to a fuzzy local composite map by taking into account the angular and radial uncertainty in sonar readings; this map

can be represented as:

$$\mathcal{M} = \{(\Pi_{\Gamma|d_i}, \Pi_{sd_i|\gamma})\}, \forall i \in I \tag{5.1}$$

where $I = \{i \mid d_i \in \text{sLocal}\}$, $\Pi_{\Gamma|d_i}$ is the angular uncertainty model associated with d_i and used to determine the orientation of the detected object as shown in Section 4.7.1. Also $\Pi_{sd_i|\gamma}$ is the shortest distance obtained between the robot and the detected object as shown in Section 4.7.2. The map in Figure 5.2 is transferred into the fuzzy local composite map and it is illustrated in Figure 5.3.

At this stage both the local map and the global map are defined. In the following section, we explain the matching process between these two maps. The outcome of this matching process gives the robot's possible location(s) in the global map.

5.2.4 Matching The Local Map to The Global Map

Once the fuzzy local composite map is constructed, it is matched to the given global map to find the robot's possible location(s) in the environment. In this matching process, the global map is searched to find the possible locations from which the robot could have obtained this fuzzy local composite map. The searching algorithm is explained by the following steps:

Step1. Initialize:

$\Phi^{temp} = 0$; Move step size=1 cm; Rotate step size=1^o.

Step2. The constructed fuzzy local composite map is transformed into the coordinates of the robot's global map. This transformation is achieved by the translation of the center of the fuzzy local map to be d_1 away from the object G_k in the global map, in the beginning $k = 1$, and by rotating the fuzzy local

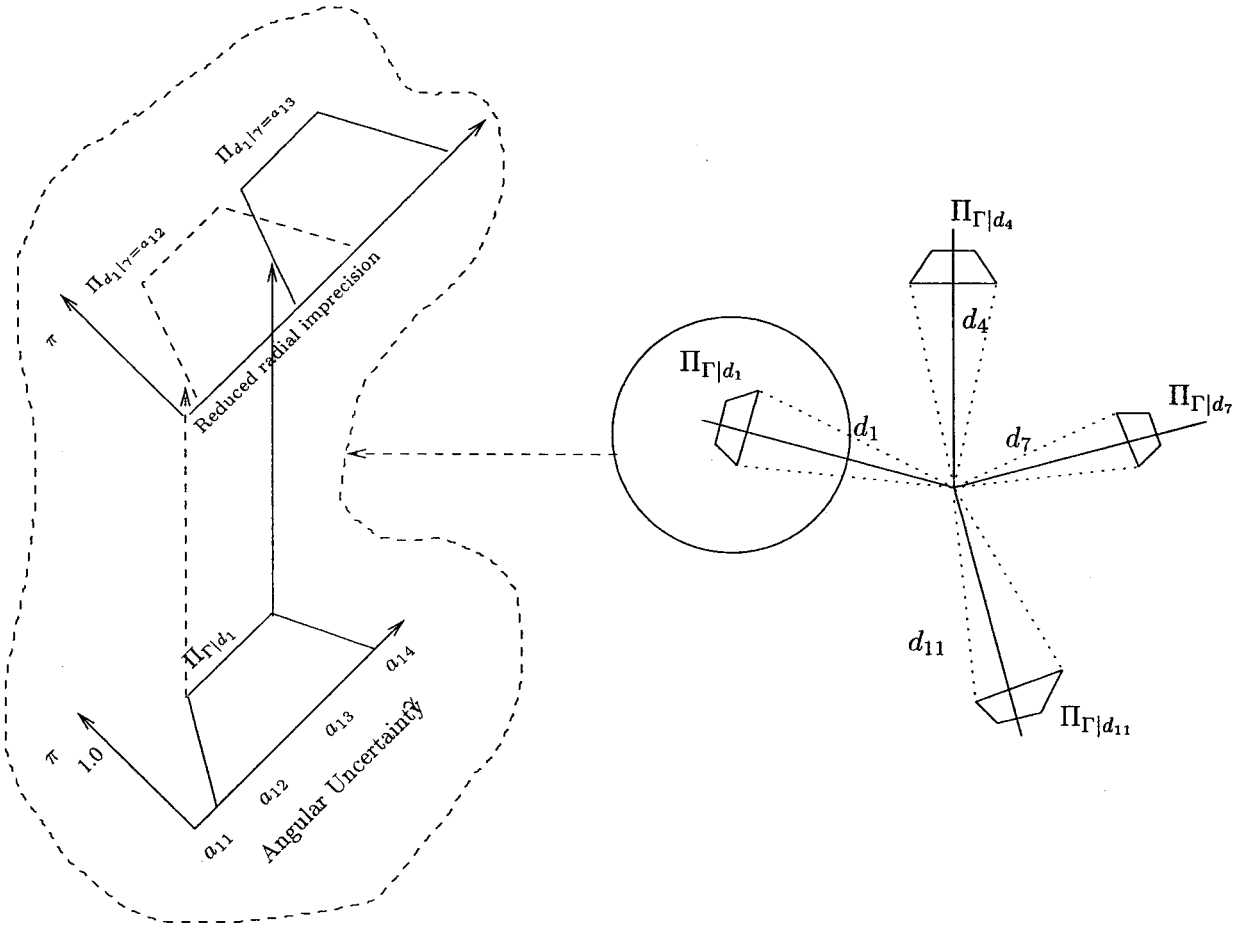

Figure 5.3: Example of a possible fuzzy local composite map of Figure 5.2.

composite map to align a_{11}, where $a_{11} \in supp\Pi_{\Gamma|d_1}$, with the angle of the first object in the global map.

Step3. For each component of the fuzzy local composite map,i.e., $i \in I$, search the global map to find an object that is d_i away from the center of the local map and where its angle belongs to $[a_{i1}, a_{i4}]$. If there is such an object record two degrees of match; the radial degree of match, Φ_{d_i}, and the angular degree of match, Φ_{Θ_i}, which are given as:

$$\Phi_{d_i} = \Pi_{sd_i}(L_k) \tag{5.2}$$

$$\Phi_{\Theta_i} = \Pi_{\Gamma|d_i}(N_k) \tag{5.3}$$

where L_k is the distance between the center of the local map and the object that is matched with i^{th} component of the local fuzzy composite map, and N_k is the angle of the object that is matched with i^{th} component of the local fuzzy composite map. If each component of the fuzzy local composite map has a matching component in the global map, the combined degree of match is recorded as follows:

$$\Phi = \min(\Phi_d, \Phi_\Theta) \tag{5.4}$$

where:

$$\Phi_d = \min_i \Phi_{d_i}, \ \forall i \in I \tag{5.5}$$

and:

$$\Phi_\Theta = \min_i \Phi_{\Theta_i}, \ \forall i \in I \tag{5.6}$$

If one of the fuzzy local composite map components does not have a matching object in the global map, then $\Phi = 0$.

Step4. Stay on the same search point and continue rotating the local map until a_{14} becomes parallel to the angle of the object G_k while continuously applying the

check in Step 2. For cases which pass the test in Step 3, update the degree of match Φ^{temp} as follows:

$$\Phi^{temp} = \max(\Phi^{temp}, \Phi) \tag{5.7}$$

Step5. If the above test fails when G_k is a wall, move to another search point by moving parallel to the current wall in a predefined step. At each new search point, repeat steps 2, 3 and 4. When the end of the wall is reached, go to Step 6. If the current object is a corner go, directly to Step 6.

Step6. Apply the following steps:

- Update the overall degree of match as follows:

$$\Phi^k = \Phi^{temp} \tag{5.8}$$

- Jump to the next object in the global map, i.e., k=k+1.
- Repeat steps 2,3, 4 and 5.

When a component of the fuzzy local composite map does not match an object in the global map, this means that this component is obtained based on the detection of an unknown object in the robot's environment. Therefore, at least two non-parallel components of the fuzzy local composite map are required to have matching objects in the global map so that the robot's candidate location can be estimated. This process is explained next.

5.2.5 Estimation of The Robot's Location

Each robot's candidate location is estimated based on the shortest distances between the robot and the detected objects in the global map. For each candidate location, the x, y and θ components of this location are computed as:

$$\Pi_X = \bigcap_{i \in I} \Pi_{X|sd_i}$$

$$\Pi_Y = \bigcap_{i \in I} \Pi_{Y|sd_i}$$

$$\Pi_\Theta = \bigcap_{i \in I} \Pi_{\Theta|sd_i}$$

where $\Pi_{X|sd_i}$, $\Pi_{Y|sd_i}$ and $\Pi_{\Theta|sd_i}$ are the possibility distributions of the x, y and θ components, respectively, coming from the elements of the fuzzy local composite map transformed into the global coordinate system. These locations are referred to as fuzzy locations due to the fact that the three location related components (x-component, y-component, and orientation) are represented with possibility distributions. One can obtain the fuzzy robot's location as a region by taking the Cartesian product of Π_X and Π_Y as shown in Figure 5.4 where each point (x, y) that belongs to this region has a degree of possibility of $\Pi_{X \times Y}(x, y) = \min\{\Pi_X(x), \Pi_Y(y)\}$ of being the actual position of the robot.

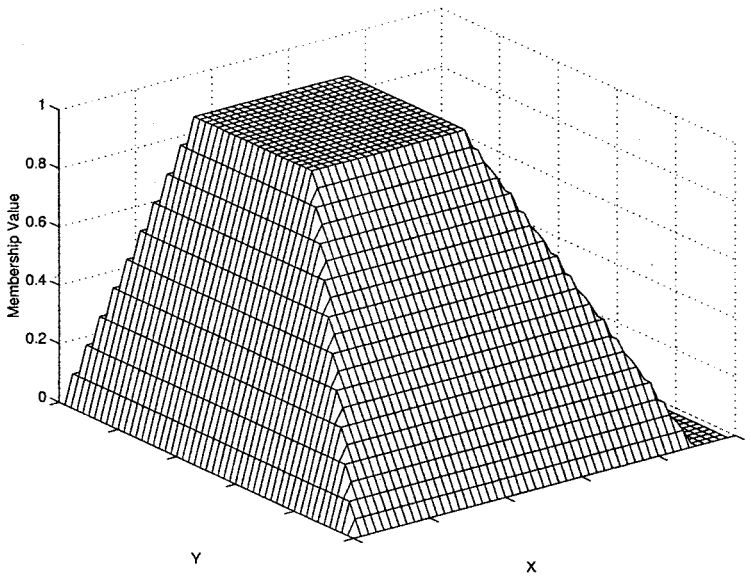

Figure 5.4: Fuzzy location region.

As mentioned earlier, when there is more than one candidate location of the robot obtained by the matching process, each location is represented as a fuzzy location in the global map. The robot travels to obtain a new local composite map from which a new set of fuzzy locations is obtained. These new locations are matched to the old locations by taking into account the distance traveled. The number of candidate locations is then reduced by applying fuzzy pattern matching. This process continues until a unique location is obtained.

5.2.6 Fuzzy Pattern Matching

When the robot extracts new features based on the sonar readings and obtains multiple fuzzy locations, it moves to a new location to obtain a new local composite map. Then the robot identifies a new set of fuzzy locations and checks for agreement with the old fuzzy locations by taking into account the distance traveled. This process is continuous until a unique location is found.

Let N, O and H represent new, old and hypothesized locations, where H is obtained from O by taking into account the traveled distance. Consider the location related components and let Π_{Xh}, Π_{Yh} and $\Pi_{\Theta h}$ represent the possibility distributions of x-component, y-component, and orientation associated with a hypothesized fuzzy location. Let Π_X, Π_Y, and Π_Θ represent the possibility distributions of x-component, y-component, and orientation associated with a new fuzzy location. Dubois and Prade [95] use possibility and necessity measures, introduced in Section 3.11, to represent the degree of match between the N and H components. These measures are denoted as $Poss(\Pi_{Ch}; \Pi_C)$ and $Nec(\Pi_{Ch}; \Pi_C)$, where C is one of the location related components. The possibility and necessity measures are defined as:

$$Poss(\Pi_{Ch}; \Pi_C) = \sup_{c \in C} \min(\pi_{Ch}(c); \pi_C(c)) \tag{5.9}$$

$$Nec(\Pi_{Ch};\Pi_C) = \inf_{c\in C} \max(\pi_{Ch}(c); 1-\pi_C(c)) \tag{5.10}$$

The degree of possibility $Poss(\Pi_{Ch};\Pi_C)$, measures to what extent it is possible that N and H belong to the same value, i.e., it represents the degree of overlap of Π_{Ch} and Π_C. On the other hand, $Nec(\Pi_{Ch};\Pi_C)$ measures to what extent it is necessary that the value to which Π_{Ch} belongs is among those that are compatible with Π_C, therefore it represents the degree of inclusion of Π_{Ch} into Π_C. Graphical representations of $Poss(\Pi_{Ch};\Pi_C)$ and $Nec(\Pi_{Ch};\Pi_C)$ are given in Figure 5.5.

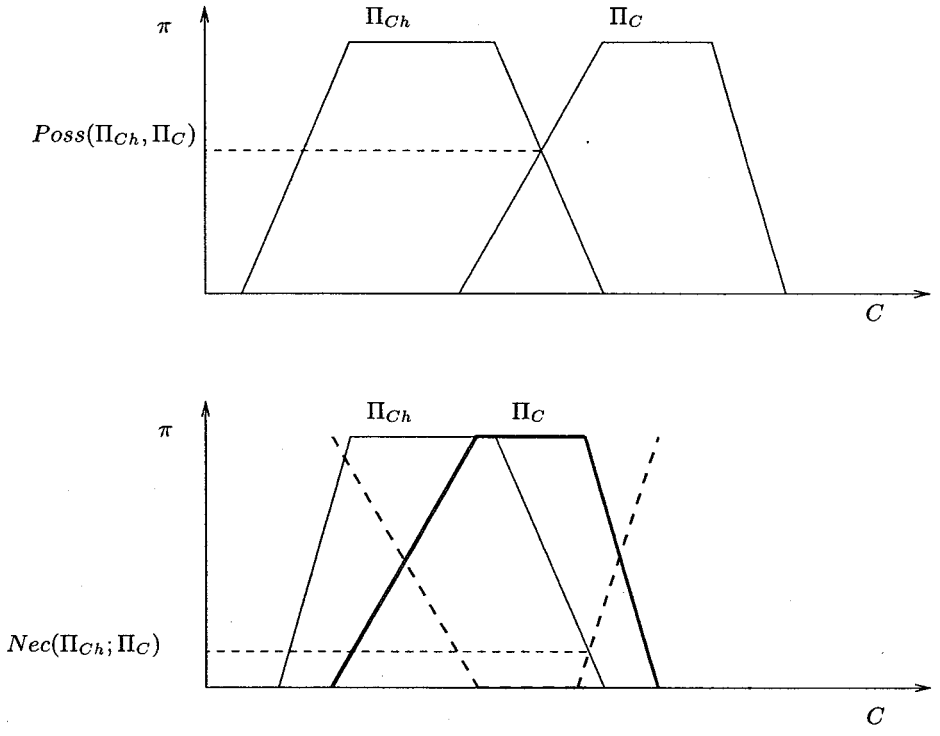

Figure 5.5: Scalar measures of matching between two fuzzy patterns.

In this thesis we are interested in the degree of overlap between two fuzzy locations, referred to as location pairs, which are composed of a new candidate location N and a hypothesized location H. Therefore, we are interested in the possibility measure $Poss(\Pi_{Ch};\Pi_C)$. If the robot actually was at the old location

and, after traveling, it actually reached the new location, then the degree of overlap (possibility) between the possibility distributions representing the components of these locations is expected to be high. Therefore, the possibility measure can be considered as a hypothesis test where location pairs with low degrees of possibility are rejected and remaining locations form the set of candidate locations. Details of this process are explained next.

In the next section, our fuzzy logic based global localization algorithm is summarized.

5.2.7 Localization Algorithm

The dynamic localization algorithm is explained in the following steps and summarized in Figure 5.6:

1. Obtain a local composite map, then form a fuzzy local composite map and match it to the given global as shown in Section 5.2.4.

   The result of this matching process may be one unique fuzzy location or multiple candidate fuzzy locations in the global map. If there is more than one candidate location, form the first set of fuzzy candidate locations, $\mathcal{L}_k^i = \{Loc_{i1}, \ldots, Loc_{ik}, \ldots, Loc_{in}\}$, where $\text{Loc}_{ik}=(\Pi_X^{[i,k]},\Pi_Y^{[i,k]}, \Pi_\Theta^{[i,n]})$, i is the index for the sets of fuzzy candidate locations, and n is the number of candidate locations. In the beginning $i = 1$. In addition, $\Pi_X^{[i,k]}$ and $\Pi_Y^{[i,k]}$ are the possibility distributions for the x and y components of fuzzy location k in the global map and are defined as follows:

$$\Pi_X^{[i,k]} = \sum_{x_j \in X} \pi_j / x_j \tag{5.11}$$

$$\Pi_Y^{[i,k]} = \sum_{y_j \in Y} \pi_j / y_j \tag{5.12}$$

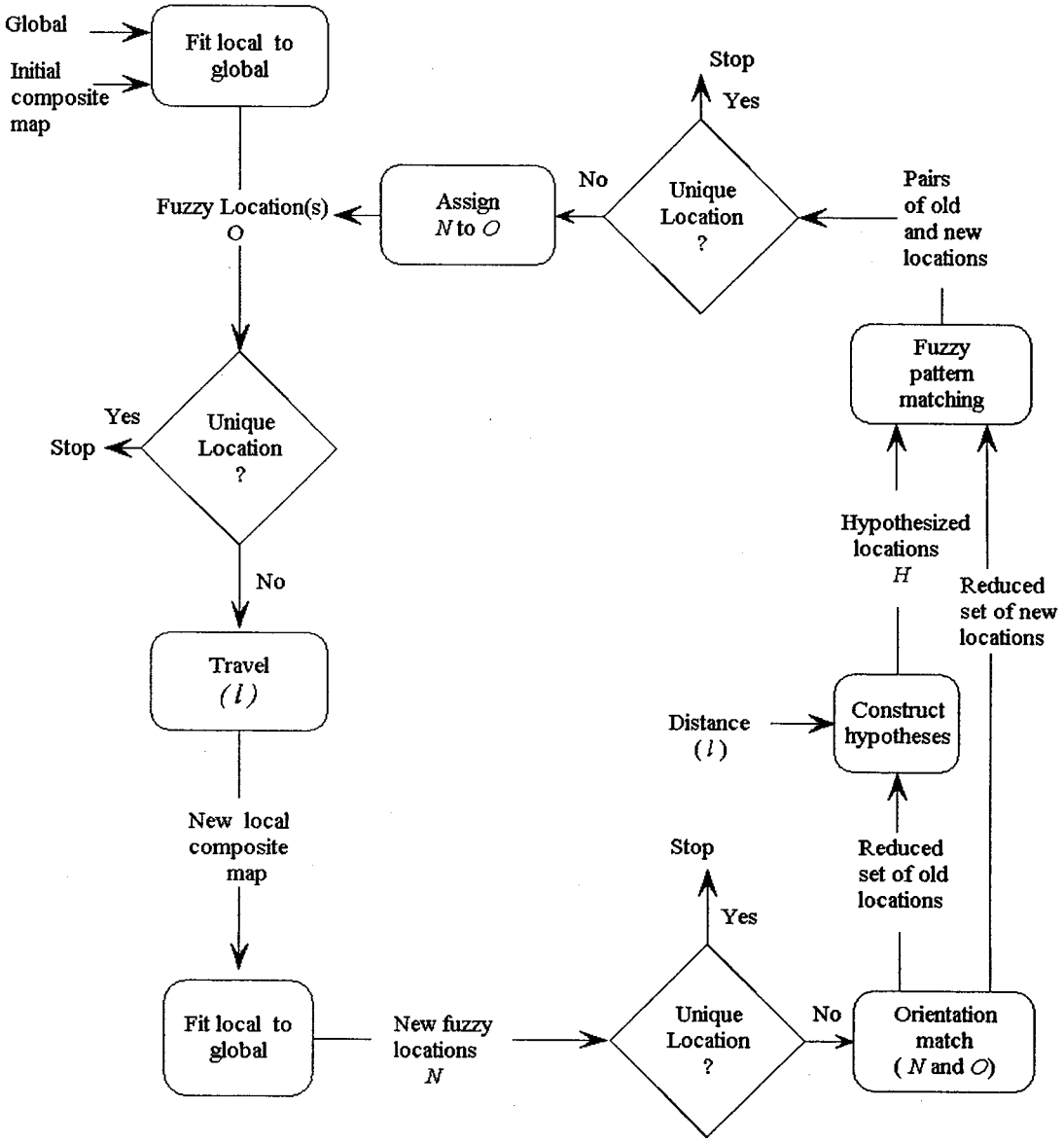

Figure 5.6: Localization algorithm.

and $\Pi_{\Theta}^{[i,k]}$ is the fuzzy orientation of this location in the global map defined as:

$$\Pi_{\Theta}^{[i,k]} = \sum_{\theta_j \in \Theta} \pi_j / \theta_j \tag{5.13}$$

Each candidate location has a value that represents the quality of matching between the local fuzzy map and the global map. This degree of matching is obtained in Section 5.2.4 as Φ^k.

2. If there is more than one candidate location, move to a new location on a straight path. Then, repeat Step 1 and obtain $\mathcal{L}_k^i = \{Loc_{i1}, \ldots, Loc_{ik}, \ldots, Loc_{im}\}$, where $i = 2$ and m is the number of new candidate locations.

3. Under the assumption that the robot's odometers are accurate when traveling short distances on a straight path, the old candidate locations are matched with the new candidate locations taking into account the distance traveled. The matching step is done by using the fuzzy pattern matching technique as explained in Section 5.2.6. This matching process helps reduce the number of candidate locations recently obtained. This is explained in the following steps:

   - For each location in the new set of fuzzy candidate locations $\mathcal{L}_k^i$, first check its orientation with the orientation of each location in the old set of fuzzy candidate locations $\mathcal{L}_k^{i-1}$, i.e., compute:

     $$\Lambda_{\Theta_{kj}}^i = \Lambda(\Pi_{\Theta}^{[i-1,k]}; \Pi_{\Theta}^{[i,j]}), \text{ for } k = 1, \ldots, n;\ j = 1, \ldots, m$$

     The location pairs (formed by a location from the old set of fuzzy locations and another from the new set of fuzzy locations) with a high degree of match (greater than a specified threshold) form the reduced sets of old and new candidate locations.

- For each location that belongs to the reduced set of old fuzzy locations obtained from the orientation test, obtain a hypothesized fuzzy location by taking into account the distance traveled l. The hypothesized x-component of an old location is obtained by:

$$\Pi_{Xh}^{[i-1,k]} = \bigcup_{\forall\theta\in supp\Pi_{\Theta}^{[i-1,k]}} \Pi_{(x+l\cos\theta)}^{[i-1,k]}, \tag{5.14}$$

where $\Pi_{(x+l\cos\theta)}^{[i-1,k]}$ is defined as:

$$\Pi_{(x+l\cos\theta)}^{[i-1,k]} = \sum_{x_j\in X} \pi_j/(x_j + l\cos\theta), \tag{5.15}$$

and the hypothesized y-component is given by:

$$\Pi_{Yh}^{[i-1,k]} = \bigcup_{\forall\theta\in supp\Pi_{\Theta}^{[i-1,k]}} \Pi_{(y+l\sin\theta)}^{[i-1,k]}, \tag{5.16}$$

where $\Pi_{(y+l\sin\theta)}^{[i-1,k]}$ is defined as:

$$\Pi_{(y+l\sin\theta)}^{[i-1,k]} = \sum_{y_j\in Y} \pi_j/(y_j + l\sin\theta). \tag{5.17}$$

It should be noted that the hypothesized x and y components above are computed using a disjunctive combination. This is due to the fact that the orientation of the robot is fuzzy, meaning that the robot could have moved in a number of directions with different degrees of possibility. Therefore, the robot could have arrived at a number of different locations, thus increasing the uncertainty of the arrived location. Therefore, this operation requires a disjunctive combination operator. This step is shown in Figure 5.7 where, for simplicity, the operation is performed only at the two limits of the core of the orientation.

- For each location that belongs to the reduced set of new fuzzy locations, match the x-component with the x-component of the hypothesized fuzzy locations, i.e., compute:

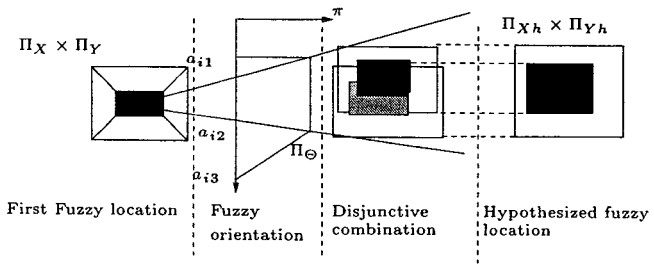

Figure 5.7: Obtaining a hypothesized location based on the traveled distance.

$$\Lambda^i_{X_{kj}} = \Lambda(\Pi^{[i-1,k]}_{Xh}; \Pi^{[i,j]}_X), \text{ for } k = 1, \ldots, n_r;\ j = 1, \ldots, m_r(k)$$

- Repeat this process for the y-component to compute $\Lambda^i_{Y_{kj}}$.
- Location pairs with high degrees of match, both in x and y components, remain candidate locations.

4. Steps 1-3 can be repeated until a unique fuzzy location is obtained.

The implementation of the algorithm is demonstrated with examples in Chapter 6.

5.3 Concurrent Localization and Map Updating

Fuzzy logic based concurrent localization and map updating algorithms for mobile robots are introduced in this section. These algorithms depend on sonar readings obtained from the robot's environment to update the robot's location and map. Sonar readings are used to construct a fuzzy composite map. This provides information about the location of detected objects in the global map. These objects either belong to the original map or are new objects in the environment that need to be added to the global map as line segments. Identification of the detected object is performed by fitting the fuzzy composite map to the global map. As a result of this fitting process, the fuzzy composite map components can be classified into two sets. The first set includes the components that have a match in the global map. These

are used to obtain the robot's location based on sonar readings, and then combined with the robot's location obtained from odometers over a short distance in order to update the robot's current location. The second set includes the components that do not have matching components in the global map. These are used to update the map itself in terms of line segments.

5.3.1 Localization Algorithm

The proposed fuzzy based localization and map updating algorithms are explained in this section. These algorithms depend upon a collection of sonar readings obtained by the robot's sensor at each sonar scan. A sonar scan consists of the sonar readings at each localization cycle which consists of sensing, localizing, and location updating. The obtained sonar readings in one scan are used to build a fuzzy composite map. This fuzzy composite map is fit into the global map. The components of the fuzzy composite map that fit into the global map are identified and grouped in one set. The same is done for the components that do not fit into the global map. For each fitting component, the shortest distance between that component and its fitted object in the global map is calculated. Each calculated shortest distance represents either an x or a y coordinate of the robot's position in the global map. All obtained x components are combined to obtain one representative coordinate. The same is done for the y components. These coordinates represent the robot's position when only taking into account the sonar readings. The odometer readings are then used to calculate the expected position of the robot. Then, information from the two locations is fused to obtain the current robot's location. The obtained location is used to correct the odometers. Finally, the set of the unfitted components is used to extract lines segments to be used in the map updating algorithm. These steps are explained in details next.

5.3.2 Fitting The Fuzzy Local Composite Map Into The Global Map

Consider a fuzzy local composite map obtained from sonar readings. The components of this map are fit into the global map. The components that fit successfully are used to update the robot's position. The ones that do not fit successfully are used to create new line segments. Next, we show how we test each component of the fuzzy map to see if it fits or does not fit into the global map. This is explained in the following steps:

- For each element of the fuzzy local composite map, search the global map of the robot to find the set of objects that have negative surface normals in the support of $\Pi_{\Theta|sd_i}$. This set is represented as:

$$\mathcal{A}_i = \{O_1, \ldots, O_j, \ldots, O_k\} \forall i \in I$$

  where O_j is an object in the global map whose negative surface normal $\in$ $supp\Pi_{\Theta|sd_i}$ and k is the number of elements in $\mathcal{A}_i$.

- For each $\mathcal{A}_i$, find the coordinates that represent this component in the global map. These coordinates are obtained as:

$$X_i = X_r + d_i \cos(\gamma_i)$$

$$Y_i = Y_r + d_i \sin(\gamma_i)$$

  where X_r is the x coordinate for the robot's current location; Y_r is the y coordinate for the robot's current location; d_i is the sonar reading obtained from the sensor that represents the i^{th} component of the fuzzy local composite map; γ_i is the angle of this sensor in the global frame.

- For each $\mathcal{A}_i$, find the relationship between each element in $\mathcal{A}_i$, i.e., O_j and (X_i, Y_i) as follows (note that for each $\mathcal{A}_i$ there is only one pair of (X_i, Y_i)):

$$\lambda^* = \frac{(X_{s_{o_j}} - X_r)(Y_{e_{o_j}} - Y_{s_{o_j}}) - (X_{e_{o_j}} - X_{s_{o_j}})(Y_{s_{o_j}} - Y_r)}{(X_r - X_i)(Y_{e_{o_j}} - Y_{s_{o_j}}) - (X_{e_{o_j}} - X_{s_{o_j}})(Y_r - Y_i)} \tag{5.18}$$

$$\mu^* = \frac{(X_{s_{o_j}} - X_r) * (Y_i - Y_r) - (X_i - X_r)(Y_{s_{o_j}} - Y_r)}{(X_r - X_i)(Y_{e_{o_j}} - Y_{s_{o_j}}) - (X_{e_{o_j}} - X_{s_{o_j}})(Y_r - Y_i)} \tag{5.19}$$

$$X_E = \frac{(X_r Y_i - Y_r X_i)(X_{s_{o_j}} - X_{e_{o_j}}) - (X_r - X_i)(X_{s_{o_j}} Y_{e_{o_j}} - X_{e_{o_j}} Y_{s_{o_j}})}{(X_r - X_i)(Y_{s_{o_j}} - Y_{e_{o_j}}) - (Y_r - Y_i)(X_{s_{o_j}} - X_{e_{o_j}})} \tag{5.20}$$

$$Y_E = \frac{(X_r Y_i - Y_r X_i)(Y_{s_{o_j}} - Y_{e_{o_j}}) - (Y_r - Y_i)(X_{s_{o_j}} Y_{e_{o_j}} - X_{e_{o_j}} Y_{s_{o_j}})}{(X_r - X_i)(Y_{s_{o_j}} - Y_{e_{o_j}}) - (Y_r - Y_i)(X_{s_{o_j}} - X_{e_{o_j}})} \tag{5.21}$$

$$D = \sqrt{(X_i - X_E)^2 + (Y_i - Y_E)^2} \tag{5.22}$$

where λ^* is a ratio that determines if there is an intersection between the line L (Figure 5.8) that links the current location of the robot and the (X_i, Y_i), and any global line segment O_j, μ^* is the ratio that determines if (X_i, Y_i) is within the start and the endpoints of any line segment that belongs to the global map, and (X_E, Y_E) is the intersection point between the line L and the object O_j. These ratios are utilized as follows:

1. If $0 \leq \mu^* \leq 1$, $0 \leq \lambda^* \leq 1$, and $D \leq \zeta_1$, then there is a match between the object O_j and the component $\mathcal{A}_i$, where ζ_1 is a threshold value determined experimentally.
2. If $0 \leq \mu^* \leq 1$, and $V \leq \zeta_2$, then there is a match between the object O_j and the component $\mathcal{A}_i$. However, in this case the line L has no intersection with the object O_j and V is the distance between (X_i, Y_i) and the object O_j.

- If one of the previous conditions is satisfied, the object O_j is used to update the robot's location.

- If the previous two conditions fail, then there is no match between the object O_j and the component i, and (X_i, Y_i) is then used as the seed for a new line segment creation.

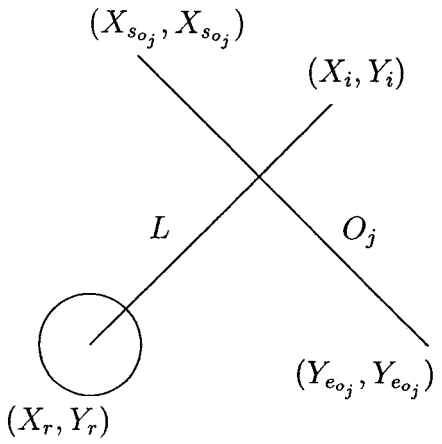

Figure 5.8: Local map

5.3.3 Fuzzy Triangulation

The obtained possibility distributions that represent the shortest distances between the robot and the detected objects (the ones that have matching components in the fuzzy local composite map) are used to update the robot's location components, x, y and θ. As mentioned earlier, the shortest distance between the robot and wall can update either the x or the y component of the robot's location in the global map. The shortest distance between the robot and the corner can update both the x and the y coordinates of the robot location in the global map. However, before updating the robot's coordinates, the shortest distances are used to calculate the x and y coordinates with respect to the detected objects. These coordinates are obtained as follows:

$$\Pi_{X|td_i} = \sum_j \pi_j / (X_{O_k} - sd_i \cos(N_k)), \forall (sd_i)_j \in supp\Pi_{sd_i} \tag{5.23}$$

$$\Pi_{Y|td_i} = \sum_j \pi_j/(Y_{O_k} - sd_i \sin(N_k)), \forall (sd_i)_j \in supp\Pi_{sd_i} \tag{5.24}$$

$$\Pi_{\Theta|td_i} = \sum_j \pi_j/(\kappa_{1i} + \lambda_i), \forall (\lambda_i)_j \in supp\Pi_{\Gamma|Sd_i} \tag{5.25}$$

The objective of the above equations is to obtain the robot's coordinates based on the shortest distances between the robot and the detected objects. This is achieved by using the global map given to the robot. The global coordinates of the detected objects are given as (X_{O_k}, Y_{O_k}, N_{O_k}). Note that according to the type of the detected objects, the parameters (X_{O_k}, Y_{O_k}, N_k) can represent the coordinates of a wall or a corner. In the case of a wall these parameters can be described as in Section 5.2.2 by ($X_{s_{OL_k}}, Y_{s_{OL_k}}, NL_k$) and in the case of a corner they become (X_{OC_k}, Y_{OC_k}, NC_k). In Equation (5.25), κ_{0i} is the angular difference between the orientation of the first sonar sensor in the sonar ring (since it represents the orientation of the robot) and the orientation of the i^{th} sensor which has the shortest distance to an object. Equation (5.25) represents the rotation of the angular possibility distributions of the sensors that provide the shortest distance information to the current orientation of the robot.

Finally, the robot's coordinates in the global map are obtained by combining all possibility distributions that represent the x, y and θ coordinates as follows:

$$\Pi_{X_{so}} = \bigcap_{i \in I} \Pi_{X|td_i} \tag{5.26}$$

$$\Pi_{Y_{so}} = \bigcap_{i \in I} \Pi_{Y|td_i} \tag{5.27}$$

$$\Pi_{\Theta_{so}} = \bigcap_{i \in I} \Pi_{\Theta|td_i} \tag{5.28}$$

These locations are referred to as fuzzy locations due to the fact that the three location related components (x-component, y-component, and orientation) are represented with possibility distributions.

For example, Figure 5.9(a) shows a fuzzy composite map fitted to the global map. In Figure 5.9(b), the shortest distance between the robot and each object is

shown. Then in Figure 5.9(c), these short distances are transformed into x and y components. In this figure there are four x components and three y components of the shortest distances that can be used to obtain the robot's coordinates. Finally, in Figure 5.9(d), Equations (5.26, 5.27, 5.28) are used to obtain the robot's x, y, and θ coordinates.

One can obtain the fuzzy robot's position as a region by taking the Cartesian product of $\Pi_{X_{so}}$ and $\Pi_{Y_{so}}$ as shown in Figure 5.4 where each point (x, y) that belongs to this region has a degree of possibility of $\Pi_{X_{so} \times Y_{so}}(x, y) = \min\{\Pi_{X_{so}}(x), \Pi_{Y_{so}}(y)\}$ of being the actual robot's position. Based on this figure, the possibility that the robot's position in the global map belongs to the flat region is 1.0.

5.3.4 Sensor Fusion for Localization

The idea of sensor fusion is to combine location information from different types of sensor. The objective of the fusion is to obtain location information with less uncertainty. In this paper, the traveled distance of the robot since the previous time-step provided by the odometers is considered to update the robot's current location. Then, this obtained location is fused with the location information obtained by the sonar. The robot's location based on the odometers is obtained as:

$$\Pi_{X_{od}} = \sum_{x_f} \pi_x / (X_f + l\cos(\bar{\theta}_f)), \forall x_f \in supp\Pi_{X_f} \tag{5.29}$$

$$\Pi_{Y_{od}} = \sum_{y_f} \pi_{y_f} / (Y_f + l\sin(\bar{\theta}_f)), \forall y_f \in supp\Pi_{Y_f} \tag{5.30}$$

$$\Pi_{\Theta_{od}} = \sum_{\theta_f} \pi_{\theta_f} / (\phi + \theta_f), \forall \theta_f \in supp\Pi_{\Theta_f} \tag{5.31}$$

where Π_{X_f}, Π_{Y_f}, and Π_{Θ_f} are the possibility distributions that represent the current coordinates of the robot. The symbols l and ϕ are the traveled distance and the angular rotation since the previous time-step provided by the odometers. Finally, $\bar{\theta}_f$ is the crisp value that represents the current location of the robot and is

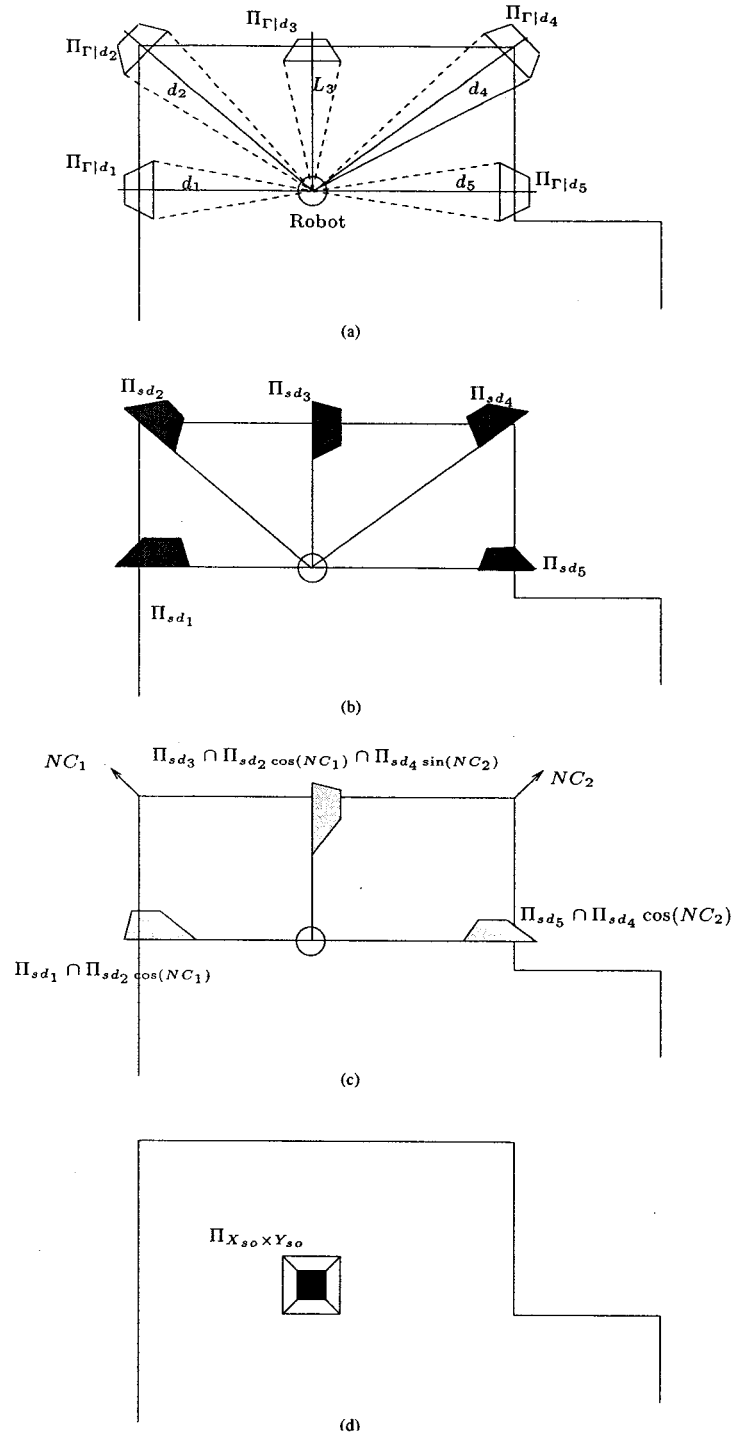

Figure 5.9: (a) Fuzzy composite map is fit to the global map; (b) Shortest distances between the robot and different objects are obtained; (c) Combination of the shortest distances; (d) The fuzzy region that represents the estimated position of the robot.

obtained using the center of gravity method as follows:

$$\bar{\theta}_f = \frac{\sum_{\theta \in supp\Pi_{\Theta_f}} \theta_f \pi(\theta_f)}{\sum_{\theta_f \in supp\Pi_{\Theta_f}} \pi(\theta_f)}$$

Since we obtain the robot's location based on two types of sensors (sonar and odometers), we can fuse these two sources of location information to obtain the robot's current location and update the robot's odometer to start a new localization cycle. The components of robot's current location after fusion are obtained as follows:

$$\Pi_{X_f} = \Pi_{X_{od}} \bigcap \Pi_{X_{so}}$$

$$\Pi_{Y_f} = \Pi_{Y_{od}} \bigcap \Pi_{Y_{so}}$$

$$\Pi_{\Theta_f} = \Pi_{\Theta_{od}} \bigcap \Pi_{\Theta_{so}}$$

To update the odometers, the above possibility distributions must be defuzzified to obtain crisp values and this is done by using the center of gravity method:

$$\bar{x}_f = \frac{\sum_{x_f \in supp\Pi_{X_f}} x_f \pi(x_f)}{\sum_{x_f \in supp\Pi_{X_f}} \pi(x_f)}$$

$$\bar{y}_f = \frac{\sum_{y \in supp\Pi_{Y_f}} y_f \pi(y_f)}{\sum_{y_f \in supp\Pi_{Y_f}} \pi(y_f)}$$

$$\bar{\theta}_f = \frac{\sum_{\theta \in supp\Pi_{\Theta_f}} \theta_f \pi(\theta_f)}{\sum_{\theta_f \in supp\Pi_{\Theta_f}} \pi(\theta_f)}$$

5.3.5 Line Segments Extraction

In this section we present a method to group sonar readings into line segments that can be used to update the global map. This process takes place in the presence of pieces of evidence that support the fact that these sonar readings are not coming from the original global map features. In other words, the components of the fuzzy local composite map which do not have matching objects in the global map are

used to build new objects. These objects are built in the form of line segments. Estimating the parameters of the new line segments requires that the robot's current location is valid. This means that there is a sufficient degree of match between the fuzzy composite map and the global map.

Fuzzy composite map components do not fit to the global map and the updated robot's current location can be used to either initialize a line segment, create a line segment, or update the parameters of a created line segment. This process is shown in Figure 5.11. The three cases of this process are explained as follows:

1. **Initialization of a new line segment**

   In this case the component of the fuzzy composite map is used to obtain the starting point and the normal to the surface of a candidate line segment. These are obtained as follows:

$$X_s = X_r + S\cos(\gamma) \tag{5.32}$$

$$Y_s = Y_r + S\sin(\gamma) \tag{5.33}$$

$$\Theta_s = \frac{\sum_{\forall\theta\in sup\Pi_{\Gamma|d_i}} \theta_i \pi_{\Gamma|d_i}(\theta_i)}{\sum_{\forall\theta\in supp\Pi_{\Gamma|d_i}} \pi_{\Gamma|d_i}(\theta_i)} \tag{5.34}$$

   where γ is the angle of the sensor that detected this new object, and S is the crisp value of the shortest distance obtained by:

$$S = \frac{\sum_{\forall d_j\in supp\Pi_{sd}} d_j \pi_{sd}(d_i)}{\sum_{\forall d_j\in supp\Pi_{sd}} \pi_{sd}(d_j)} \tag{5.35}$$

   The above obtained parameters are considered the initial information about a newly detected object in the environment. This information will be stored for use in the process of the creation of a new line segment as will be discussed next.

2. **Create a new line segment**

   If we have an initialized line segment and a component of the fuzzy composite

map that does not fit into the global map, the coordinates of this component are then checked with the initialized segment parameters to see if a relationship exists between them. This relation is determined as follows:

$$\sqrt{(X_s - X_i)^2 + (Y_s - Y_i)^2} \leq \tau \tag{5.36}$$

$$\pi_{\Gamma|d_i}(\theta_s) \geq \alpha \tag{5.37}$$

where τ and α are threshold values determined experimentally. Equation(5.36) determines the distance of the newly obtained (X_i, Y_i), which is associated with a component of the fuzzy map that does not fit into the global map, from the starting point of an initialized line segment. Equation(5.37) determines the orientation of (X_i, Y_i) with respect to an initialized segment. If both of these relationships are satisfied, the coordinates of the component are considered as the ending coordinates of the initialized line segment. This step will complete the parameters of the initialized segment and results in a newly created segment.

3. **Updating the parameters of a created segment**

   If we have a created line segment and a component of the fuzzy composite map that does not fit into the global map, the coordinates of this component can be used to update the parameters of the line segment. Figure 5.10 shows a line segment and the coordinates of two different components labeled as A and B. The A coordinates are used to update the starting coordinates of the line segment. Similarly, the B coordinates are used to update the ending coordinates of the line segment. For the A coordinates to be used to update the starting coordinates of the line segment, the value of the parameter μ^*, given by Equation(5.19) must be less than zero, when applied to the parameters of the created line segment and the A coordinates. This means that the coordinates

of A are outside the boundaries of a new line segment. Then, if this is satisfied, we proceed by checking how far A is from the starting coordinates of the new line segment. If the distance between the starting coordinate of the new line segment and A is less than a threshold value, then the A coordinates can be used to update the starting coordinates of the line segment. Similarly, this is applied to the B coordinates, however, the μ^* value must be greater than 1 so that the B coordinates can be used to update the ending coordinates of a new line segment.

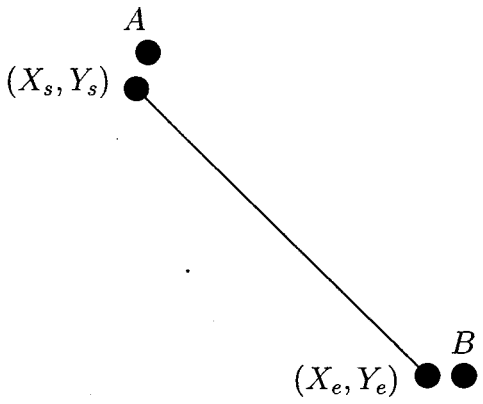

Figure 5.10: Created line segment.

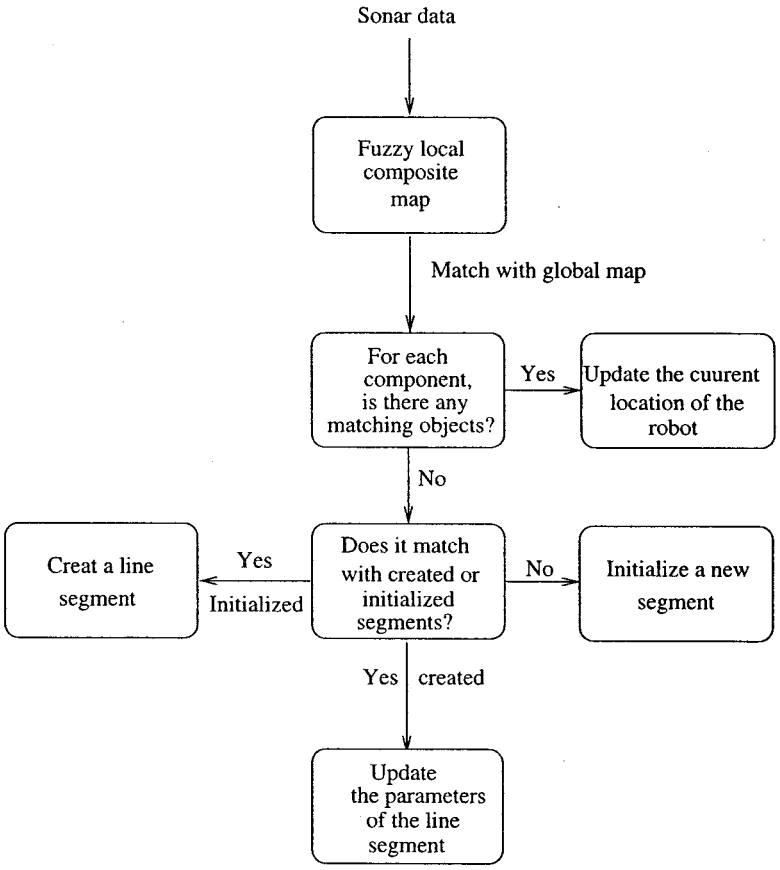

Figure 5.11: Line segments extraction algorithm.

Chapter 6

Experimental Results and Discussions

In this chapter we implement our proposed fuzzy logic based localization and map updating algorithms on a Nomad 200 mobile robot. This chapter includes two sections. The first section deals with the global localization problem and the second one deals with the concurrent localization and map updating problems.

6.1 Applications of The Global Localization Problem

6.1.1 Example

For this example, consider the map given in Figure 6.1. The robot is located at an arbitrary location in the environment, i.e., it has no knowledge of its global location. The first step is for the sonar sensors to collect data from the robot's environment. Then, sonar readings coming from adjacent sensors are considered to be coming from the same object if the difference between the neighboring readings is within a

predefined tolerance which is determined experimentally as 10 cm. Combining adjacent sonar readings also helps eliminate false reflections, reducing angular and radial uncertainty in sonar readings as explained in Section 5.2.3, and then constructing the robot's local composite map. Each element in the local composite map consists of at least two sonar readings coming from the same object. This local composite map is represented as:

$$\text{Local}_1 \quad = \quad \{(d_9 = 1596, d_{10} = 1520), (d_{13} = 3653, d_{14} = 3603)\}(mm)$$

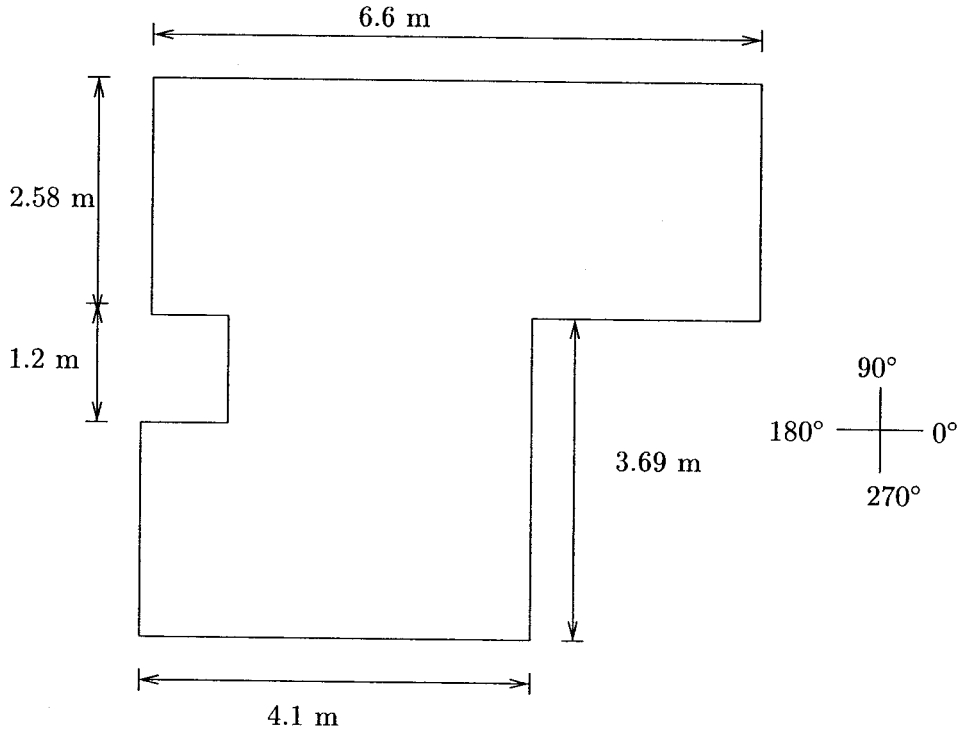

Figure 6.1: The global map.

This local composite map is transferred into the fuzzy local composite map by taking into account the angular and radial uncertainty of the sonar readings. This fuzzy local composite map is shown in Figure 6.2.

By matching the fuzzy local composite map with the global map, we can obtain candidate locations of the robot in the environment by applying the first

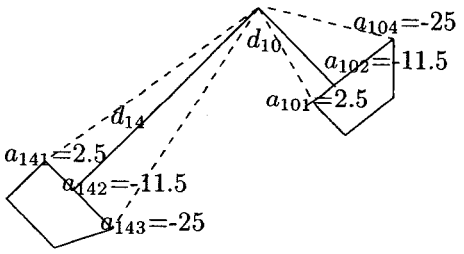

Figure 6.2: Angular uncertainty of the fuzzy local composite map.

step in our proposed localization algorithm (Section 5.2.7). These locations are shown in Figure 6.3 and are labeled as Loc_{11}, Loc_{12}, Loc_{13}, and Loc_{14}.

The x, y and θ components of the candidate locations are computed as explained in Section 5.2.5 and shown in Figure 6.4 for Loc_{12} [1] .

After getting all candidate locations, the robot moves to a new location for a new local composite map, which is given as:

$$\text{Local}_2=\{(d_5 = 3044, d_6 = 2988),\ (d_9 = 1596, d_{10} = 1545)\ \}(\text{mm}).$$

Then we obtain the candidate locations Loc_{21}, Loc_{22}, Loc_{23}, Loc_{24} as shown in Figure 6.5. The x, y and θ components for Loc_{23} are shown in Figure 6.6.

Now we obtain hypothesized fuzzy locations for the fuzzy locations obtained in the previous local composite map using Equations (5.14) and (5.16) and the x and y components shown in Figure 6.7 for $Loc_{12,h}$.

First, we match the orientations and then the x, and y components of the locations that have agreement in the orientation. The degree of possibility of matching in each case is computed by using Equation (5.9). This process is explicitly demonstrated between $Loc_{12,h}$ and Loc_{23} in Figure 6.8. In this figure, the degree of match between orientations is 1.0, and between x and y components is 1.0 and 1.0, respectively. After matching all of the hypothesized fuzzy locations with all of the current fuzzy locations, we obtain the decision tree shown in Figure 6.9. In this

[1] Loc_{12} is the actual location of the robot.

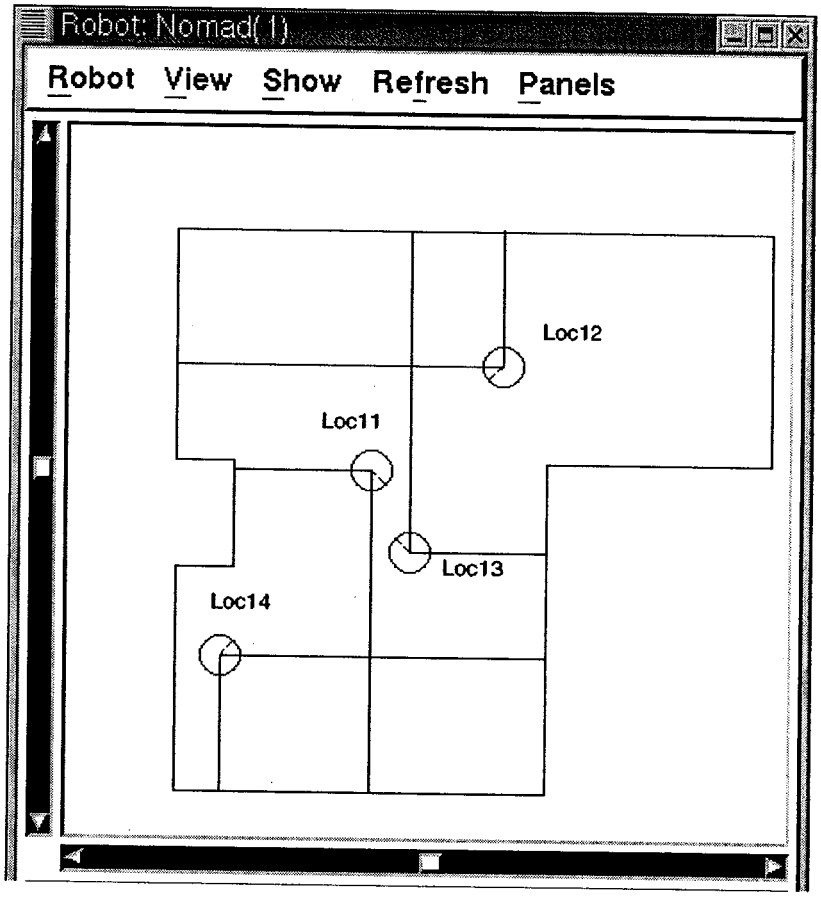

Figure 6.3: Candidate locations of the robot.

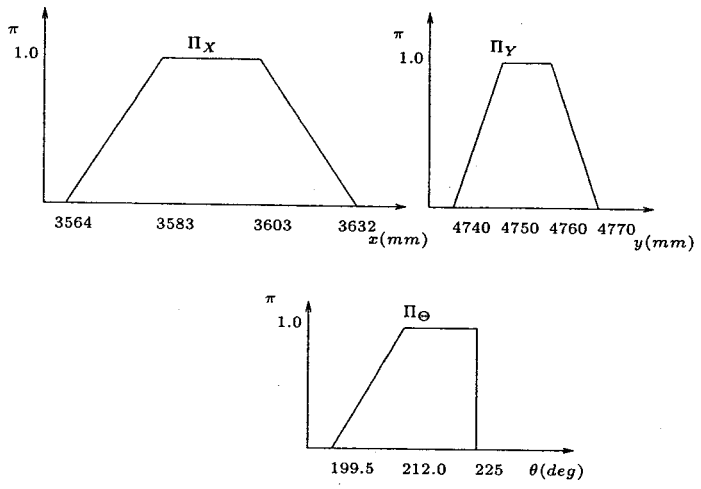

Figure 6.4: The x, y and θ components of Loc_{12}.

figure, the orientation and the x component are matched between Loc_{11} and Loc_{22}, however, there is no match between the y components of these two locations. There is a match in the orientation and x components of Loc_{13} and Loc_{24} but there is no match between the y components. Locations Loc_{14} and Loc_{21} match in the orientation and y components, however, there is no match between their x components. Therefore, we obtain Loc_{23} as the actual current location and Loc_{12} as the actual previous location.

Figure 6.10 shows the two sets of candidate locations in the same map. From this figure it is clear that Loc_{12} is the previous location and Loc_{23} is the current location.

6.1.2 More Examples

Figure 6.11 shows the different results obtained by applying the proposed algorithm at different locations in the robot's environment. In these experiments we obtain unique candidate locations of the robot represented by black circles.

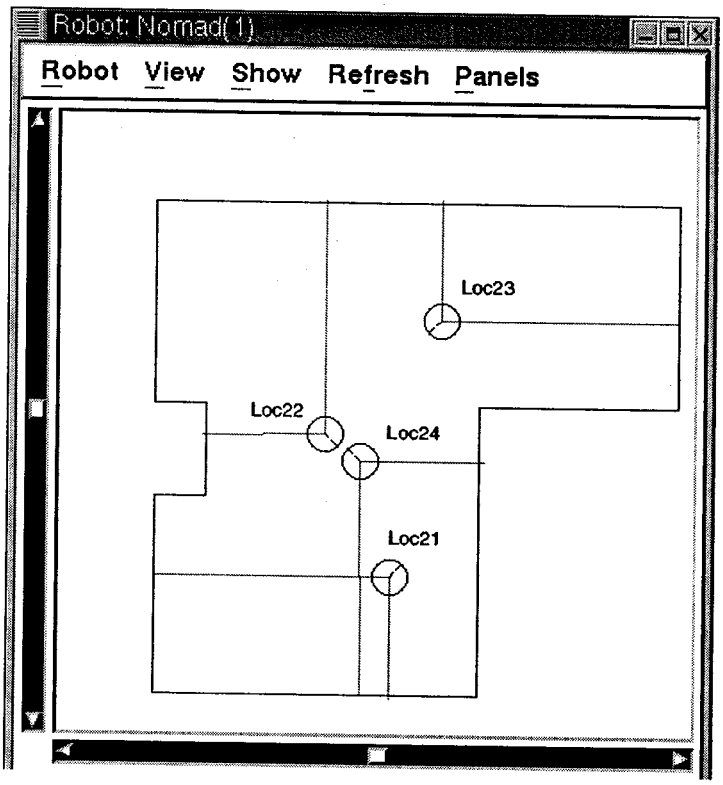

Figure 6.5: Fuzzy candidate locations in the second scan.

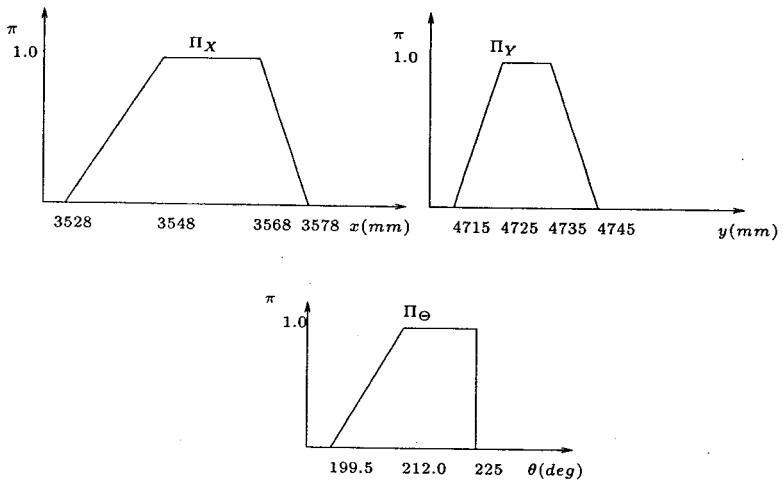

Figure 6.6: The x, y and θ components of Loc_{23}

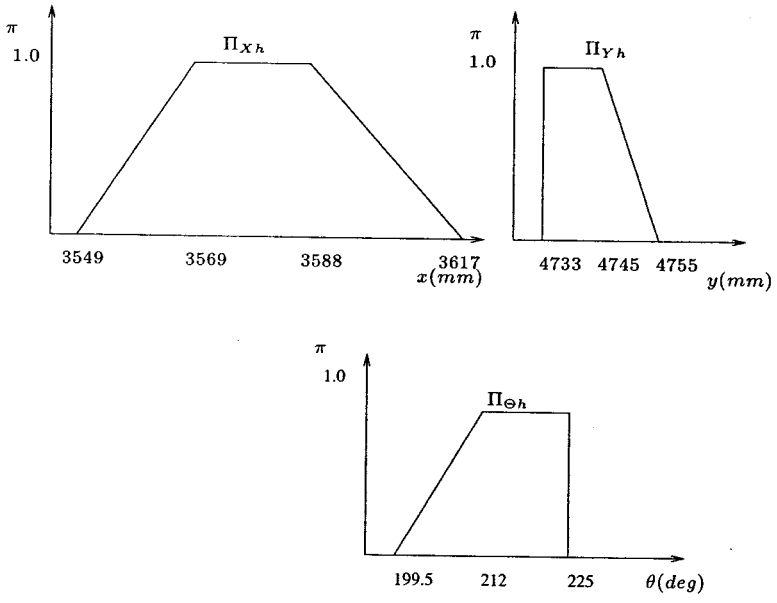

Figure 6.7: Hypothesized fuzzy location, $Loc_{12,h}$.

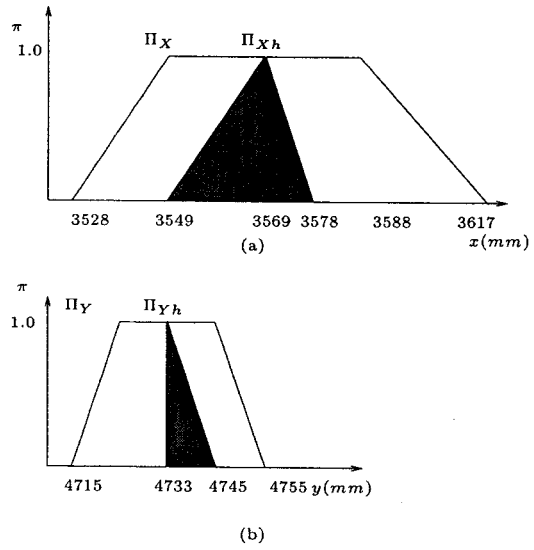

Figure 6.8: Fuzzy matching between Loc_{12} and Loc_{23}: (a) x-components match, (b) y-components match.

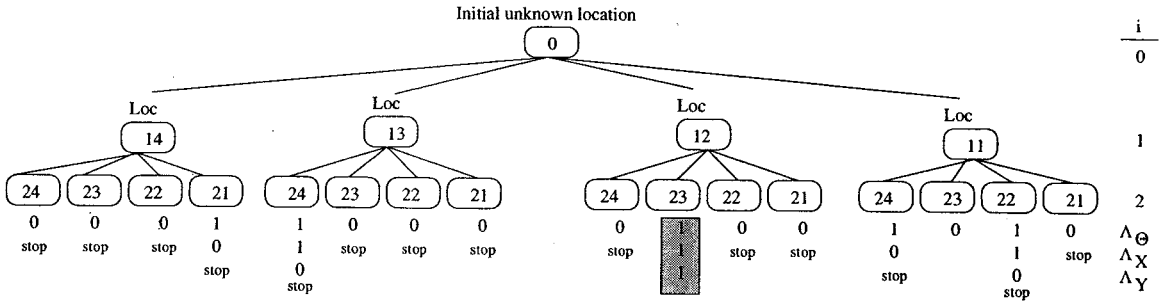

Figure 6.9: Tree search to obtain the current location.

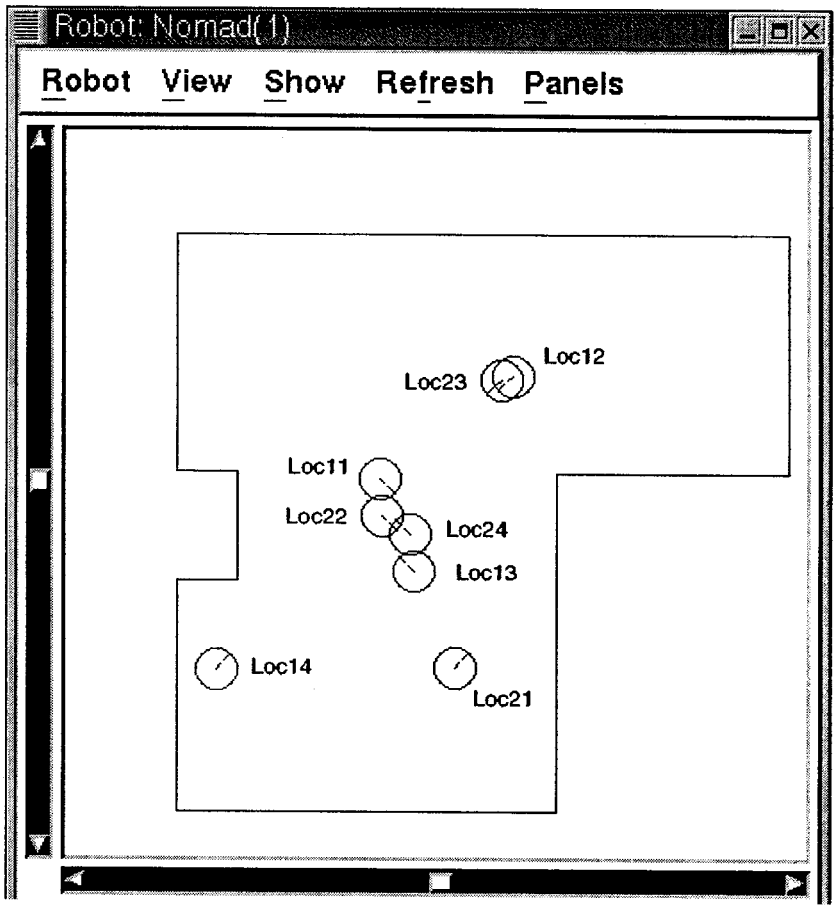

Figure 6.10: The two sets of candidate locations shown in the same map.

In Figure 6.11(a), the robot was able to obtain one unique location after several attempts. The last sonar scan resulted in two candidate locations. However, one of these locations conflicted with the robot and environment geometries since the robot ring was in contact with one of the environment walls. This impossible location was eliminated and then one unique location was identified. Figure 6.11(b) shows a situation where the robot had enough sensory information to uniquely localize itself. In Figures 6.11(c,d,f), during its movements the robot had multiple candidate locations. When new sonar information became available, the robot was able to reduce the number of these locations and obtain one unique location. Finally, in Figure 6.11(e), the robot initially attempted to localize itself based on the sonar readings obtained from only two walls. As a result, the robot obtained three candidate locations. Then, after its movement, the robot was able to detect a new wall which reduced the number of candidate locations into two competing locations. In the end, the robot was able to recognize two corners in addition to the walls which gave the robot the ability to obtain one unique location. The detection of the two corners reduced the number of iterations needed to find a unique location.

Table 6.1 reports the location components as the parameters of the possibility distributions that are associated with these locations. The possibility distributions that represent the X and Y coordinates are used to obtain the fuzzy region that describes the robot's position in the global map. This is done by taking the Cartesian product of Π_X and Π_Y as shown in Figure 6.12. This fuzzy region identifies a collection of the robot's positions, each with a certain degree of possibility. Table 6.2 provides the number of iterations needed to obtain each unique location, the total number of candidate locations obtained until the robot identified unique locations, and the degree of match between the fuzzy local composite map and the global map for these locations. Table 6.3 provides the actual measurements of the unique fuzzy locations.

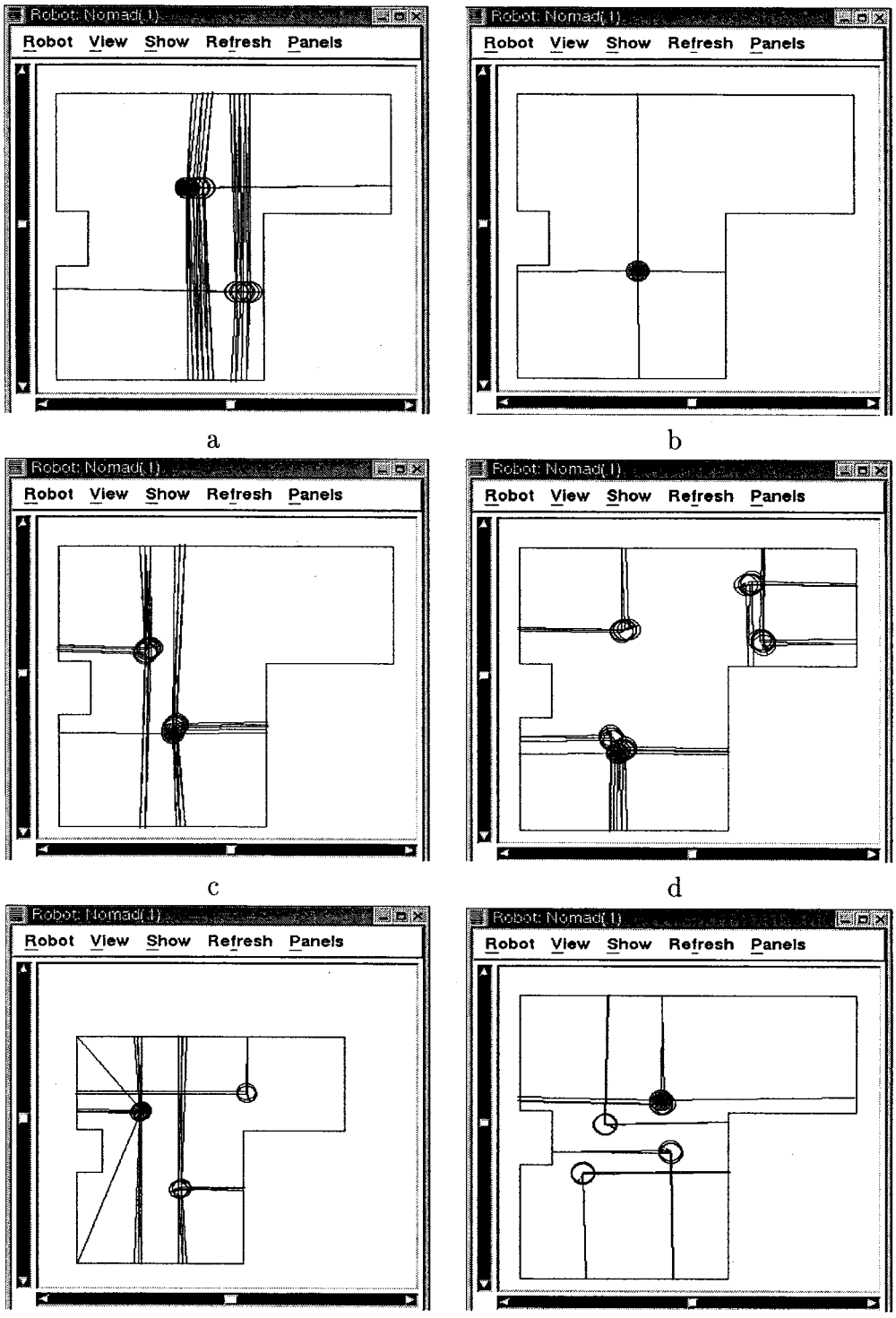

Figure 6.11: Different unique fuzzy locations in the global map.

Table 6.1: Components of identified fuzzy unique locations in the global map.

Test	X (mm)	Y (mm)	Θ (deg)
a	(2590,2610,2640,2660)	(4194,4203,4213,4233)	(152.5,152.5,166.5,180)
b	(2385,2385,2393,2403)	(2328,2347,2377,2396)	(242.5,256.5,270,270)
c	(2227,2237,2247,2257)	(2077,2087,2097,2106)	(220,220,233.5,247.5)
d	(1879,1899,1928,1948)	(1690,1700,1729,1729)	(175,188.5,202.5,202.5)
e	(1575,1585,1614,1614)	(4251,4271,4273,4283)	(355,8.5,22.5,22.5)
f	(2793,2813,2843,2843)	(3960,3980,4010,4030)	(85,85,90,90)

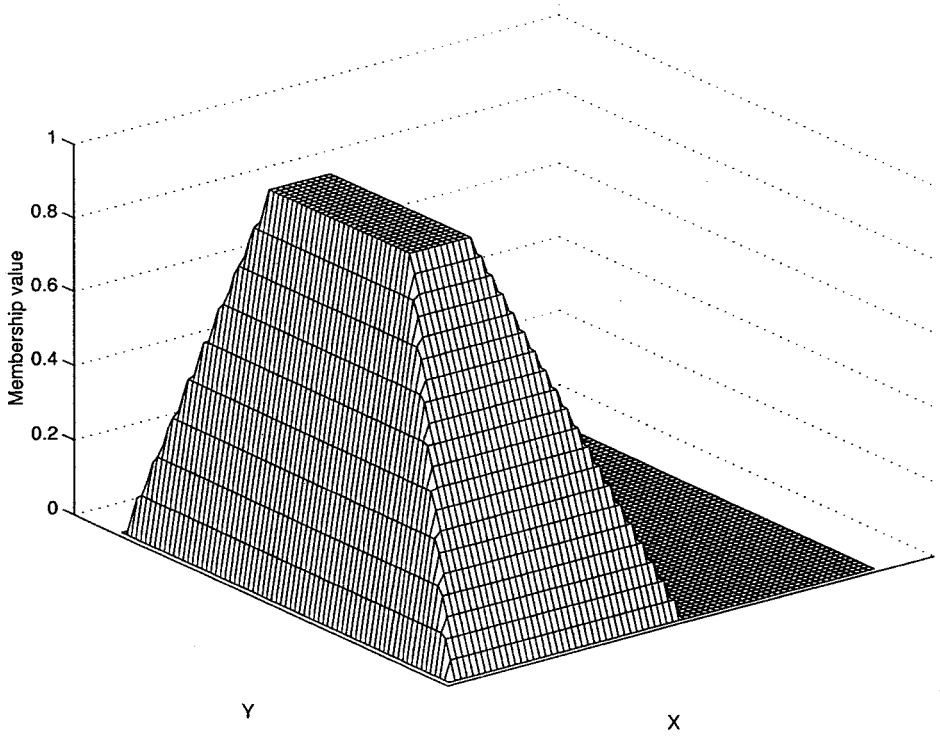

Figure 6.12: Fuzzy location region.

Table 6.2: Number of iterations and candidate locations obtained until a unique location is identified.

Test	Number of Iterations	Number of Locations	Φ
a	7	14	0.93
b	1	1	0.92
c	9	17	0.85
d	6	26	0.94
e	6	13	0.83
f	3	11	0.88

Table 6.3: Actual components of the unique locations in the global map.

Test	Xact (mm)	Yact (mm)	Θact (deg)
a	2615	4205	157
b	2390	2382	267
c	2239	2088	225
d	1916	1720	195
e	1595	4270	24
f	2820	3995	88

6.2 Applications of The Concurrent Localization and Map Updating Problem

In this section we implement our location and map updating algorithms in a real environment at the Fuzzy Systems Research Lab.

The Nomad 200 is programmed to follow the path illustrated in Figure 6.13. The robot has initial knowledge about its location in the global map. While the robot moved along its path, it was stopped at places A, B, C, and D (as shown in Figure 6.13) to obtain measurements of its position. In addition, the robot's position obtained from the odometers was registered. Then, the error in the robot's position was calculated as the difference between the measured position and the position provided by the odometers. This error is obtained as follows:

$$error = \sqrt{(y_{measured} - y_{odometer})^2 + (x_{measured} - x_{odometer})^2} \tag{6.1}$$

The obtained error versus the localization iterations is plotted using a dashed line as shown in Figure 6.14. This figure demonstrates that the error obtained by relying only on the odometers accumulates with time. For example, when the robot is at location A, the error provided by the odometers is 73 cm (see Figure 6.13 for the robot's path). This error is accumulated over the robot's path until it reaches location A. This error comes from the error in the x and y coordinates of the robot's position. However, the contribution to error from the y coordinate is larger since the robot was traveling along the y direction. At location B, the error is 93 cm and accumulated as a result of the turns performed by the robot. The accumulated error at location B starts to decrease until the robot reached location C, where it increased to 82 cm as a result of the robot's movement in an opposite direction to its original movements. Finally, at location D the error is 187 cm and accumulated as a result of the robot's turns and the movement of the robot in the x direction. These results support the fact that odometers are not reliable over long paths. This

is due to unequal wheel diameters, misalignment of wheels, finite encoder resolution, uneven floors, and wheel slippage.

In a second test, the robot followed the same path, however, our proposed localization algorithm is used to update the robot's position while it is moving along its path. The robot stopped at places A, B, C, and D as shown in Figure 6.13 so that measurements of its position could be taken. At the same time we registered the position information obtained from the proposed localization algorithm at these locations. We calculated the error in the robot's position as the difference between the position obtained by the measurements and the position obtained by the proposed algorithm. This error is obtained as explained in Equation (6.1). The error versus the number of localization iterations needed to reach each point is plotted and shown by the dashed-dotted line in Figure 6.14. This line shows that the error in the robot's position, corrected by our localization algorithm, is very small and its maximum value is around 2 cm. This is an acceptable range of error when using sonar sensors for localization. Similar approaches introduced by other researchers [43] show a larger range of errors when using sonar sensors for location updating in a similarly sized environment as the one used for our experiments.

The Nomad 200 is programmed to follow another path as shown in Figure 6.15. The robot was stopped at locations A and B so that measurements of its location could be taken. From Figure 6.16, the error obtained by our proposed localization algorithm is 1.9 cm. The error obtained by the odometers at location A was 95 cm and 190 cm at location B.

As Figures 6.14 and 6.16 show, the error obtained by our localization algorithm is not only less than the one obtained by the odometers, but also less than what is reported in the literature [43, 40]. This result shows the usefulness of the localization algorithm for mobile robot applications when specific tasks are to be achieved by the robot.

Our proposed localization algorithm is designed for mobile robots with a ring

configuration. This is a very important feature to mention since this configuration allows the detection of objects that are in different directions from the robot, and because the coordinates of these objects are used to update the robot's location. Therefore, this helps in increasing the frequency of location updates as shown in Figures 6.13 and 6.15. The intensive marks that are shown on the original map boundaries are the sonar points that are used to update the robot's location while the robot is following its path. Other algorithms are implemented on different robot configurations where these configurations impose some restrictions on the time when the robot can update its location [27]. In [27], the robot has to stop to accumulate a certain number of localization iterations to update its location.

The proposed localization algorithm is very robust to noisy sonar data. This is due to the fact that we filter erroneous sonar readings by combining range information obtained from adjacent sonar sensors. In addition, the modeling of angular and radial uncertainty of sonar readings results in obtaining location information with a small amount of error. The black dots shown in Figures 6.13 and 6.15 are noisy sonar readings that we chose not to use for localization or map updating. Some of the noisy readings are shown to be consistent with the global map, however, they are obtained in different scans by using only one sonar sensor.

Our map updating algorithm relies on the robot's current location to identify new objects in the robot's environment. Then, these objects are represented in the form of line segments and are added to the robot's global map. To make sure that the robot's current location is reliable, we implement the map updating algorithm concurrently with the location updating algorithm. The map updating algorithm is implemented in a real environment as shown in Figures 6.13 and 6.15. In Figure 6.13, one object was added to the robot's environment and while the robot was following its path, this object was identified using sonar readings that did not have matching components in the global map. Those sonar readings were used to initialize, create, and update a line segment that represented this object. During this process, the

number of the line segments in the robot's environment increased as a result of updating the robot's map by adding this line segment. In Figure 6.15, two objects were added to the robot's environment and our map updating algorithm was able to identify these two objects and form line segments that represented these objects. The number of the line segments in the robot's map increased by two as a result of updating the robot's environment.

Figure 6.13: Experimental verification of the proposed localization algorithm.

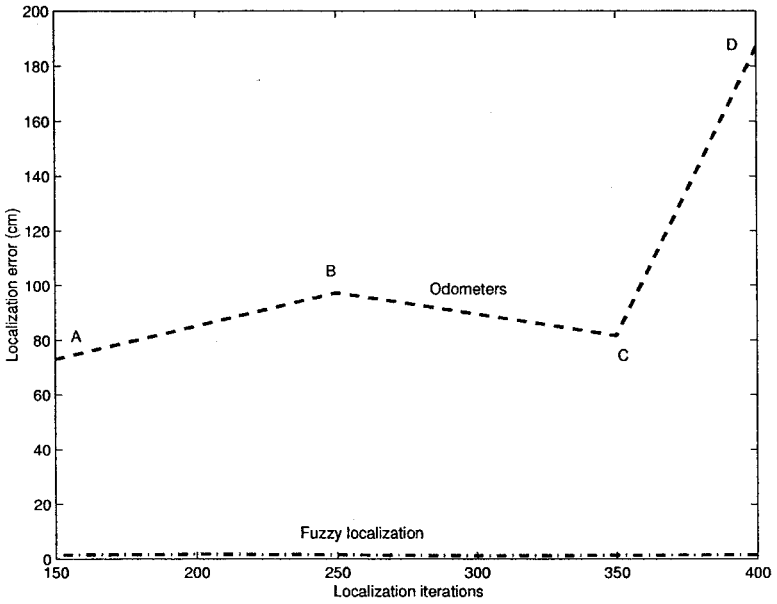

Figure 6.14: Localization error versus localization iterations.

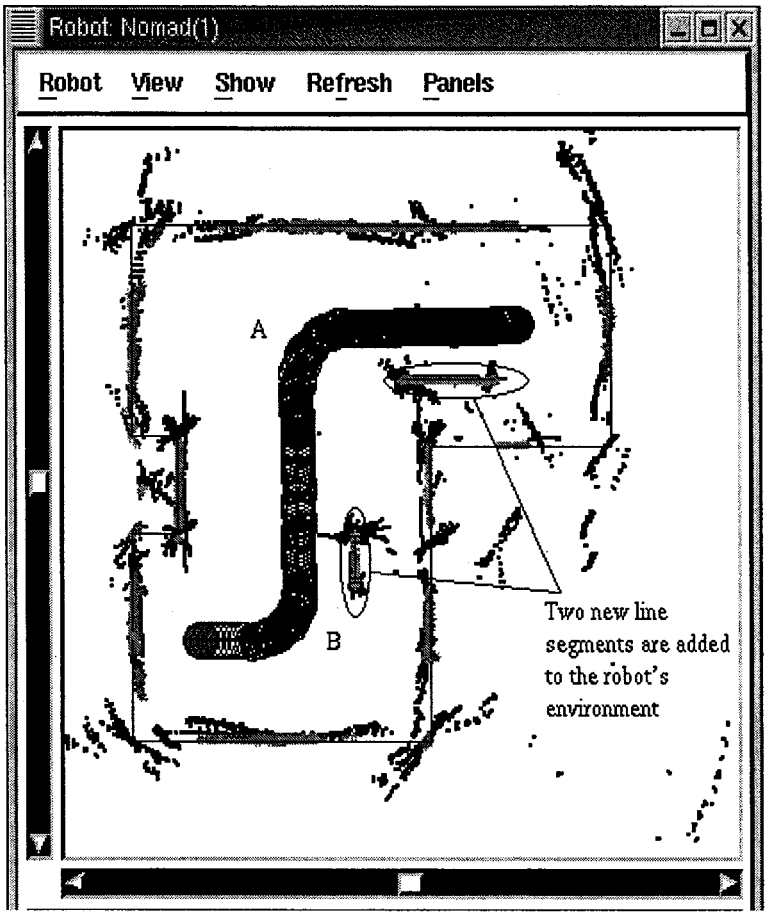

Figure 6.15: Experimental verification of the proposed localization algorithm.

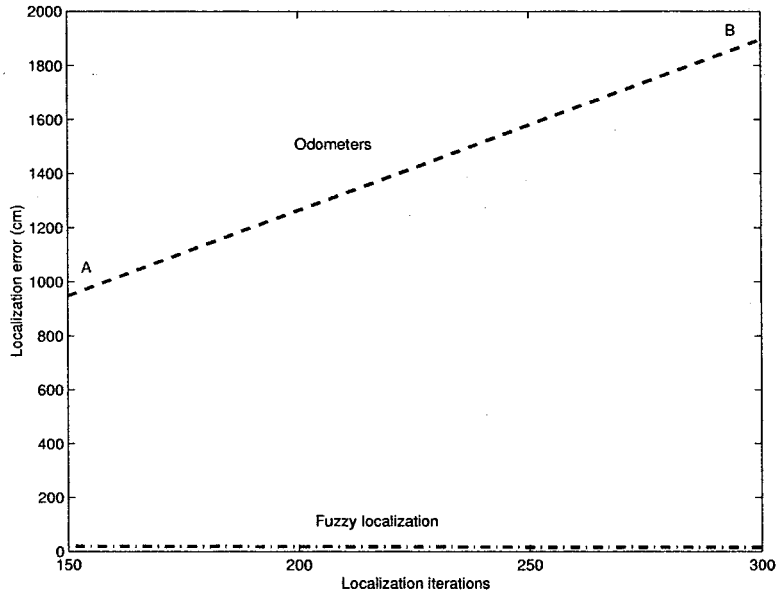

Figure 6.16: Localization error versus localization iterations.

Chapter 7

Conclusions and Future Work

In this chapter we conclude this thesis and introduce our future work plans.

7.1 Conclusions

This thesis introduced three fuzzy logic based algorithms for mobile robots equipped with a ring of sonar sensors. The first algorithm solves the global localization problem of mobile robots, the second algorithm solves the location updating problem, and the third solves the map updating problem. The three algorithms are dynamic algorithms, i.e., they run while the robot is moving.

Our localization algorithms depend on sonar readings to estimate the robot's location and update its map. Sonar sensors are chosen because they are inexpensive and provide range information in real-time. However, they suffer from drawbacks that limit their performance, especially when used for localization and map updating. There are two main drawbacks that affect any sonar based localization or map updating algorithm: the beam width of the sonar sensor and false reflections. The beam width introduces uncertainty in the position and orientation (*radial* and *angular* uncertainty, respectively) of the detected objects, and therefore affects quality of the location information provided by the localization algorithms. False reflections

provide inaccurate information about the robot's surroundings, and these inaccuracies affect the functionality of the localization algorithms.

These drawbacks can be overcome by studying the behavior of sonar sensors when they detect objects in the robot's environment. This is achieved by providing an appropriate experimental setup and carrying out various experiments that enable us to understand the behavior of sonar sensors. The experiments here studied the behavior of the sonar readings reacting to walls and corners since these two objects are available in the environments of any mobile robot. Based on the experimental results, we constructed fuzzy logic based models (possibility distributions) that represent the angular and radial uncertainty in sonar readings obtained by one sensor. Moreover, the false reflections problem was avoided by combining range information from adjacent sensors. Adjacent sonar sensors with small differences in the range readings are considered to be reflected from the same object. Combining information from adjacent sensors introduces reduced models of uncertainty in sonar readings when they are reflected from walls and corners. The reduced models are derived based on the knowledge of the angle between any two adjacent sensors in the sonar ring and the number of the adjacent sensors detecting the same object. In addition, we show how we can select the appropriate uncertainty models based on the range information and the number of adjacent sensors detecting the same object. These models are then used to identify objects in the robot's environment by estimating their position and orientation with respect to the robot. The coordinates of these objects are used in the proposed localization algorithms to estimate the robot's location. The method used to construct the uncertainty models can be generalized for any robot with a ring configuration.

We have proposed a fuzzy logic based solution for the global localization problem of mobile robots, that is, the estimation of the robot's location when it is completely lost in a known human-made indoor environment. The proposed approach uses sonar readings collected from a ring of sonar sensors mounted around the robot.

Consecutive sonar readings with close readings are considered to be reflected from the same object in the global map. These readings are associated with the appropriate uncertainty models which are given in the form of possibility distributions (fuzzy sets). This results in constructing a fuzzy local composite map which represents the current proximity of the robot. This map consists of a set of components, each of which represents the shortest distance between the robot and a detected object, and the orientation of the detected object with respect to the robot. These components are represented by possibility distributions (fuzzy sets).

In our proposed global localization algorithm, a matching algorithm is developed to match the fuzzy local composite map and the robot's global map to obtain all of the possible robot's locations in the global map. For the matching process to be successful, at least two non-parallel components of the fuzzy local composite map must be associated with objects in the robot's global map. Generally, the result of the matching process is either one candidate location or a number of candidate locations of the robot in the global map. Since x, y and θ components of an identified location are represented by possibility distributions, these locations are referred to as fuzzy locations. To reduce the number of candidate locations, the robot is moved to a new location and a new local fuzzy composite map is constructed. Then, a new set of candidate fuzzy locations is obtained. By considering the robot's movement, a set of hypothesized locations is identified from the old set of candidate locations. The hypothesized locations are matched with the new candidate locations and the candidates with a low degree of match are eliminated. The matching process is performed using the fuzzy pattern matching technique. If the robot actually was at the old location and, after traveling, it actually reached the new location, then the degree of match between the possibility distributions representing the components of these locations is expected to be high. Therefore, the degree of match can be used to test this hypothesis. The location pairs with low degrees of possibility are rejected and remaining locations are selected as the set of candidate locations. This

process continues until a unique location is identified, provided that the environment has a sufficient number of unique features.

The proposed algorithm is implemented on a Nomad 200 mobile robot. The effectiveness of the algorithm is demonstrated by many examples. In each example, the robot's location is initialized from a completely lost situation. In situations where there is more than one candidate location, the algorithm is able to reduce these locations into one unique location based on the processing of the gathered range information provided by the robot's sonar sensors in real-time. The proposed algorithm is capable of dealing with the uncertainties and false reflections associated with these sensors. This is reflected on the precision of the location information provided by this algorithm. Our proposed localization algorithm makes use of all available information provided by the robot's sensors while the robot is navigating its environment. This has a major effect on the process of the reduction of steps necessary to obtain one unique location. The experiments show how the recognition of corners in the robot's environment reduces the steps needed to obtain one unique location. The fuzzy local composite map provides location information about the detected objects in the robot's environment. This map is constructed based on sonar readings, i.e., the construction of this map is done in real-time given that there is no need to store large amounts of sensory data to build such a map. This is superior to the process of constructing local maps in terms of line segments which requires more time and the storing of extensive sensory readings while the robot is navigating its environment. Since our proposed algorithm provides the location of the robot in the form of fuzzy sets, it can be implemented with fuzzy logic based path planning, wall following and obstacle avoidance algorithms. The proposed algorithm is a generic algorithm for a class of mobile robots with a ring of sonar sensors.

We have proposed a fuzzy logic based location updating algorithm. This algorithm relies on the principle of sensor fusion to estimate the current location of the robot. The current location of the robot is found by combining the location of

the robot obtained by the odometers over short traveled distances and the location of the robot obtained based on the sonar readings. To estimate the robot's location based on sonar readings, the components of the fuzzy local composite map are transformed into global coordinates. As a result of this transformation, we identify two sets of the fuzzy local composite map components. The first set consists of the components that have matching components in the global map. The second set consists of non-matching components. Fuzzy triangulation technique is applied to each component of the first set to estimate either the x or the y coordinates of the robot's location. As a result of this triangulation technique, more than one component may describe the x or the y coordinate. Then, the principle of combining information from different sources is applied to obtain one x and one y coordinate. The result of this combination is the robot's location based on sonar readings. The robot's location is also estimated based on the odometer readings by taking into account the previous robot's location and the traveled distance. Then, a fuzzy logic based fusion technique is applied to the location obtained based on the sonar readings and the measurement from the odometers. The result of the fusion operation is the current location of the robot. This location is obtained in the form of possibility distributions (fuzzy sets). A defuzzification technique is applied on these distributions to obtain crisp values that can be used to update the robot's odometers.

The proposed location updating algorithm is able to update the current location of the robot continuously as long as there are sonar readings reflected from the robot's environment. Moreover, the algorithm does not depend on large amount of sonar data to be used in the location updating process. The proposed algorithm depends on the detection of natural landmarks such as walls and corners which are available in any indoor environment. In other words, structuring the robot's environment with artificial landmarks is not necessary for this algorithm to function. This algorithm is robust to noisy sonar readings and it provides location information with a small amount of error. This is due to the fact that this algorithm depends on

modeling the radial and angular uncertainty of sonar readings in the form of possibility distributions. The proposed location updating algorithm is tested on a Nomad 200 robot in a real environment. Experimental results are compared with the results obtained by relying only on the odometers to estimate the robot's location. These experiments demonstrate that the proposed algorithm has a small amount of error in estimating the robot's location.

We propose a map updating algorithm that enables the robot to update its global map while navigating. This algorithm is used to update the robot's map by adding new line segments. This is achieved by relying on the set of non-matching components to identify new objects in the robot's environment. The process of updating the robot's environment consists of three parts. The first part is responsible for initializing new line segments, the second part is responsible for creating new line segments from initialized segments, and the third part is responsible for updating the created line segments. Updating the robot's map requires that the current robot's location is reliable. Therefore, the location updating algorithm is implemented concurrently with the map updating algorithm. The proposed algorithm does not wait to obtain large amounts of sonar data to establish line segments. Additionally, the algorithm is able to handle the uncertainty associated with sonar readings. The proposed algorithm is implemented on a Nomad 200 mobile robot and the effectiveness of the algorithm is demonstrated experimentally.

7.2 Future Work

We can summarize our plans for future work as follows:

- In this thesis we introduced a fuzzy logic based dynamic global localization algorithm for mobile robots working in structured environments. Our algorithm can be used in many applications where the robot has to work in such environments. It is important also to introduce a global localization algorithm

where the robot has to work in cluttered environments. For this reason, we are planning to introduce a fuzzy logic based map building algorithm based on the well known fuzzy c-mean clustering. The cluster centers, obtained from the fuzzy c-mean algorithm, represent objects in the global map. Then, fuzzy logic based global localization can be designed where a local fuzzy map, obtained as cluster centers, can be matched with the global map to identify the robot's location in the global map.

- We are planning to implement our fuzzy logic based location updating algorithm concurrently with a fuzzy logic based goal approaching algorithm. The goal approaching algorithm needs reliable robot locations to enable the robot to reach its goal. The location updating algorithm is capable of providing a reliable robot's location continuously.

- We are planning to implement our fuzzy logic based location updating algorithm concurrently with a path following algorithm. The path that is followed by the robots may have different shapes such as a circle, square, etc. Usually a feedback controller is designed to allow the robot to follow its path. However, many researchers rely on odometers as a feedback device to estimate the robot's current location while the robot is following its path. This is applicable on the robot's simulator but not on the real robot. Therefore, our location updating algorithm can be used to provide feedback about the robot's current location on its path.

Bibliography

[1] L. Sciavicco and B. Siciliano, *Modeling and Control of Robot Manipulators.* McGraw-Hill, 1996.

[2] J. Craig, *Introduction to Robotics.* Addison-Wesley, 1989.

[3] F. Lamiraux and L. Kavraki, "Planning paths for elastic objects under manipulation constraints," *International Journal of Robotics Research*, vol. 20, no. 3, pp. 188–208, 2001.

[4] M. HAMZA, *Robotics and Applications.* ACTA Press, 2001.

[5] M. HAMZA, *Robotics and Manufacturing.* ACTA Press, 2001.

[6] I. J. Cox and G. T. Wilfong, *Autonomous Robot Vehicles.* Springer-Verlag, 1990.

[7] J. L. Jones and A. M. Flynn, *Mobile Robots: Inspiration to Implementation.* A K Peters, Wellesley, MA, 1993.

[8] M. Siegal and P. Guanatilake, *Remote Inspection Technologies for Aircraft Skin Inspection.* Technical report, Carnegie Mellon University. Pittsburgh, PA, 1997.

[9] I. Ulrich, F. Mondada, and J.-D. Nicoud, "Autonomous vacuum cleaner," *IEEE Transactions on Robotics and Automation*, vol. 19, no. 3-4, pp. 233–245, 1997.

[10] H. A. Yanco, "Development of outdoor navigation for a robotic wheelchair system," in *Proceedings of the Fifteenth National Conference on Artificial Intelligence*, p. 1208 AAAI Press/MIT Press, 1998.

[11] M. Ollis, *Perception Algorithms for a Harvesting Robot.* Doctoral dissertation, Carnegie Mellon University. Pittsburgh, PA, 1997.

[12] H. Schempf, D. Apostolopoulos, and J. West, "Tilebot: Mobile robot for automatic installation of floor tiles," in *IEEE Int. Conf. on Robotics and Automation (ICRA '96), April, 199*, 1996.

[13] J. Leonard and H. F. Durrent-White, "Mobile robot localization by tracking geometric beacons," *IEEE Transactions on Robotics and Automation*, vol. 7, no. 3, pp. 376–382, 1991.

[14] J. Borenstein, "Measurement and correction of systematic odometry errors in mobile robots," *IEEE Transactions on Robotics and Automation*, vol. 12, pp. 139–148, Spring 1995.

[15] K. Demirli, I. Türkşen, and M. Molhim, "GMP based fuzzy reasoning : An application to sonar based navigation," *Journal of Advanced Computational Intelligence*, To appear.

[16] A. Zelinsky, "Mobile robot map making using sonar," *Journal of Robotic Systems*, vol. 8, no. 5, pp. 557–577, 1991.

[17] B. Barshan and R. Kuc, "Differentiating sonar reflection from corners and planes by employing an intelligent sensor," *IEEE Transactions on Pattern Analysis and Machine Intelligence*, vol. 12, pp. 560–569, June 1990.

[18] R. Kuc and M. Siegel, "Physically based simulation model for acoustic sensor robot navigation," *IEEE Transactions on Pattern Analysis and Machine Intelligence*, vol. PAMI-9, pp. 766–778, November 1987.

[19] O. Bozma and R. Kuc, "Building a sonar map in a specular environment using a single mobile sensor," *IEEE Transactions on Pattern Analysis and Machine Intelligence*, vol. 13, pp. 1260–1269, December 1991.

[20] O. Bozma and R. Kuc, "Single sensor map-building based on physical principles of reflection," in *Proc. IEEE/RSJ International Workshop on Intelligent Robots and Systems IROS'91. Nov 3-5*, pp. 1038–1043, 1991.

[21] D. Miller, "Two dimensional mobile robot positioning using onboard sonar," *The International Journal of Robotics Research*, vol. 4, pp. 56–66, Spring 1985.

[22] Y. Nagashima and S. Yuta, "Ultrasonic sensing for mobile robot to recognize an environment-measuring the normal direction of walls-," in *Proceedings of the IEEE/RSJ International Conference on Intelligent Robots and Systems*, pp. 805–812, 1992.

[23] M. Piasecki, "Global localization for mobile robots by multiple hypothesis tracking," *Robotics and Autonomous Systems*, vol. 16, pp. 93–104, 1995.

[24] J. Castellanos and J. Tardós, *Mobile Robot Localization and Map Building: A Multisensor Fusion Approach.* Kluwer Academic Publishers, 1999.

[25] J. J. Leonard and H. F. Durrant-Whyte, "Simultaneous map building and localization for an autonomous mobile robot," in *in IEEE/RSJ Int. Workshop on Intelligent Robots and Systems, Osaka, Japan*, pp. 1442–1447, 1991.

[26] J. Crowley, "World modeling and position estimation for a mobile robot using ultrasonic ranging," in *Proceedings of the IEEE International Conference on Robotics and Automation*, pp. 674–680, 1989.

[27] J. Gasós and A. Martín, "Mobile robot localization using fuzzy maps," in *Lecture Notes in Artificial Intelligence* (A. Ralescu and T. Martin, eds.), Springer Verlag, 1996.

[28] K. Demirli and I. Türkşen, "Sonar based mobile robot localization by using fuzzy triangulation," *Robotics and Autonomous Systems*, vol. 33, pp. 109–123, December 2000.

[29] K. Demirli and I. Türkşen, "Fuzzy logic based mobile robot localization with sonar data," in *Canada-Japan bilateral Workshop on Intelligent Manufacturing and Process, Design*, Toronto, Canada, April 28-30, 1996.

[30] A.Elfes, "Sonar-based real-word mapping and navigation," *IEEE Journal of Robotics and Automation*, vol. RA-3, pp. 249–265, June 1987.

[31] D. Cho and J. Lim, "A new certainty grid based mapping and navigation system for an autonomous mobile robot," *The International Journal of Advanced Manufacturing Technology*, vol. 10, pp. 139–148, Spring 1995.

[32] L. Kleeman and R. Kuc, "Mobile robot sonar for target localization and classification," *International Journal of Robotics Research*, vol. 14, pp. 295–318, August 1995.

[33] L. Guibas, R. Motwani, and P. Raghavan, "The robot localization problem," in *Algorithmic Foundations of Robotics* (K. G. D. Halperin, J. Latombe, and R. Wilson, eds.), pp. 269–282, A. K. Peters, 1995.

[34] O. Karch and H.Noltemeier, "Robot localization - theory and practice," in *IEEE/RSJ Int Conf. Intelligent Robots and Systems, pp. 850-856*, Grenoble, France, 1997.

[35] G. Dudek, K. Romanik, and S. Whitesides, "Localizing a robot with minimum travel," *SIAM J. comput*, vol. 2, pp. 583–604, April 1998.

[36] M. Drumheller, "Mobile robot localization using sonar," *IEEE Transactions on Pattern Analysis and Machine Intelligence*, vol. PAMI-9, pp. 325–332, March 1987.

[37] J. Crowley, F. Wallner, and B. Schiele, "Position estimation using principal components of range data," *Robotics and Autonomous Systems*, vol. 23, pp. 267–276, 1998.

[38] T. Duckett and U. Nehmzow, "Mobile robot self-localization and measurement of performance in middle-scale environments," *Robotics and Autonomous Systems*, vol. 24, pp. 57–69, 1998.

[39] J. Mota and M. Ribeiro, "Mobile robot localization on reconstructed 3D models," *Robotics and Autonomous Systems*, vol. 31, pp. 17–30, 2000.

[40] O. Wijk and H. I. Christensen, "Localization and navigation of a mobile robot using natural point landmarks extracted from sonar data," *Robotics and Autonomous Systems*, vol. 31, pp. 31–42, 2000.

[41] A. Saffiotti and L. Wesley, "Perception-based self localization using fuzzy locations," in *Reasoning with Uncertainty in Robotics* (M. V. Lambalgen, ed.), pp. 368–386, Springer LNCS, 1996.

[42] I. J. Cox, "Blanche: An autonomous robot vehicle for structured environments," in *in IEEE International Conf. Robotics and Automation, Philadelphia, PA, USA*, pp. 978–982, 1988.

[43] P. Hoppenot and E. Colle, "Real time localizing of a low-cost mobile robot with poor ultrasonic data," *Control Engineering Practice*, vol. 6, pp. 925–934, 1998.

[44] J. N. J. Tardos, J. Horn, and G. Schmidt, "Fusing range and intensity images for mobile robot localization," *IEEE Transactions on Robotics and Automation*, vol. 6, pp. 76–84, February 1999.

[45] H. Beom and H. Cho, "Mobile robot localization using a single rotating sonar and two passive cylinders beacons," *Fuzzy Sets and Systems*, vol. 13, pp. 243–252, 1995.

[46] L. Matthies and A. Elfes, "Integration of sonar and stereo range data using a grid-based representation," in *IEEE Int. Conf. Robotics and Automation*, pp. 727–733, Philadelphia, PA, USA, 1988.

[47] F. Freyberger, P. Kampmann, and G. Schmidt, "Constructing maps for indoor navigation of mobile robot using an active 3D range imaging devise," in *IEEE Int. Workshop on Intelligent Robots and Systems*, pp. 143–148, Munich, Germany, 1990.

[48] G. U. M. Poloni and M. Vendittelli, "Fuzzy logic and autonomous vehicles: Experiments in ultrasonic vision," *Fuzzy Sets and Systems*, vol. 69, pp. 15–27, 1995.

[49] R. Urick, *Principles of Underwater Sound.* McGraw-Hill, New York, 1983.

[50] J. Borenstein, H. R. Everett, and L. Feng, *Navigating Mobile Robots: Systems and Techniques.* A K Peters, Ltd, Wellesley, Massachusetts, 1996.

[51] J. J. Leonard and H. F. Durrent-Whyte, *Directed Sonar Sensing for Mobile Robot Navigation.* Kluwer Academic Publisher, 1992.

[52] M. Molhim, *Possibilistic Sonar Modeling and Localization for Mobile Robots.* Master's thesis, Concordia University, Department of Mechanical Engineering, 1997.

[53] H. Zimmerman, "Uncertainty modelling and fuzzy sets," in *To appear in Proceedings of Workshop on Modeling Uncertainty.*

[54] G. Klir, "Where do we stand on measure of uncertainty, ambiguity, fuzziness, and the like," *Fuzzy Sets and Systems*, vol. 24, pp. 141–160, 1987.

[55] D. Dubois and H. Prade, *Possibility Theory.* Plenum Press, New York, 1988.

[56] A. Elfes, "Multi-source spatial data fusion using bayesian reasoning," in *Data Fusion in Robotics and Machine Intelligence* (A. Abidi and C. Gonzalez, eds.), pp. 137–163, Academic Press, Inc., 1992.

[57] K. Konolige, "Improved occupancy grids for map," *Autonomous Robots*, vol. 4, pp. 351–367, 1997.

[58] J. Borenstein and U. Raschke, "Real-time obstacle avoidance for non-point mobile robots," *ASME Transactions on Robotics Research*, vol. 2, pp. 2.1–2.10, 1992.

[59] G. Klir, "Generalized information theory," *Fuzzy Sets and Systems*, vol. 40, pp. 127–142, 1991.

[60] G. Klir and B. Yuan, *Fuzzy Sets and Fuzzy Logic.* Prentice Hall, New York, 1995.

[61] Z. Wang and G. Klir, *Fuzzy Measure Theory.* Plenum Press, New York, 1992.

[62] D. G. Kendall, "Foundations of a theory of random sets," in *Stochastic Geometry* (E. F. Harding and N. G. Kendall, eds.), pp. 322–376, Wiley, New York, 1974.

[63] G. Shafer, *Mathematical Theory of Evidence.* Princeton University Press, Princeton, NJ, 1976.

[64] J. Cliff, *Possibilistic Process for Complex Systems Modeling, Ph.D dissertation, Suny Binghamton.* UMI Dissertation Services, Ann Arbor MI, 1994a.

[65] L. Zadeh, "Fuzzy sets," *Information and Control*, vol. 8, pp. 338–353, 1965.

[66] L. Zadeh, "Outline of a new approach to the analysis of complex systems and decision process," *IEEE Transaction on Systems, Man and Cybernetics*, vol. 1, pp. 28–44, 1973.

[67] M. Sugeno and T. Yasukawa, "A fuzzy logic based approach to qualitative modeling," *IEEE Transactions on Fuzzy Systems*, vol. 1, pp. 7–31, February 1993.

[68] J. Bezdek, "Cluster validity with fuzzy sets," *Journal of Cybernetics*, vol. 3, pp. 58–71, 1974.

[69] S. L. Chiu, "Fuzzy model identification based on cluster estimation," *Journal of Intelligent and Fuzzy Systems*, vol. 2, pp. 267–278, 1994.

[70] K. Demirli and I. Türkşen, "Mobile robot navigation with generalized modus ponens type fuzzy reasoning," in *IEEE International Conference on Systems, Man and Cybernetics*, pp. 3724–3729, Vancouver, BC, Canada, October 22–25, 1995.

[71] K. Demirli, S. X. Cheng, and P. Muthukumaran, "Fuzzy modeling of job sequencing with subtractive clustering," *Fuzzy Sets and Systems*, To appear.

[72] M. R. Emami, I. Türkşen, and A. Goldenberg, "Development of systematic methodology of fuzzy logic modeling," *IEEE Transactions on Fuzzy Systems*, vol. 6, pp. 346–361, August 1998.

[73] D. Demirli and P. Muthukumaran, "Fuzzy system identification with higher order subtractive clustering," *Journal of Intelligent and Fuzzy Systems*, vol. 2, pp. 267–278, 1994.

[74] B. Schweizer and A. Sklar, *Probabilistic Metric Spaces*. North-Holland, Amsterdam, 1983.

[75] R. R. Yager, "Connectives and quantifiers in fuzzy sets," *Fuzzy Sets and Systems*, vol. 40, pp. 39–75, 1991.

[76] M. Mizumoto, "Fuzzy sets and their operations," *Information and Control*, vol. 48, pp. 30–48, 1981.

[77] K. Demirli, *A Unified and Extended Framework for Operator Selection in Generalized Modus Ponens Type Fuzzy Reasoning.* University of Toronto, Ph.D Thesis, 1995.

[78] D. Dubois and H. Prade, *Fuzzy Sets and Systems: Theory and Applications.* Academic Press, New York, 1980.

[79] M. M. Gupta and J. Qi, "Theory of t-norms and fuzzy inference methods," *Fuzzy Sets and Systems*, vol. 40, pp. 431–450, 1991.

[80] R. Bellman and M. Giertz, "On the analytic formalism of the theory of fuzzy sets," *Information Sciences*, vol. 5, pp. 149–156, 1973.

[81] R. R. Yager, "On a general class of fuzzy connectives," *Fuzzy Sets and Systems*, vol. 4, pp. 235–242, 1980.

[82] D. Dubois and H. Prade, "Fuzzy sets aggregation connectives," *Information Sciences*, vol. 36, pp. 85–121, 1985.

[83] L. Zadeh, "Fuzzy sets as a basis for a theory of possibility," *Fuzzy Sets and Systems*, vol. 1, pp. 3–28, 1978.

[84] G. Klir and T. A. Folger, *Fuzzy Sets, Uncertainty, and Information.* Prentice Hall, Englewood Cliffs, NJ, 1988.

[85] P. Z. Wang and X. H. Liu, "Set valued statistics," *Journal of Engineering Mathematics*, vol. 1, no. 1, pp. 43–54, 1984.

[86] D. Dubois and H. Prade, "Fuzzy sets, probability and measurement," *European Journal of Operational Research*, vol. 40, no. 2, pp. 135–154, 1989.

[87] D. Dubois and H. Prade, "Evidence, knowledge and belief functions," *International Journal of Approximate Reasoning*, vol. 6, no. 3, pp. 295–320, 1992.

[88] J. Cliff, "Possibilistic measurement and set statistics," in *Proceedings of NAFIPS, 1992, vol.2,*, pp. 458–467, 1992.

[89] J. Cliff, "Empirical possibility and minimal information distortion," in *Fuzzy Logic : State of the art, editor R. Lowen, Kluwer*, 1993a.

[90] J. Cliff, "Some new results on possibilistic measurement," in *Proc of NAFIPS*, pp. 227–231, Allentown, Pennsylvania, 1993b.

[91] J. Cliff, "Possibilistic semantic and measurements methods in complex systems," in *Proc. 2nd International Symposium on Uncertainty Modeling and Analysis, Bilal Ayyub editor, IEEE Computer Society Press*, pp. 208–215, 1993c.

[92] J. Cliff, "Possibilistic approach to qualitative model-based diagnosis," *Telematic and Informatics*, vol. 11, no. 4, pp. 365–384, 1994b.

[93] K. Demirli, M. Molhim, and A. Bulgak, "Possibilistic sonar modeling for mobile robots," *International Journal of Uncertainty, Fuzziness, and Knowledge-based Systems*, vol. 7, p. 177, April 1999.

[94] D. Dubois and H. Prade, "Combination of fuzzy information in the framework of possibility theory," in *Data Fusion in Robotics and Machine Intelligence* (A. Abidi and C. Gonzalez, eds.), pp. 481–505, Academic Press, Inc., 1992.

[95] D. Dubois, H. Prade, and C. Testemale, "Weighted fuzzy pattern matching," *Fuzzy Sets and Systems*, vol. 28, pp. 313–331, 1988.

Appendix A

Incidence angle (γ)	Actual distance (cm)	Sonar reading (cm)	Error (cm)
0	49.58	48.26	-1.32
1	49.59	48.26	-1.33
2	49.61	48.26	-1.35
3	49.66	48.26	-1.40
4	49.71	48.26	-1.46
5	49.79	48.26	-1.53
6	49.89	48.26	-1.63
7	50.00	48.26	-1.74
8	50.13	48.26	-1.87
9	50.18	50.8	0.42
10	50.44	50.8	0.36
11	50.63	48.26	-2.37
12	50.83	48.26	-2.57
13	51.05	48.26	-2.79
14	51.29	50.8	-0.49
15	51.55	50.8	-0.75
16	51.83	50.8	-1.03
17	52.13	50.8	-1.33
18	52.46	50.8	-1.66
19	52.80	50.8	-2.00
20	53.17	50.8	-2.37
21	53.56	50.8	-2.76
22	53.97	50.8	-3.17
23	54.40	50.8	-3.61
24	54.87	50.8	-4.10
25	55.36	50.8	-4.56

Table A.1: Sonar readings from a wall approximately 50 cm away from the sensor for $0 \leq \gamma \leq 25$.

Incidence angle (γ)	Actual distance (cm)	Sonar reading (cm)	Error (cm)
-1	49.58	48.26	-1.33
-2	49.61	48.26	-1.35
-3	49.65	48.26	-1.37
-4	49.71	48.26	-1.45
-5	49.79	48.26	-1.53
-6	49.89	48.26	-1.62
-7	50.00	48.26	-1.74
-8	50.12	48.26	-1.86
-9	50.28	48.26	-2.01
-10	50.44	48.26	-2.18
-11	50.62	50.8	0.17
-12	50.82	48.26	-2.57
-13	51.05	48.26	-2.79
-14	51.29	50.8	-0.49
-15	51.55	50.8	-0.75
-16	51.83	50.8	-1.03
-17	52.13	50.8	-1.33
-18	52.45	50.8	-1.65
-19	52.80	50.8	-2.00
-20	53.16	50.8	-2.37
-21	53.56	50.8	-2.76
-22	53.96	50.8	-3.17
-23	54.40	50.8	-3.61
-24	54.86	50.8	-4.06
-25	55.35	50.8	-4.55

Table A.2: Sonar readings from a wall approximately 50 cm away from the sensor for $0 > \gamma \geq -25$.

Incidence angle (γ)	Actual distance (cm)	Sonar reading (cm)	Error (cm)
0.00	95.68	93.98	-1.70
1.00	93.95	93.98	0.03
2.00	92.30	96.52	4.21
3.00	90.74	96.52	5.78
4.00	89.25	96.52	7.27
5.00	87.84	96.52	8.68
6.00	86.50	96.52	10.02
7.00	85.22	96.52	11.30
8.00	84.00	96.52	12.52
9.00	82.84	96.52	13.68
10.00	81.74	96.52	14.78
11.00	80.69	96.52	15.83
12.00	79.69	99.06	19.37
13.00	78.74	96.52	17.78
14.00	77.83	96.52	18.68
15.00	76.98	96.52	19.54
16.00	76.16	96.52	20.36
17.00	75.38	96.52	21.14
18.00	74.65	96.52	21.88
19.00	73.94	96.52	22.58
20.00	73.28	99.06	25.78
21.00	72.65	99.06	26.41
22.00	72.05	99.06	27.00
23.00	71.48	99.06	27.57
24.00	70.96	99.06	28.11
25.00	70.45	99.06	28.61

Table A.3: Sonar readings from a corner approximately 100 cm away from the sensor for $0 \leq \gamma \leq 25$.

Incidence angle (γ)	Actual distance (cm)	Sonar reading (cm)	Error (cm)
-1.00	93.95	93.98	0.03
-2.00	92.30	93.98	1.68
-3.00	90.74	93.98	3.24
-4.00	89.25	93.98	4.73
-5.00	87.84	93.98	6.13
-6.00	86.49	93.98	7.48
-7.00	85.22	96.52	11.30
-8.00	84.00	96.52	12.52
-9.00	82.84	96.52	13.67
-10.00	81.74	96.52	14.77
-11.00	80.69	96.52	15.82
-12.00	79.69	96.52	16.82
-13.00	78.74	96.52	17.77
-14.00	77.83	96.52	18.68
-15.00	76.97	96.52	19.54
-16.00	76.16	96.52	20.36
-17.00	75.38	96.52	21.13
-18.00	74.64	96.52	21.87
-19.00	73.94	96.52	22.57
-20.00	73.28	99.06	25.78
-21.00	72.65	99.06	26.41
-22.00	72.05	99.06	27.00
-23.00	71.49	99.06	27.57
-24.00	70.96	99.06	28.11
-25.00	70.45	99.06	28.61
-25.00	70.45	99.06	28.61

Table A.4: Sonar readings from a corner approximately 100 cm away from the sensor for $0 > \gamma \geq -25$.